UNIVERSITY OF SOUTHAMPTON

FACULTY OF SOCIAL, HUMAN AND MATHEMATICAL SCIENCES

Mathematical Sciences

A Study on Weighted and Structured Low Rank Matrix Optimization Problems

by

Jian Shen

Thesis submitted for the degree of Doctor of Philosophy

January 2021

UNIVERSITY OF SOUTHAMPTON

ABSTRACT

FACULTY OF SOCIAL, HUMAN AND MATHEMATICAL SCIENCES

MATHEMATICAL SCIENCES

Doctor of Philosophy

A STUDY ON WEIGHTED AND STRUCTURED LOW RANK MATRIX OPTIMIZATION PROBLEMS

by Jian Shen

This thesis focuses on the weighted and structured low rank approximation problem (wSLRA). This problem arises from a wide range of applications such as signal recovery, image processing and matrix learning. Due to the non-convexity of low rank matrix set, this problem is NP-hard and difficult to tackle. In this thesis we firstly focus on weighted low rank Hankel matrix optimization problem, which has become one of the main approaches to the signal extraction from noisy series or signals of finite rank by selecting the suitable weight matrix.

Two guiding principles for developing an approach are (i) the Hankel matrix optimization should be computationally tractable, and (ii) the objective in the optimization should be a close approximation to the original weighted least-squares. In this thesis we firstly introduce an approach that satisfies (i) and (ii) called Sequential Majorization Method (SMM). The framework of majorization method introduces guaranteed convergence by successfully solving the subproblem of each iterate, which ensures the sandwich inequality. At the same time, the latest gradient information is used when solving the subproblem of SMM, leading to more accurate approximations to the objective. However, the SMM scheme still has some drawbacks. The $(\mathbf{q}, \mathbf{p})$-norm introduced by SMM

to approximate weight norm are not mathematically equivalent, and the alternating projection method is used when optimizing the subproblem which has no convergence guarantees.

We further propose a new scheme as Penalised Method of Alternating Projection (pMAP). The proposed method inherits the favourable local properties of MAP and has the same computational complexity. Moreover, it is capable of handling a general weight matrix, is globally convergent, and enjoys local linear convergence rate provided that the cutting off singular values are significantly smaller than the kept ones. Furthermore, the new method also applies to complex data. Extensive numerical experiments demonstrate the efficiency of the proposed method against several popular variants of MAP.

This pMAP scheme is further extended to solve a wider rang of structured low rank matrix optimization problems such as robust matrix completion and robust principal component analysis with small noise. We use these two examples to demonstrate the approach to extend pMAP framework while keeping its advantages in dealing with low rank matrix approximation problems including computing efficiency and convergence results. Numerical experiments are conducted for both examples to illustrate the competitiveness of pMAP comparing with some state-of-the-art solvers

Contents

List of Figures

List of Tables

List of Algorithms

Declaration of Authorship

I, Jian Shen, declare that the thesis entitled *A Study on Weighted and Structured Low Rank Matrix Optimization Problems* and the work presented in the thesis are both my own, and have been generated by me as the result of my own original research. I confirm that:

- This work was done wholly or mainly while in candidature for a research degree at this University;
- Where any part of this thesis has previously been submitted for a degree or any other qualification at this University or any other institution, this has been clearly stated;
- Where I have consulted the published work of others, this is always clearly attributed;
- Where I have quoted from the work of others, the source is always given. With the exception of such quotations, this thesis is entirely my own work;
- I have acknowledged all main sources of help;
- Where the thesis is based on work done by myself jointly with others, I have made clear exactly what was done by others and what I have contributed myself;
- Parts of this work have been published as Qi et al. [2017] and Shen [2018].

Signed: .....

Date: .....

Acknowledgements

Throughout the writing of this dissertation I have received a great deal of support and assistance.

First of all, I would like to express my sincere gratitude to my supervisor Professor Hou-Duo Qi for for his consistent support and guidance throughout this research project. His insight and knowledge into the subject matter steered me though this research, and his expertises was invaluable for writing this thesis.

I would like to acknowledge my supervisor, Professor Zu-Di Lu for his his wonderful suggestions and collaborations. I would also thank my project progression examiners, Dr.Tri-Dung Nguyen and Dr.Alain Zemkoho for their insightful suggestions and feedbacks that pushed me to continuously improve my work. With many thanks to Professor Jein-Shan Chen from National Taiwan Normal University and Professor Nai-Hua Xiu from Beijing Jiaotong University for all their patient sharing and guidances. I would like to thank my Thesis Defense Committss, Dr.Jonathan Gillard and Dr.Tri-Dung Nguyen for all their careful reading and comments.

And my biggest thanks to my family for all the support you have shown me through my PhD. For my parent, Yi-Peng Shen and Chang-Li Yan, thanks for all your unfailing support, trust and encouragement. For my wife Xiang-Yu, thanks for all your unconditional support and patience. This trip would have not been possible without you.

Chapter 1

Introduction

This thesis studies the weighted low rank with structure constraint matrix approximation problem. We will firstly focus on approximating a low rank Hankel matrix such that the weighted distance to the observations is minimised. This problem arise from many areas such as signal processing, statistics, system identification and image processing, to name just a few.

By assuming a signal can be represented using only a few coefficients in a discrete basis (e.g., Fourier or wavelet basis), the embedding matrix from such a signal with some certain structures like Hankel or Toeplitz is of low rank. As a result, the structured low rank matrix approximation approach can be employed in many applications. Comparing with classical approaches which aim to approximate coefficients in finite discrete bases, this rank minimization technique enjoys various benefits such as high-resolution solution and free of bases selection because it works on the continuous domain directly. Due to these advantages, the rank minimization technique attracts a lot of attention in recent researches.

However, solving this problem is not easy. The non-convexity of low rank matrix constraint makes this problem to be NP-hard and difficult to solve in a tractable approach. Convex relaxation method is widely introduced for this problem and enjoys the best global optimal guarantee, but it also suffers a heavy computing cost at the same time.

There are some non-convex heuristic methods for this problem such as alternating projection and matrix factorization. However, their convergence behaviours are often unidentified or influenced by the starting point.

In this study we propose several new methods for this NP-hard problem via a sequential majorization approach. We will show that by introducing suitable majorization surrogate functions, this problem can be tackled via an iterative approach while admits some convergence results. Numerical experiments are conducted to demonstrate the performance of our proposed method comparing with some state-of-the-art solvers. We will also show that this majorization framework can be easily extended to other similar problems, such as robust matrix completion (RMC) and robust principal component analysis (RPCA) with noise.

1.1 Introduction

The low rank matrix optimization problems are widely raised in several applications such as matrix completion (e.g. [Candès and Recht, 2009, Jain et al., 2013, Vandereycken, 2013, Saeed et al., 2018]), matrix decomposition (e.g. [Mobahi et al., 2011, Shi, 2013]) and Hankel/Toeplitz matrix learning (e.g. [Usevich and Comon, 2016, Gillard and Zhigljavsky, 2016, Guo et al., 2017]). In general, the structured low rank matrix approximation problem can be formulated as:

$$\begin{aligned} &\min_{X\in\mathbb{R}^{l\times k}} f(X) \\ &\text{s.t.} \quad X \in \mathcal{C} \end{aligned} \tag{1.1}$$

where the subspace $\mathcal{C} \subset \mathcal{M}$ corresponds to the intersection of two or more matrix subsets while one is a low rank matrix set and others are structural constraints. $\mathcal{M}$ is the set of matrix of size $l \times k$ and $f(X)$ is a non-negative loss function that to be minimized. Because Problem (1.1) aims to minimise the cost function with non-convex low rank constraint, solving this problem is thought to be NP-hard and not tractable.

In this thesis we will focus on a particular type of Problem (1.1), known as weighted low rank Hankel matrix approximation problem (WLRH, in short). Let the cost function $f(X)$ to be the weighted distance between variable matrix and observed matrix as

$$f(X) = \|X - Y\|_W^2 = \|W \circ (X - Y)\|^2$$

In this formulation Y is the input Hankel matrix with observations and W stands for the weight matrix with non-negative elements. $\circ$ is used to denote the pairwise inner product between two matrix, i.e., $(A \circ B)_{ij} = A_{i,j}B_{i,j}$. In this thesis we have

Assumption 1: W is non-negative (i.e., $W_{i,j} \geq 0$ for all (i, j)).

Let us introduce two specific matrix subsets widely used in this thesis:

- Hankel matrix subset, defined as

$$\mathcal{H} : \left\{ X \in \mathbb{R}^{l \times k} \middle| X_{i,j} = X_{p,q}, \text{ if } i + j = p + q, \ \forall\ 1 \leq i, p \leq l \text{ and } 1 \leq j, q \leq k. \right\}$$

  In another word, elements of a Hankel matrix at the same ascending skew-diagonal from left to right are the same. Below is a simple 3×5 Hankel matrix with 7 unique elements as an example:

$$\begin{bmatrix} a_1 & a_2 & a_3 & a_4 & a_5 \\ a_2 & a_3 & a_4 & a_5 & a_6 \\ a_3 & a_4 & a_5 & a_6 & a_7 \end{bmatrix}$$

- r-rank matrix subset, defined as

$$\mathcal{M}_r : \left\{ X \in \mathbb{R}^{l \times k} \middle| \text{rank}(X) \leq r. \right\}$$

Let the subspace $\mathcal{C}$ be the intersection of above two subsets as $\mathcal{C} = \mathcal{H} \cap \mathcal{M}_r$. For a given Hankel matrix Y, we consider the following problem:

$$\min_{X \in \mathbb{R}^{l \times k}} \ f(X) := \frac{1}{2}\|W \circ (X - Y)\|^2 \tag{1.2}$$

$$\text{s.t.} \quad X \in \mathcal{H} \cap \mathcal{M}_r$$

The objective of this optimization problem is to find $X \in \mathbb{R}^{l \times k}$ that closet to Y in terms of weighted distance. X is constrained that 1) its rank should be smaller or equal to r and 2) it should be a Hankel matrix. Throughout this thesis, we assume that both weight matrix W and the objective rank r to be known and user-selected. Here W with non-negative entries measures the importance or correctness of data in Y, e.g., assigning high weights to data that are believed to be measured accurately or more important and giving relevant low weights to data that are less important or with high noise.

1.2 Motivation and Practical Applications

1.2.1 Singular Spectrum Analysis (SSA)

Our work is greatly inspired by Spectrum Spectrum Analysis (SSA) which introduced the low rank technique into time series analysis studies. We refer to the works by Hassani [2007] and Golyandina and Korobeynikov [2014] that provide comprehensive introductions on SSA. SSA aims to decompose the original time series into the sum of independent sub-series including long-term trend, period cycles and noise. It provides a novel and powerful approach to get insight at the each component of a time series. This tool is widely employed in various applications such as 1) removing noise from a time series, 2) identifying the trend or seasonal facts, 3) forecasting the future data or filling the missing data in a series and 4) detect outlier or structure change, to name just a few.

1.2.1.1 Basic SSA

Phase 1: Decomposition

The implementation of basic SSA includes two phases known as Decomposition and Reconstruction. The basic idea behind decomposition is that a time series is determined

or influenced by a set of discrete and independent variables. Following this assumption, the original time series can be represented as the sum of independent components while each component corresponds to a variable. To implement the decomposition, the first step of SSA is to embed the original time series into a structured matrix using lagged copies. Considering a real time series with n elements

$$\mathbf{a} = (a_1, a_2, ..., a_n)$$

while its i-th lagged copies is constructed as $\mathbf{a}_i = (a_i, a_{i+1}, ...a_{i+k-1})^T$. Then its trajectory matrix A takes the following format

$$A = \mathcal{H}(\mathbf{a}) = [\mathbf{a}_1, \mathbf{a}_2, ..., \mathbf{a}_l] = \begin{bmatrix} a_1 & a_2 & \cdots & a_l \\ a_2 & a_3 & \cdots & a_{l+1} \\ \vdots & \vdots & \vdots & \vdots \\ a_k & a_{k+1} & \cdots & a_n \end{bmatrix}$$

Here $\mathcal{H}$ represent the embedding operator that projects a time series into a Hankel matrix. Without loss of generality, we always assume $l \leq k$ throughout this thesis. There are also other ways to embed a time series into a structured trajectory matrix like using Toeplitz matrix (for example, see Condat and Hirabayashi [2015]). In this thesis we will insist on Hankel matrix since both approaches play a similar role in SSA. The next step is to decompose the Hankel matrix A using Singular Value Decomposition (SVD). For a real valued matrix $A \in \mathbb{R}^{l,k}$, we always have the following decomposition

$$A = U\Sigma V^T$$

where $U \in \mathbb{R}^{l \times l}$ and $V \in \mathbb{R}^{k \times k}$ are unitary matrices. $\Sigma = \text{diag}(\sigma_1, \sigma_2, ..., \sigma_l)$ is a $l \times k$ diagonal matrix, while its $\{i, i\}$-th element correspond to the i-th singular value of A. By default, we always arrange σ_i in the non-increasing order with respect to its index i, i.e., $\sigma_1 \geq \sigma_2 \geq \sigma_3 \geq ... \geq \sigma_l$.

Using SVD, the Hankel trajectory matrix A can be decomposed as the sum of matrices

$$A = \sum_{i=1}^{l} A_i \tag{1.3}$$

where $A_i = \sqrt{\lambda_i} U[i,:] V[i,:]^T$ and $U[i,:]$ stands for the i-th row in U. It completes the Decomposition phase of SSA. To provide a insight analysis on the decomposition phase of SVD, let us consider a well-known real life time series example, Australia monthly fortified wine sales from 1980 to 1992, as plotted in Fig.1.1 with 156 observations.

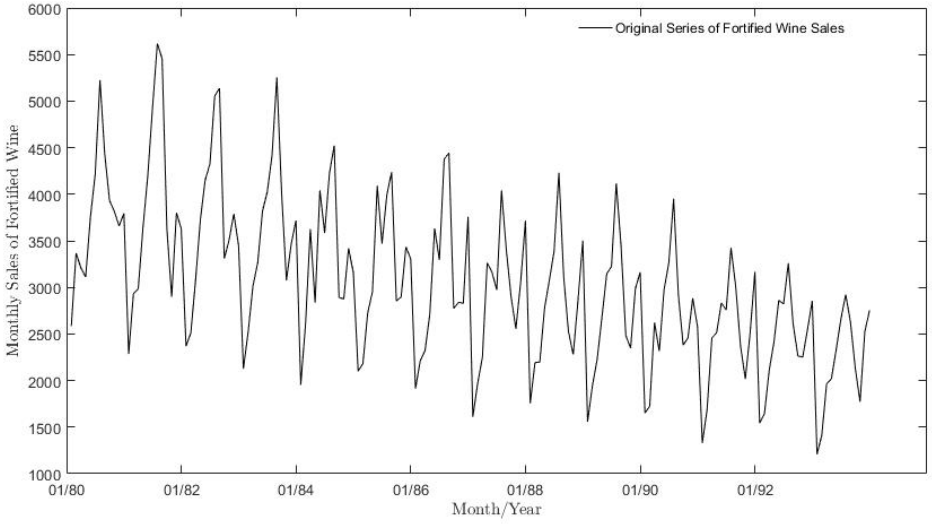

FIGURE 1.1: Monthly Fortified Wine Sales Series from 1980 to 1992

We apply the decomposition phase of SSA on this dataset to get a set of matrices using equation (1.3). Following suggestions by Gillard and Usevich [2018], l is set as 84. To visualization each one-rank matrix A_i, we apply diagonal averaging which projects a given matrix to the subspace of Hankel matrix such that a time series can be extracted. The detailed implementation of diagonal averaging will be discussed in the following Reconstruction phase. The visualization result of each A_i is plotted in Fig.1.2. The first submatrix A_1 can be interpreted as the long term trend of the series which has the largest influence on the data validity. Following 11 submatrices represents the cyclical fluctuations in the original series with different frequencies. With the decreasing of corresponding singular value, the cyclical fluctuation admits higher frequencies and lower amplitude.

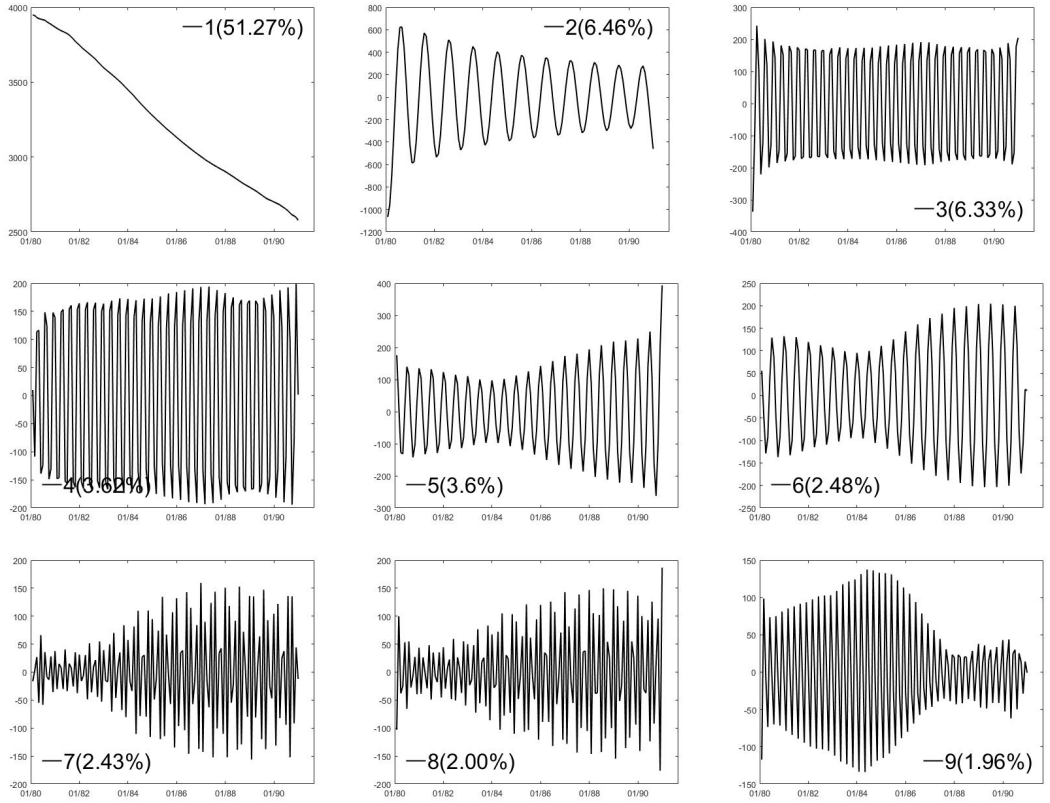

FIGURE 1.2: Singular Value Decomposition of Wines Sales Series

Phase 2: Reconstruction

The Reconstruction phase of SSA comes after Decomposition to extract a time series from decomposed Matrix. Define the indices set $\mathcal{I} = \{i_1, i_2, ..., i_r\}$ as the subset of indices $\{1, 2, ..., l\}$, the reconstructed $\widetilde{A}$ is obtained by

$$\widetilde{A} = \sum_{j=1}^{r} A_{i_j}$$

following the submatrix A_i computed by SVD. This procedure is called regrouping. The selection strategy of r depends on the purpose of SSA. For example, in de-noising or data approximation application, the subset indices is selected as $i_j = j$ which means SSA will keep the r-largest singular values.

The final step of SSA is to project this reconstructed $\widetilde{A}$ into a Hankel matrix by diagonal averaging. This step averages the matrix entries in $\widetilde{A}$ over antidiagonals. Let $\widetilde{A_{i,j}}$ represent the (i, j)-th element in $\widetilde{A}$, diagonal averaging will result to the following Hankel

matrix

$$\begin{bmatrix} \widehat{a}_1 & \widehat{a}_2 & \cdots & \widehat{a}_\ell \\ \widehat{a}_2 & \widehat{a}_3 & \cdots & \widehat{a}_{\ell+1} \\ \vdots & \vdots & \vdots & \vdots \\ \widehat{a}_k & \widehat{a}_{k+1} & \cdots & \widehat{a}_n \end{bmatrix}$$

where $\widehat{a}_i$ is computed by

$$\widehat{a}_i = \frac{1}{|\mathcal{I}_i(p,q)|} \sum_{p+q-1=i} \widetilde{A_{p,q}}$$

$\mathcal{I}_i(p,q)$ is the indices set that includes all unique combinations of $\{p,q\}$ such that $p+q-1=i$ while $|\mathcal{I}|$ denotes the set size of $\mathcal{I}$. Following the step of diagonal averaging, SSA finally returns the approximated time series

$$\widehat{\mathbf{a}} = (\widehat{a}_1, \widehat{a}_2, ..., \widehat{a}_n)$$

This finishes the implementation of SSA.

Let us use the Australia wine sales example again to demonstrate the reconstruction phase of SSA. The reconstruction results of Australia wine sale series are plotted in Fig.1.3 by keeping r largest singular values. We observed that following reconstruction phase, SSA generates a "smoothed" series with different resolutions. The higher rank choices on r will lead to the smoothed series closer to the observations.

1.2.1.2 SSA Related Works

SSA is believed to be a powerful tool that widely applied in many areas such as social science, economics, physics, biological, market research and so on. One major empirical application of SSA is to approximate the missing or future values in a series in areas such as energy usage [Li et al., 2014], health care pressure [Gillard and Knight, 2014], stock market [Lahmiri, 2018], climate change [Unnikrishnan and Jothiprakash, 2018] and so on. Another popular application scenario of SSA is removing the noise component in a signal, for example, in the work by Zabalza et al. [2015b] on hyper-spectral image data and the work by Lari et al. [2019] on field seismic data. SSA is also widely applied

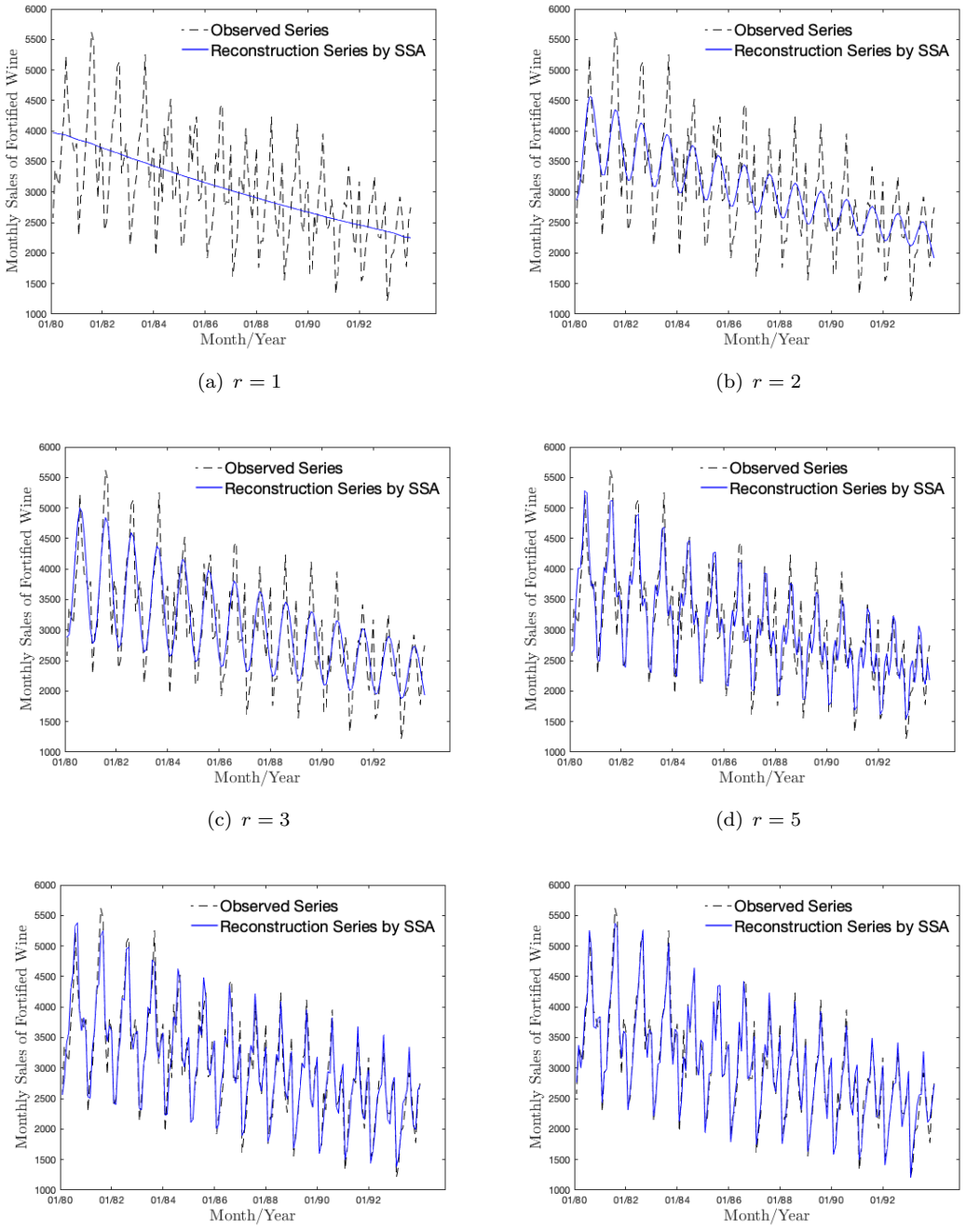

(a) $r = 1$ (b) $r = 2$

(c) $r = 3$ (d) $r = 5$

(e) $r = 10$ (f) $r = 15$

FIGURE 1.3: Reconstruction result of Australian wine sales series using different sub-matrice re-grouping choices, various from $r = 1$ in Fig. 1.3(a) to $r = 15$ in Fig. 1.3(f).

for outlier or structural change detection in a signal data. Lang [2019] applied SSA to detect the outlier in heart rate variability data while Xu et al. [2017] and Bhowmik et al. [2019] used this technique to identify the structural damages in a signal data.

Some researches tried to establish the relationship between SSA and popular time series

decomposition solvers, such as Fourier or wavelet transformation. In fact, SSA generalises these techniques by working on a continuous variable dictionary in the frequency domain when assuming that a time series can have discrete representation in a specific frequency domain. As a result of introducing rank technique, SSA enjoys a huge benefit that it provides "high resolution solutions" comparing with classical compressed sensing techniques such as MUSIC (Schmidt [1986]) and ESPRIT (Roy and Kailath [1989]). Matrix rank reduction technique can effectively avoid the issue of "basis mismatch" (Chi et al. [2011]), which often occurs when the variables or coefficients of a true time series fail to locate on the pre-prepared discrete dictionary precisely. One most recent research applying rank technique on compressed sensing problem with convincing results is completed by Cai et al. [2019].

Some theoretical works are proposed at the same time to further improve the performance of SSA via different approaches. Rahmani [2017] proposed the Bayesian SSA to tackle the scenario when the underlying system moves from one homogeneous state to another rapidly. The Monte Carlo SSA proposed by Groth and Ghil [2015] to avoid taking some stochastic noise as oscillations when extracting interpretable components in a signal. A novel augmented Lagrange multiplier algorithm-based solver is by Feng et al. [2018] to avoid the singular value computing at the decomposition phase of SSA. All these empirical and theoretical works drive us to further propose more robust and efficient schemes to handle Problem (1.2).

1.2.2 Applications

There is a long history to employ low rank matrix approximation approach to deal with time series and signal analysis problems. Some recently researches applied this WLRH problem to tackle spectral sparse signal processing (Condat and Hirabayashi [2015], Cai et al. [2019]), image processing (Nguyen et al. [2013], Jin and Ye [2015]), time series analysis (Markovsky and Usevich [2013], Gillard and Usevich [2018]) and tensor completion (Ying et al. [2017]), to name just a few. In this section we provide three different applications of WLRH. Also since there are several variant problems that

can be tackled using the framework we proposed for WLRH, we introduce two further applications for these variants.

1.2.2.1 Time Series De-noising

In this application all data in a time series are assumed to be observed with random and coherent noise. The actual low rank structure in high dimension data can be identified by extracting the noiseless data from noisy observations. Fig.1.4 presents the coefficients of a spectral sparse signal in a discrete Fourier domain without noise. Its true signal is plotted in Fig. 1.5 (blue solid line) [1] and as well as its noisy observations (red dotted line). Assuming only the information of noisy observations are captured, signal denoising aims to recover the true signal and re-establish the coefficients. Some recent researches includes Condat and Hirabayashi [2015] and Gillard and Zhigljavsky [2016]. More detailed information can be found in Section 4.4.1.

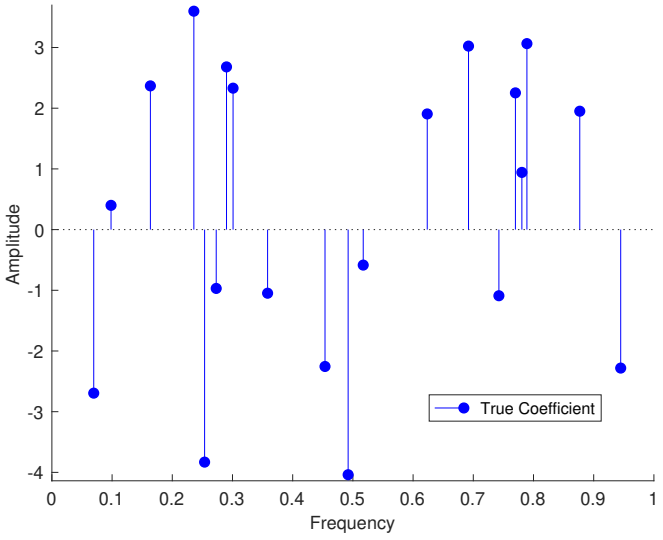

FIGURE 1.4: Example of signal denoising: Discrete presentation of a signal with 20 coefficients in the frequency domain.

[1] For the illustration convenience, only the real part of the complex-valued signal is plotted in this figure

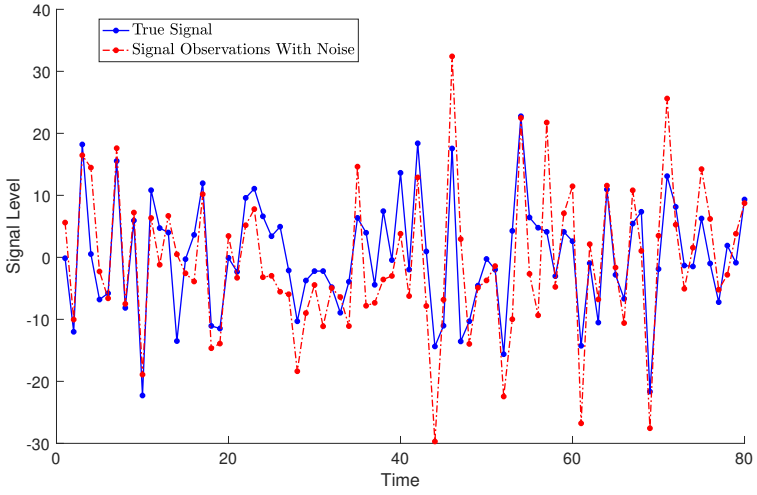

FIGURE 1.5: Example of signal denoising: True and observed signal with 80 observations in the time domain. The coefficients of true signal in the frequency domain is presented in Fig.1.4.

1.2.2.2 Incomplete Signal Recovery

In some applications, the observations of a signal are not complete due to several reasons like plotted in Fig.1.6. Incomplete Signal Recovery aims to approximate these missing values from observed data by assuming the whole signal has sparse representation in a specific domain (like in Fig.1.5). If the signal can be successfully recovered, its coefficient locations and amplitudes can be precisely established as well. Some recent works focusing on this application can be seen in Tang et al. [2013], Chen and Chi [2014] and Cai et al. [2019]. Furthermore, time series forecasting can be formulated as a special application of missing data recovery by considering the future data as missing values at the end of a signal. We refer some recent works by Butcher and Gillard [2017] and Gillard and Usevich [2018]. Section 3.3 conduct two numerical experiments to forecast the future data in a time series and Section 4.4.2 provides detail experiments on the sparse signal recovery.

1.2.2.3 Image Processing: A step to high dimensional data

In many applications, the data may be collected from higher dimensions, for example, in the applications of multi-channel time series analysis and image processing (see Huang

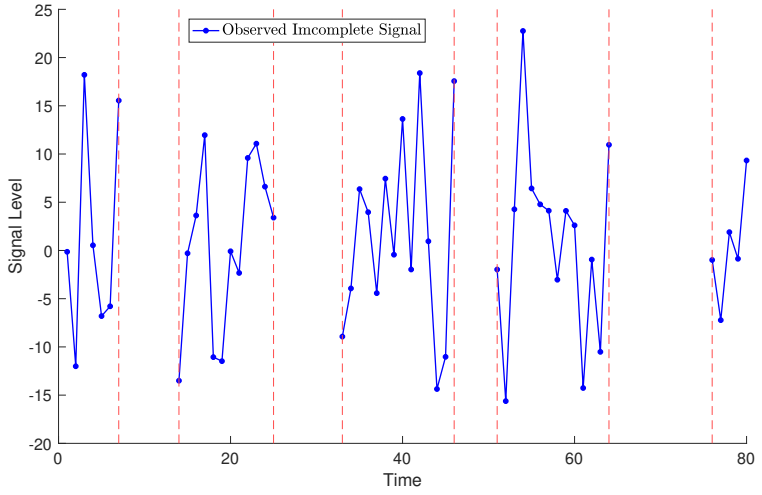

FIGURE 1.6: Procedure of Majorization Minimization

et al. [2016], Silva et al. [2018], Lee et al. [2016] and Ying et al. [2018]).

We show WLRH approach still works under this situation. Assume we have a matrix consisted by a set of series as $X = \{\mathbf{x}_1, \mathbf{x}_2, ..., \mathbf{x}_m\} \in \mathbb{R}^{m \times n}$ and each series $\mathbf{x}_i = \{x_{i,1}, x_{i,2}, ..., x_{i,n}\}^T \in \mathbb{R}^n$. The 2-dimension matrix X can be embedded into the following block Hankel matrix:

$$\mathcal{H}(X) = \begin{pmatrix} \mathcal{H}(\mathbf{x}_1) & \mathcal{H}(\mathbf{x}_2) & \mathcal{H}(\mathbf{x}_3) & \dots & \mathcal{H}(\mathbf{x}_{l'}) \\ \mathcal{H}(\mathbf{x}_2) & \mathcal{H}(\mathbf{x}_3) & \mathcal{H}(\mathbf{x}_4) & \dots & \mathcal{H}(\mathbf{x}_{l'+1}) \\ \mathcal{H}(\mathbf{x}_3) & \mathcal{H}(\mathbf{x}_4) & \mathcal{H}(\mathbf{x}_5) & \dots & \mathcal{H}(\mathbf{x}_{l'+2}) \\ \dots & \dots & \dots & \dots & \dots \\ \mathcal{H}(\mathbf{x}_{k'}) & \mathcal{H}(\mathbf{x}_{k'+1}) & \mathcal{H}(\mathbf{x}_{k'+2}) & \dots & \mathcal{H}(\mathbf{x}_m) \end{pmatrix} \tag{1.4}$$

where l' and k' is selected such that $l' + k' - 1 = m$. Each Hankel matrix $\mathcal{H}(\mathbf{x}_i)$ is constructed as

$$\mathcal{H}(\mathbf{x}_i) = \begin{pmatrix} \mathcal{H}(x_{i,1}) & \mathcal{H}(x_{i,2}) & \mathcal{H}(x_{i,3}) & \dots & \mathcal{H}(x_{i,l}) \\ \mathcal{H}(x_{i,2}) & \mathcal{H}(x_{i,3}) & \mathcal{H}(x_{i,4}) & \dots & \mathcal{H}(x_{i,l+1}) \\ \mathcal{H}(x_{i,3}) & \mathcal{H}(x_{i,4}) & \mathcal{H}(x_{i,5}) & \dots & \mathcal{H}(x_{i,l+2}) \\ \dots & \dots & \dots & \dots & \dots \\ \mathcal{H}(x_{i,k}) & \mathcal{H}(x_{i,k+1}) & \mathcal{H}(x_{i,k+2}) & \dots & \mathcal{H}(x_{i,n}) \end{pmatrix} \tag{1.5}$$

There are multiple approaches to construct a block Hankel matrix from 2-dimensional data and in (1.4) we just provide one popular approach of them. Similar constructing approach can be extended to higher dimensional data, for example, [Cai et al., 2019, Section 2.4] proposed the block Hankel matrix constructing method for 3-dimension data. This embedding approach enables us to employ the low rank matrix approximation methods for tackling multi-channel data from higher dimensions.

1.2.2.4 Movie Recommendation Engine

The main target of movie recommendation engines (MRE) is recommending suitable movies to each movie user by approximating their potential ratings on these movies. Assume we have a matrix Y containing the rating data from an audience to a specific movie, i.e., $Y_{i,j}$ stands for rating of i-th audience to j-th movie. This dataset is usually large scaled since there are thousands of movies and millions of audiences on the market. Following figure provides a simple example of movie rating matrix, consisted by four audiences and four films.

Alice	4			4
Bob		5	4	
Joe		5		
Sam	5			

FIGURE 1.7: Examples of movie rating matrix by four movies and four users. 6 out of 16 ratings are known and MRE aims to find good recommendations by approximating rest 10 ratings.

In most case the rating matrix Y is incomplete because it is impossible for each audience to provide ratings for all movies. As a result, this film recommendation engine application aims to recover the missing ratings and then recommand movies to audiences accordingly. However, establishing movie recommendation engine based on the rating

set in real business is considered to be very challenge because normally the percentage of known ratings are very small, thus attracts a lot of attentions. Problem formulation MRE will be discussed in Section 5.1 and the application details can be seen from Section 5.1.4.

1.2.2.5 Sparse Noise Detection

Sparse noise detection or removal problem comes from scenarios where observations are polluted by sparse outlier noise, for example, video foreground/background decomposition and fault detection. This application assumes the observations $Y \in \mathcal{M}$ is consisted by two components as $Y = L + S$. $L \in \mathcal{M}$ is a low rank matrix which contains useful information. $S \in \mathcal{M}$ is a sparse matrix which means most elements are zeros while a few non-zero elements represent the noise. Hence the objective of this problem is to recover L from given observations Y. For example in the video foreground/background decomposition problem, the observed matrix can be decomposed in to a 1-rank matrix representing the stable background and a sparse matrix representing the moving objects in the video (Bouwmans et al. [2017]). In Section 5.2 we will discuss our proposed scheme to formulate and tackle this problem.

1.3 Problem Formulation and Contributions

1.3.1 Problem Formulation

It is worth noting that by applying SVD, the matrix $\widetilde{A}$ obtained by SSA regrouping is exactly of rank r if $\sigma_r(A) \neq 0$. Let us consider the most common situation that SSA always selects the r largest singular values in the regrouping phase. In this case, SSA aims to find the closest low rank Hankel matrix to A. However, it is worth noting that in most cases, the output of SSA is quite far from r-rank matrix set unless the original time series enjoys perfect separability (Hassani et al. [2011]).

To improve the result of SSA, some researches (for example, see [Gillard, 2010, Sec 3.4]) proposed the following optimization problem based on the idea of SSA

$$\begin{aligned} \min_{X \in \mathbb{R}^{m \times n}} & \|X - Y\|^2 \\ \text{s.t.} \quad & X \in \mathcal{H} \cap \mathcal{M}_r \end{aligned} \tag{1.6}$$

which aims to find a intersect point between Hankel and low rank matrix set while also minimising the distance to the original Hankel matrix. To further motivate our investigation on Problem (1.2), let us consider a complex-valued time series $\mathbf{a} = (a_1, a_2, \ldots, a_n)$ of finite rank [Golyandina et al., 2001, Chp. 5]:

$$a_t = \sum_{s=1}^{m} P_s(t) \lambda_s^t, \quad t = 1, 2, \ldots, n \tag{1.7}$$

where $P_s(t)$ is a complex polynomial of degree $(\nu_s - 1)$ (ν_s are positive integers) and $\lambda_s \in \mathbb{C} \setminus \{0\}$ are distinct. Define $r := \nu_1 + \ldots + \nu_m$ (":=" means "define"). Then it is known [Usevich, 2010, Prop. 2.1] that the rank of the Hankel matrix A generated by $\mathbf{a}$ must be r, i.e., $\operatorname{rank}(\mathcal{H}(\mathbf{a})) = r$ where the choice of (k, ℓ) satisfies $n = k + \ell - 1$ and $r \leq k \leq n - r + 1$.

Suppose now that the time series $\mathbf{a}$ is contaminated and/or has missing values. To reconstruct $\mathbf{a}$, a natural approach is to computing its nearest time series $\mathbf{x}$ by the least squares:

$$\min \sum_{i=1}^{n} w_i |a_i - x_i|^2, \qquad \text{s.t.} \quad \operatorname{rank}(X) \leq r, \quad X = \mathcal{H}(\mathbf{x}), \tag{1.8}$$

where $\mathbf{w} = (w_1, \ldots, w_n) \geq 0$ is the corresponding weight vector emphasizing the importance of each elements of $\mathbf{a}$. The equivalent reformulation of (1.8) as (1.2) is obtained by setting

$$W := \mathcal{H}(\sqrt{\mathbf{v}} \circ \sqrt{\mathbf{w}}) \qquad \text{and} \qquad v_i = \begin{cases} 1/i & \text{for } i = 1, \ldots, k-1 \\ 1/k & \text{for } i = k, \ldots, n-k+1 \\ 1/(n-i+1) & \text{for } i = n-k+2, \ldots, n, \end{cases}$$

where $\mathbf{v}$ is known as the averaging vector of Hankel matrix of size $k \times \ell$ ($k \leq \ell$) and $\sqrt{\mathbf{w}}$

is the elementwise square root of $\mathbf{w}$. We note that the widely studied (1.2) with $W_{ij} \equiv 1$ corresponds to $w_i = 1/v_i$, which is known as the trapezoid weighting. Another popular choice for financial time series is the exponential weights $w_i = \exp(\alpha i)$ for some $\alpha > 0$. We refer to [Gillard and Usevich, 2018, Sect. 2.4] for more comments on the choice of weights.

A special type of the time series of (1.7) arises from the spectral compressed sensing, which has attracted consideration attention lately (Chen and Chi [2014]). In its one dimensional case, a_t is often a superposition of a few complex sinusoids:

$$a_t = \sum_{s=1}^{r} d_s \exp\left\{(2\pi j\omega_s - \tau_s)t\right\}, \tag{1.9}$$

where $j = \sqrt{-1}$, r is the model order, ω_s is the frequency of each sinusoid, and $d_s \neq 0$ is the weight of each sinusoid, and $\tau_s \geq 0$ is a damping factor. We note that (1.9) is a special case of (1.7) with $P_s(t) = d_s$ (hence $\nu_s = 1$) and $\lambda_s = \exp(2\pi j\omega_s - \tau_s)$. If a_t is sampled at all integer values from 1 to n, we get a sample vector $\mathbf{a} \in \mathbb{C}^n$. Consequently, the rank of $\mathcal{H}(\mathbf{a})$ must be r.

However, in practice, only a subset Ω of the sampling points $\{1, \ldots, n\}$ may be observed (possibly contaminated), leading to the question how to best reconstruct $a(t)$ based on its partial observation a_i on Ω. This has led to the Hankel matrix completion/approximation problem of (1.2), see [Chen and Chi, 2014, Sect. II.A] and [Cai et al., 2018, Sect. 2.1]. A popular choice of W in the spectral compressed sensing is $W_{i,j} = 1$ for all (i, j) (uniform weighting), resulting in the distance between X and A in (1.2) being measured by the standard Frobenius norm.

1.3.2 Contributions

The main contribution of this thesis can be summarized as following:

- **Sequential Majorization Minimization:**

  We firstly propose a new approximation scheme via majorization, a technique that has been widely used in dealing with hard optimization problems, to tackle the

Problem (1.2). Rather than approximating the original hard problem, this new scheme yields a sequential approximations which are hoped to provide more and more an accurate approximation each step. Each approximation subproblem of our scheme enjoys the form of SSA and hence it is relatively easy to solve. For example, the latest gradient information was used to construct the new approximation once a new iterate was obtained.

The approximation can be improved through a smaller $(\mathbf{p}, \mathbf{q})$ weight, which can be refined by linear programming (cheap computational cost). The method was guaranteed to converge if the sandwich inequality is satisfied at each iterate.

- **Penalized Method of Alternating Projections:**

  We further propose a new penalty function and develop a penalized method to tackle the Problem (1.2) whose main step is the alternating projections. We call it the penalized MAP (pMAP). We establish the following convergence result of pMAP.

  - The objective function sequence $F(X^\nu, \rho)$ will converge and $\|X^{\nu+1} - X^\nu\|$ converges to 0. Moreover, any limiting point of X^ν is an approximate KKT point of the original problem (1) provided that the penalty parameter is above certain threshold.
  - If X is an accumulation point of the iterate sequence $\{X^\nu\}$, then the whole sequence converges to $\widehat{X}$ at a linear rate provided that $\sigma_r(\widehat{X}) \gg \sigma_{r+1}(\widehat{X})$.

  We will extend these results to the complex case, thanks to a technical result (Prop. 2) that the subdifferential of $g_r(X)$ in complex domain can also be computed in a similar fashion as in the real domain. To our best knowledge, this is the first variant of MAP that can handle general weights and enjoys both global convergence and locally linear convergence rate under a reasonable condition (i.e., $\sigma_r \gg \sigma_{r+1}$)

  We also show this pMAP scheme can be easily extended to handle more rank minimization problems such as robust matrix completion and robust principal component analysis while some of the convergence results still hold.

Thesis work leads to the following academic papers:

- Publication entitled with: *A sequential majorization method for approximating weighted time series of finite rank.* H.D.Qi, J.Shen and N.H.Xiu. Statistics and Its Interface, 2018, 11(4): 615-630.
- Presentation and publication in the proceedings of the conference entitled with: *Daily Crude Oil Price Analysis and Forecasting Based on the Sequential Majorization Method.* J.Shen. Transforming Energy Markets, 41st IAEE International Conference, Jun 10-13, 2018. International Association for Energy Economics, 2018.
- Paper submitted for publication entitled with: *A penalized method of alternating projections for weighted low-rank Hankel matrix optimization.* J.Shen, J.S.Chen, H.D.Qi and N.H.Xiu.

1.4 Organization of the Thesis

The rest of this thesis is organized as following.

In Chapter 2 we will set up our standard notation and some background preliminaries for weighted matrix projection and majorization minimization framework. Recent literatures focused on solving this low rank matrix learning problems will be reviewed and discussed.

Chapter 3 develops the sequential approximation scheme based on the majorization technique, named as SMM for Sequential Majorization Method. We will introduce linear programming to improve our approximation. Two real-life testing problems are conducted to compare our method with some candidate solvers.

Chapter 4 further proposes another new scheme, named as pMAP for Penalized Method of Alternating Projection. We will establish some convergence results for pMAP and also extend this framework to complex-valued cases. Two popular testing problems

(time series denoising and incomplete signal recovery) will be introduced to compare this pMAP method with some state-of-the-art methods. The comparison between SMM and pMAP will be discussed in this chapter.

In Chapter 5, we extend our proposed scheme to deal with a wider rang of low rank matrix learning problems. We will show that our proposed framework in Chapter 4 can be easily extended to tackle other problems such as robust matrix completion and robust principal component analysis. Numerical experiments and results are provided to show the effectiveness of our approaches.

The main results and conclusions will be discussed in Chapter 6.

Chapter 2

Methodology and Literature Review

The WLRH approach has shown its great potential in tackled signal data analysis applications such as incomplete signal recovery and time series forecasting. However, solving this problem directly is not an easy task. WLRH is highly non-convex due to the present of non-convex rank constraint, for which reason there are no efficient and tractable methods to compute the global optimum solution ([Ottaviani et al., 2014]). Following the introductions in Chapter 1, this chapter will provide some preliminaries and also literature reviews on the existing researches to tackle this non-convex problem.

2.1 Preliminaries and Methodology

2.1.1 Notations

In this section we introduce the notation used in this thesis. We use $\mathbb{R}$ to denote real numbers and $\mathbb{C}$ to denote complex numbers. The Euclidean space of dimension n is denoted as $\mathbb{R}^n$. A vector is denoted using bold lower-case letter, e.g., $\mathbf{x}$ while is i-th element in $\mathbf{x}$ is denoted as x_i. A matrix is denoted by capital letters, e.g., X. $X_{i,j}$ stands for its (i,j)-th element. The identity matrix with dimension $n \times n$ is denoted by I_n.

We use $\mathbf{1_{m,n}} \in \mathbb{R}^{m \times n}$ to denote a matrix when all of its entries equal to 1. As already discussed, $\circ$ denotes the Hadamard product, i.e., $(A \circ B)_{i,j} = A_{i,j}B_{i,j}$. The operator diag($\mathbf{x}$) produces a diagonal matrix X with $X_{i,i} = x_i$.

Throughout this thesis several entrywise matrix norms will be discussed. p-norm of a matrix $X \in \mathbb{C}^{m \times n}$ is denoted by $\|X\|_p$, which is calculated as

$$\|X\|_p = (\sum_{i=1}^{m}\sum_{j=1}^{n}|x_{i,j}|^p)^{1/p}.$$

In the case of $p = 2$, we have $\|X\|_2 = \|X\|_F$ is known as Frobenius norm (or Euclidean norm). In this thesis we also use $\|X\|$ to denotes Frobenius norm for the sake of simplicity. In some cases we may use the term "weighted norm", $\|X\|_W$, defined as following:

$$\|X\|_W = \|W \circ X\|_F = (\sum_{i=1}^{m}\sum_{j=1}^{n}|W_{i,j}X_{i,j}|^2)^{1/2}.$$

The ℓ_0-norm is used to denote the number of non-zero elements in a matrix as $\|X\|_0 = \sum_{i,j}\mathcal{I}(X_{i,j})$, where $\mathcal{I}(x)$ is the non-zero indicator, i.e., $\mathcal{I}(x) = 0$ if and only if $x = 0$ and $\mathcal{I}(x) = 1$ if x is not zero.

Let X have singular value decomposition as $X = U\Sigma V^T$ where both $U \in \mathbb{R}^{l \times l}$ and $V \in \mathbb{R}^{k \times k}$ are unitary matrix and $\Sigma \in \mathbb{R}^{l \times k}$ is a diagonal matrix. $\lambda_i(X) = \Sigma_{i,i}$ stands for the i-th singular value of matrix X which is arranged following the non-increasing order with respect to i. We use $\|X\|_*$ to denote the nuclear norm of matrix X, calculated as

$$\|X\|_* = \sum_{i=1}^{min\{l,k\}}\lambda_i(X).$$

For the superscripts used in this report, X^{-1}, X^T, $\overline{X}$ and X^H stands for the inverse, transpose, complex conjugate and conjugate transpose respectively. The operator $\mathcal{H} : \mathbb{C}^{l+k-1} \to \mathbb{C}^{l \times k}$ stands for the mapping operator from a vector to a Hankel matrix. Consider $\mathbf{y} \in \mathbb{C}^t = [y_1, y_2, ..., y_t]^T$ given $t = l + k - 1$, its trajectory Hankel matrix

$Y = \mathcal{H}(\mathbf{y})$ is constructed as

$$Y = \mathcal{H}(\mathbf{y}) := \begin{bmatrix} y_1 & y_2 & y_3 & \cdots & y_l \\ y_2 & y_3 & y_4 & \cdots & y_{l+1} \\ \vdots & \vdots & \vdots & \ddots & \vdots \\ y_k & y_{k+1} & y_{k+2} & \cdots & y_t \end{bmatrix}$$

i.e., $Y_{i,j} = y_{i+j-1}$. The inverse operator of Hankel mapping is denoted by $\mathcal{H}^{-1} : \mathbb{C}^{l\times k} \to \mathbb{C}^{l+k-1}$, standing for the mapping from a Hankel matrix back to a vector, i.e., $\mathcal{H}^{-1}(Y) = \mathbf{y}$.

Finally let us introduce the matrix projection operator which is widely used in this thesis. We use $\Pi_{\mathcal{C}}(Y)$ to denote the optimal solution to the following constrained matrix projection least square problem:

$$\Pi_{\mathcal{C}}(Y) = \arg\min_{X} \|X - Y\| \qquad \text{s.t } X \in \mathcal{C} \tag{2.1}$$

which tried to find the matrix $X \in \mathcal{C}$ such that its distance to Y is minimised under Frobenius norm. Problem (2.1) can be considered as a special case of the following weighted projection problem

$$\min_{X} \|W \circ (X - Y)\| \qquad \text{s.t } X \in \mathcal{C} \tag{2.2}$$

where W is the non-negative weight matrix. We denote the optimal solution to Problem (2.2) as $\Pi_{\mathcal{C}}^{W}(Y)$, which represents the weighted projection of Y on the matrix set $\mathcal{C}$ under weight W.

2.1.2 Background on Weighted Matrix Projection

In this section we will discuss the weighted constrained least square problem with particular focus on rank constrained and Hankel structure constrained least square problem under arbitrary weight.

a. Weighted projection onto Hankel matrix set. Consider the weighted Hankelization problem under Frobenius norm:

$$\min_{X} \|W \circ (X - Y)\| \qquad \text{s.t } X \in \mathcal{H} \tag{2.3}$$

This problem aims to find a Hankel matrix X such that the weighted distance to observed matrix Y can be minimised. Then for any matrix $Y \in \mathbb{R}^{l\times k}$, above problem has closed form solutions denoted as detailed in the following proposition.

Proposition 2.1. *The closed form solution to (2.3) can be computed by the following weighted diagonal averaging.*

$$\Pi^{W}_{\mathcal{H}}(Y)_{i,j} =: \begin{cases} \frac{\sum_{p,q:p+q=i+j} W_{p,q}Y_{p,q}}{\sum_{p,q:p+q=i+j} W_{p,q}} & \text{if } \sum_{p,q:p+q=i+j} W_{p,q} \neq 0 \\ \frac{\sum_{p,q:p+q=i+j} Y_{p,q}}{i+j-1} & \text{if } \sum_{p,q:p+q=i+j} W_{p,q} = 0 \end{cases} \tag{2.4}$$

for $1 \leq i,p \leq l$ *and* $1 \leq j,q \leq k$.

Proof. Because of the Hankel structure constraint on X, it always holds that

$$x_{i,j} = x_{p,q} \text{ if } i+j = p+q, \qquad \forall 1 \leq i,p \leq m \text{ and } 1 \leq j,q \leq n.$$

From the definition of Frobenius norm we have

$$\begin{aligned} \|W \circ (X-Y)\|^2 &= \sum_i \sum_j (W_{i,j}(X_{i,j} - Y_{i,j}))^2 \\ &= \sum_{g=1}^{n+m-1} \sum_{i+j-1=g} (W_{i,j}(X_{i,j} - Y_{i,j}))^2 \end{aligned}$$

Since (2.3) is a quadratic optimization problem, it is minimised when

$$\frac{\partial \|W \circ (X-Y)\|^2}{\partial X_{i,j}} = 0 \text{ and } \frac{\partial^2 \|W \circ (X-Y)\|^2}{\partial^2 X_{i,j}} > 0$$

Consequently we have

$$\begin{aligned}\frac{\partial\|W\circ(X-Y)\|^2}{\partial X_{i,j}} &= \frac{\partial\sum_{p+q=i+j}(W_{p,q}(X_{i,j}-Y_{lp,q}))^2}{\partial X_{i,j}}\\ &= \sum_{p+q=i+j}(W_{p,q}(X_{i,j}-Y_{p,q}))\end{aligned}$$

i. If $W_{l,k}=0$ for all $p+q=i+j$, then Problem (2.3) is independent to $X_{i,j}$ hence is always minimised.

ii. If there exists at least one $W_{p,q}\neq 0$ for all $p+q=i+j$, then the first-order derivative of objective function is 0 only when

$$X_{i,j}=\frac{\sum_{p,q:p+q=i+j}W_{p,q}Y_{p,q}}{\sum_{l,k:p+q=i+j}W_{p,q}}$$

At the same time, we have

$$\begin{aligned}\frac{\partial^2\|W\circ(X-Y)\|^2}{\partial^2 X_{i,j}} &= \frac{\partial\sum_{p+q=i+j}W_{p,q}(X_{i,j}-Y_{p,q})}{\partial X_{i,j}}\\ &= \sum_{p+q=i+j}W_{p,q}\\ &> 0\end{aligned}$$

The last inequality is because the non-negativity of W. This completes our proof. □

b. Weighted projection onto low rank matrix set. Now consider the weighted r-rank nearest matrix approximation problem, formulated as following:

$$\min_X\|W\circ(X-Y)\| \qquad \text{s.t } X\in\mathcal{M}_r \tag{2.5}$$

Before discussing above weighted least square problem, we firstly discuss a special case of W. Let $W=\mathbf{1_{l,k}}$, the projection of Y on $\mathcal{M}_r$ under weight $\mathbf{1_{l,k}}$ can be calculated through the standard singular value decomposition (SVD). Assume $Y\in\mathbb{R}^{l\times k}$ has SVD as

$$Y=U_Y\Sigma(Y)V_Y^T$$

where $U_Y \in \mathbb{R}^{l\times l}$ and $V_Y \in \mathbb{R}^{k\times k}$ are unitary matrices. $\Sigma(Y)$ is a $l \times k$ diagonal matrix, while its $\{i, i\}$-th element correspond to the i-th singular value of Y, denoted as $\sigma_i(Y)$. Note that $\sigma_i(Y)$ is arranged in the non-increasing order with respect to its index i. Given these information, we have the following:

Theorem 2.2. *(Mazeika [2016], Thm 4.21) For any given matrix $Y \in \mathbb{R}^{l\times k}$ which has the singular value decomposition as discussed above, one of its projection onto r-rank matrix set under weight $\mathbf{1}_{\mathbf{L},\mathbf{K}}$, $\Pi_{\mathcal{M}_r}(Y)$, can be computed as*

$$\Pi_{\mathcal{M}_r}(Y) := U_Y \Sigma_r(Y) V_Y^T \tag{2.6}$$

where $\Sigma_r(Y)$ is obtained through

$$\Sigma_r(Y)_i := \begin{cases} \sigma_i(Y) & \text{if } \ i \leq r \\ 0 & \text{otherwise.} \end{cases}$$

When $\sigma_r = 0$ or $\sigma_r \neq \sigma_{r+1}$, Equation (2.6) provides the unique analytical solution to the low rank approximation problem.

However when the weight W is selected arbitrarily, there is no closed form solution for $\Pi^W_{\mathcal{M}_r}(Y)$ unless W has some specific structure. There are some approximation methods to estimate $\Pi^W_{\mathcal{M}_r}(Y)$, for example, Srebro and Jaakkola [2003] proposed an EM-based

method as Alg.1.

Algorithm 1: Algorithm: Two-Stage EM-Based Algorithm for Weighted Low Rank Approximation

initialization $X^0 \to 0$ and the objective rank r. Set $k \to 0$;

Stage 1

while $r - k + 1 \leq k$ **do**

$X^{k+1} = \Pi_{\mathcal{M}_{r-k}}(W \circ Y + (1 - W) \circ X^k)$;

$k = k + 1$

Stage 2

while *Stop condition is not satisfied* **do**

$X^{k+1} = \Pi_{\mathcal{M}_k}(W \circ Y + (1 - W) \circ X^k)$;

$k = k + 1$

output: X^k

However, the iterative approach of Alg.1 will arise heavy computing costs since a partial SVD is performed at each iterate. At the same time, its convergence result significantly depends on the initial guess X^0.

Another approach is to rewrite the objective function to keep the availability of singular value decomposition when calculating the low rank approximations. Zvonarev and Golyandina [2015] introduced a Cadzow(C) scheme by using $\|X - Y\|_C^2 := \|C^{1/2}(X - Y)\|^2$ to approximate the objective function of Problem (1.2), where $C \in \mathbb{R}^{k \times l}$ is a non-negative semidefinite diagonal matrix. Then they proposed to handle Problem (2.7):

$$\begin{aligned} \min \ \|X - Y\|_C^2 := \|C^{1/2}(X - Y)\|^2 = Tr\left((X - Y)C(X - Y)^T\right) \\ \text{s.t.} \ \ X \in \mathcal{M}_r \end{aligned} \tag{2.7}$$

A similar but more generalized scheme is proposed by Gillard and Zhigljavsky [2016] as (Q,R)-norm approach by introducing $\|X - Y\|_{(Q,R)}^2 := \|Q^{1/2}(X - Y)R^{1/2}\|^2$ to approximate $\|W \circ (X - Y)\|^2$ as

$$\|X - Y\|_{(Q,R)}^2 := \|Q^{1/2}(X - Y)R^{1/2}\|^2 \approx \|W \circ (X - Y)\|^2$$

where $Q \in \mathbb{R}^{l\times l}$ and $R \in \mathbb{R}^{k\times k}$ are diagonal matrices with positive diagonal elements. Then the estimated low rank matrix is obtained through solving the following problem instead of solving the original Problem (2.5):

$$\begin{aligned} \min \ \|X-Y\|^2_{(Q,R)} &:= \|Q^{1/2}(X-Y)R^{1/2}\|^2 = \mathrm{Tr}\Big(Q(X-Y)R(X-Y)^T\Big) \\ \text{s.t.} \ \ X &\in \mathcal{M}_r \end{aligned} \tag{2.8}$$

Now we generally illustrate how to solve (2.8).

Proposition 2.3. *[Gillard and Zhigljavsky, 2016, Theorem 2] Assume Y has the singular value decompositions as $Y = U_Y\Sigma(Y)V_Y$, its low rank approximation under (Q,R)-norm is calculated as*

$$\hat{X} = \Pi^{Q,R}_{\mathcal{M}_r}(Y) := \hat{U}\hat{\Sigma}^{(r)}\hat{V}^T \tag{2.9}$$

where $\hat{U} = (Q^{-1/2})\widetilde{U}$, $\hat{V} = (R^{-1/2})\widetilde{V}$ and $\hat{\Sigma}^{(r)} = \widetilde{\Sigma}^{(r)}$, while $\widetilde{U},\widetilde{V}$ and $\widetilde{\Sigma}^{(r)}$ comes from the singular value decomposition $Q^{1/2}YR^{1/2} = \widetilde{U}\widetilde{\Sigma}\widetilde{V}$. $\widetilde{\Sigma}^{(r)}$ is obtained from $\widetilde{\Sigma}$ by replacing σ_i by 0 for $i = (r+1),...,\min\{l,k\}$.

Problem (2.7) can be also solved through Prop.2.3, since it can be considered as a special case of (2.8) by taking $Q = \mathbf{1}_{\mathbf{L},\mathbf{K}}$ and $R = C$. One should note that although Prop.2.3 introduced a closed form solution to the low rank matrix projection problem under (Q,R)-norm, both of the two problems discussed above are not equivalent to the original problem because the objective function in (2.7) and (2.8) are just the approximations to the original weighted norm in most cases when W is selected arbitrarily, apart from some specific classes of W as mentioned in Gillard and Zhigljavsky [2016]. Hence, the solutions obtained through Prop.2.3 may be far away from the optimal solutions to the original WLRH problem depending on the $\{Q,R\}$ approximation quality.

2.1.3 Majorization Minimization Method

In many optimization problems, the objective function $f(x)$ is difficult to tackle directly, e.g., the objective function is not convex or not smooth. In that case, the majorization

minimization (MM) method provide a scheme to minimizing a majorization surrogate function iteratively while keep the objective functional value non-increasing. This technique has been widely used in dealing with hard optimization problems such as missing data filling [Simon and Abell, 2010], low-rank correlation matrix problem [Sun, 2010], low rank matrix decomposition [Hu et al., 2012], convex semidefinite programming [Jiang et al., 2012], the Euclidean distance matrix problem with low-embedding dimensions [Qi and Yuan, 2014] and large scaled machine learning [Mairal, 2015]. Some applications and examples of surrogate functions in recent research have been well summarized in Sun et al. [2017].

Consider the constrained optimization problem

$$\begin{aligned} &\arg\min f(X) \\ &s.t. X \in \mathcal{C} \end{aligned}$$

where $\mathcal{C} \subset \mathcal{M}$. Let us firstly define the surrogate majorization function for $f(X)$:

Definition 2.4. Given the function $f(X)$, $f(X, Z)$ is called as the surrogate majorization function of $f(X)$ when the following two conditions are satisfied:

$$f(X, Z) \geq f(X) \tag{2.10}$$

$$f(X, X) = f(X) \tag{2.11}$$

For all $X, Z \in \mathcal{M}$.

As a common practice, the majorization minimization method aims to iteratively minimize the surrogate function instead of minimising the original objective function $f(X)$ directly. At step ν, the current iterate X^ν is often used to construct the objective function at the next iterate as $X^{\nu+1} = \arg\min f(X, X^\nu)$. The implementation procedure of

majorization minimization method can be seen as Alg.2.

Algorithm 2: Algorithm: Majorization Minimization Method

initialization $X^0, \nu \to 0$;

while *Stop condition is not satisfied* **do**

$X^{\nu+1} = \arg\min_X f(X, X^\nu) \;\; s.t. X^{\nu+1} \in \mathcal{C}$;

$\nu = \nu + 1$

output: X^ν

Clearly at each iterate this method will 1) minimise the current surrogate function and then 2) construct the next surrogate function using the current iteration point. Then we have the following convergence result.

Theorem 2.5. *Let X^ν be the sequence generated by Alg.2. Then the following inequality chain holds.*

$$f(X^{\nu+1}) \leq f(X^{\nu+1}, X^\nu) \leq f(X^\nu, X^\nu) \leq f(X^\nu) \tag{2.12}$$

This inequality chain is known as sandwich inequality. This inequality chain guarantees that the cost function $f(X^\nu)$ monotonically decreases after each iteration when solving hard optimization problems. Proof of above sandwich inequality is quite straightforward.

Proof. Let X^ν be the sequence generated by Alg.2. Then the following inequality chain holds, then proof for Theorem.2.5 can be established by the following facts:

- $f(X^{\nu+1}) \leq f(X^{\nu+1}, X^\nu)$ comes from the definition of surrogate majorization function as Equation (2.10).
- $f(X^{\nu+1}, X^\nu) \leq f(X^\nu, X^\nu)$ holds because $X^{\nu+1} \in \mathcal{C}$ is one of the solution that minimise $f(X, X^\nu)$ at the current iterate.
- $f(X^\nu, X^\nu) \leq f(X^\nu)$ also comes from the definition of surrogate majorization function as Equation (2.11).

With all three above facts holds, the Theorem.2.5 holds as a result. □

Remarks

(R.1) One can find that it is not necessary to solve the sub-problem at each iterate of MM algorithm to guarantee inequalities chain (2.12), since in many cases the sub-problem $f(X, X^\nu)$ is still hard to minimise. To establish the sandwich inequality, we just need to ensure that the $f(X^{\nu+1}, X^\nu) \leq f(X^\nu, X^\nu)$ holds at each iterate.

(R.2) Majorization minimization technique can only guarantee the non-increasing of objective function value sequence, and also ensure the convergence to a limit if the objective function is bounded below. However, it is not proved whether the sequence $\{f(X^\nu)\}$ can converge to a local minima or even a stationary point without any other assumptions. Here we further introduce a convergence result for MM algorithm given some assumptions:

Proposition 2.6 (Sun et al. [2017]). *Assume the constraint set $\mathcal{C}$ is convex and the objective function $f(X)$ continuously differentiable. Let function $M(x)$ denote the projection operator in each iterate, i.e., $X^{\nu+1} = M(X^\nu)$. The stationary point is defined as*

$$\mathcal{C}^* = \{X | \partial f(X)^T (Y - X) \geq 0, \forall Y \in \mathcal{C}\}$$

We further make the following three assumptions:

1. *The sublevel set $lev_{\leq f(X_0)} f := \{X \in \mathcal{C} | f(X) \leq f(X_0)\}$ is compact given that $f(X_0) < +\infty$;*
2. *$f(X, X^\nu)$ is also continuously differentiable with respect to X;*
3. *$f(X, X^\nu)$ is continuous in X and X^ν.*

Then we have the following results:

1. *Any limit point X_∞ of $\{X^\nu\}_{\nu \in N}$ is a stationary point of f;*
2. *$f(X^\nu) \downarrow f^*$ monotonically and $f^* = f(X^*)$ with $X^* \in \mathcal{C}^*$;*
3. *If $f(M(X)) = f(X)$, then $X \in \mathcal{C}^*$ and $X \in \arg\min f(Z, X)$;*
4. *If X is a fixed point of M, then X is a convergent point of MM and belongs to $\mathcal{C}^*$*

(R.3) Although MM majorization provides a framework to deal with some hard optimization problems, however, it is not easy to find a suitable surrogate majorization function in real practice. On the one hand, the solution quality might be better when the shape of surrogate majorization function is closer to the original objective function. But at the same time, the surrogate function $f(X, X^\nu)$ should be easily minimised so that we can compute the sub-problem efficiently at each iterate of MM. As a result, this surrogate function should has several features including separability in variables, convexity, smoothness and the existence of a closed form minimizers [Sun et al., 2017]. Here we provide some widely used approach for majorization function constructing:

- First Order Taylor Expansion.

  The first order Taylor expansion is widely used in many researches. Consider a differentiable concave function $f(.)$, then we have the following inequality

  $$f(x) \leq f(x_t) + \partial f(x_t)^T (x - x_t)$$

  Then $f(x_t) + \partial f(x_t)^T (x - x_t)$ will be a natural majorization surrogate function of $f(x)$. For example, Sun [2010] proposed a penalization function as

  $$p(X) := \langle I, X \rangle - \sum_{i=1}^{r} \lambda_i(X), \quad \forall X \in \mathcal{S}^n$$

  where $\lambda_1 \geq \lambda_2 \geq .. \geq \lambda_n$ are the eigenvalues of X and $\mathcal{S}^n$ stands for the space of $n \times n$ symmetric matrix. Since $p(X)$ is concave, we have

  $$p(X) \leq p(X^\nu) + \langle U^\nu, X - X^\nu \rangle, \quad \forall U^\nu \in \partial p(X^\nu)$$

  Finally we can define the majorization of $p(X)$ as $m_k^p(X, X^\nu) = p(X^\nu) + \langle U^\nu, X - X^\nu \rangle$.

- Second Order Taylor Expansion.

Let $f(x)$ be a smooth convex function with Lipschitz continuous gradient, then there exists a self-adjoint and positive semi-definite linear operators $\sum_f$, such that:

$$f(x) \leq f(x^\nu) + \langle x - x^\nu, \partial f(x^\nu) \rangle + \frac{1}{2}\|x - x^\nu\|^2_{\sum_f}$$

One example of using second order Taylor expansion is the research by Jiang et al. [2012], which aims to solve the generated minimization problem

$$\min\{F(x) := f(x) + g(x) : x \in \mathcal{X}\}$$

where both $f(x)$ and $g(x)$ are proper, lower semi-continuous convex functions (possibly nonsmooth). Assume $dom(g)$ is closed and f is continuously differentiable on $\mathcal{X}$, and its gradient is s Lipschitz continuous with modulus L on $\mathcal{X}$, defined as

$$\|\partial f(x) - \partial f(y)\| \leq L\|x - y\|, \quad \forall x, y \in \mathcal{X}$$

Then the majorization surrogate function of $f(x)$ is defined as:

$$F^p(x) := f(x^\nu) + \langle \partial f(x), x - x^\nu \rangle + \frac{1}{2}\langle x - x^\nu, \mathcal{H}^\nu(x - x^\nu) \rangle + g(x)$$

where $\mathcal{H}^\nu$ is a self-adjoint positive definite linear operator that is chosen by the user.

- Other Inequalities

  There are also some other inequalities used in recent researches for constructing the majorization surrogate function. One example is proposed by Lin et al. [2017], where the triangular inequality of norms and Cauchy-Schwartz inequality are combined together when tackling the following problem:

$$\min H_k(\Delta U, \Delta V) := \|W \circ (M - (U^\nu + \Delta U)(V^\nu + \Delta V)^T)\|_1$$

$$+ \frac{\lambda}{2}\|U^\nu + \Delta U\|^2_F + \frac{\lambda}{2}\|V^\nu + \Delta V\|^2_F$$

Using triangular inequality of norms, we have

$$H^{\nu}(\Delta U, \Delta V) \leq \|W \circ (M - U^{\nu}()V^{\nu})^T - \Delta U(V^{\nu})^T - U^{\nu}\Delta V^T)\|_1$$

$$+\|W \circ (\Delta U \Delta V^T)\| + \frac{\lambda}{2}\|U^{\nu} + \Delta U\|_F^2 + \frac{\lambda}{2}\|V^{\nu} + \Delta V\|_F^2$$

Using Cauchy-Schwartz Inequality, we further have

$$\|W \circ (\Delta U \Delta V^T)\| \leq \frac{\lambda}{2}\|\mathcal{A}_u \Delta U\|_F^2 + \frac{\lambda}{2}\|\mathcal{A}_v \Delta V\|_F^2$$

where $\mathcal{A}_u = \sqrt{W_{(i,)} + \epsilon}$ and $\mathcal{A}_v = \sqrt{W_{(,j)} + \epsilon}$. So finally we have

$$H^{\nu}(\Delta U, \Delta V) \leq \|W \circ (M - U^{\nu}(V^{\nu})^T - \Delta U(V^{\nu})^T - U^{\nu}\Delta V^T)\|_1$$

$$+\frac{\lambda}{2}\|\mathcal{A}_u \Delta U\|_F^2 + \frac{\lambda}{2}\|\mathcal{A}_v \Delta V\|_F^2 + \frac{\lambda}{2}\|U^{\nu} + \Delta U\|_F^2$$

$$+\frac{\lambda}{2}\|V^{\nu} + \Delta V\|_F^2$$

2.2 Literature Review

2.2.1 Convex Relaxation

Many state-of-the-art methods have been proposed to deal with the non-convexity of structured low rank matrix approximation problems. One popular and successful approach to tackle optimization problem with nonconvex objective function is to employ the convex envelopes and relax this problem into a convex optimization one. We refer the definition of convex envelope demonstrated in Recht et al. [2010] as

Definition 2.7. [Recht et al., 2010, Chp. 2] Let $\mathcal{C}$ denote a convex set and a function $f : \mathcal{C} \to R$ which may be non-convex. Its convex envelope function g is defined as the largest convex function such that $g(X) \leq f(X)$ for all $X \in \mathcal{C}$.

The optimal solution to minimise the convex envelope function over a set of constraints can be seen as an approximation of original problem. It is also proved that the nuclear norm is the convex envelope of rank(X).

Theorem 2.8. *[Recht et al., 2010, Theo.2.2] The convex envelope of rank(X) on the set $X \in \mathbb{R}^{l\times k} : \|X\| \leq 1$ is the nuclear norm $\|X\|_*$.*

where nuclear norm of a given matrix is defined as the sum of all its singular values. This approach has been successfully implemented in many existing structured low rank matrix learning researches such as active subspace selection [Hsieh and Olsen, 2014], robust principle component analysis [Chandrasekaran et al., 2011], matrix completion [Candès and Recht, 2009], generalized low rank matrix learning [Jawanpuria and Mishra, 2018], and also for WLRH (e.g., see [Tang et al., 2013, Usevich and Comon, 2016]). Applying convex relaxation, one may solve the following penalised problem:

$$\begin{aligned} \min \ \ & f(X) := \frac{1}{2}\|W \circ (X - Y)\|^2 + \rho\|X\|_* \\ \text{s.t.} \ \ & X \in \mathcal{H} \end{aligned} \tag{2.13}$$

Here ρ is the penalty parameter that balance the weighted least square item and the nuclear norm item. Fazel [2003] proposed that Problem (2.13) can be recast into the following trace minimization problem:

$$\begin{aligned} \min \ & \frac{1}{2}\|W \circ (X - Y)\|^2 + \rho(Tr(Y) + Tr(Z)) \\ \text{s.t.} \ \ & X \in \mathcal{H} \\ & \begin{bmatrix} Y & X \\ X^T & Z \end{bmatrix} \geq 0 \end{aligned} \tag{2.14}$$

where both $Y \in \mathbb{R}^{l\times l}$ and $Z \in \mathbb{R}^{k\times k}$ are symmetric matrices. (2.14) is a convex optimization problem with respect to three variables X, Y and Z, hence can be solved efficiently by some off-the-shelf semi-definite programming solvers such as SDPT3 (Toh et al. [1999] and Chen and Chi [2014]), interior-point method [Liu and Vandenberghe,

2009] or CVX toolbox ([Grant et al., 2008] and Butcher and Gillard [2017]), to name just a few.

However, one issue caused by convex semi-definite program optimization is the high computational complexity, especially when the dimension of input data matrix is large [Netrapalli et al., 2014]. Another drawback of nuclear norm minimization method is the output estimated matrix may not be strictly low rank.

2.2.2 Matrix Factorization

The second approach introduced to tackle the WLRH problem is matrix factorization, e.g., assuming $X = UV^T$ where $U \in \mathbb{R}^{l\times r}$ and $V \in \mathbb{R}^{r\times k}$. Then one can optimize the cost function over two matrix variables U and V. This approach is introduced in many studies related to low rank matrix learning, such as matrix completion [Wen et al., 2012], deep neural network training [Sainath et al., 2013] and matrix separation [Shen et al., 2014]. Chi et al. [2018] provided a comprehensive study in using matrix factorization solving low rank optimization problem. The global optimality of generalized low rank matrix optimization problems using matrix factorization approach is been discussed by Zhu et al. [2018], provided that some iterative matrix factorization optimization algorithms can lead to the global convergence if the objective function satisfies some assumptions.

Similarly, there exists studies that implement this matrix factorization approach in solving WLRH problem. For example, Ishteva et al. [2014] approximated low rank matrix as a product of two factors with reduced dimension and also introduced the penalty method in the objective function to convert the original problem into a unconstrained optimization problem. Based on the structure property of Hankel matrix, Ying et al. [2018] further extended this scheme to solve a specific incomplete exponential signal recovery problem. Considering for any matrix $A \in \mathcal{M}$, its nuclear norm can be computed through

$$\|A\|_* = \min_{U\in\mathbb{R}^{L\times r}, V\in\mathbb{R}^{K\times r}} \frac{1}{2}(\|U\|_F^2 + \|V\|_F^2) \qquad s.t.\ A = UV^T$$

As a result, the WLRH problem can be reformulated in the following way:

$$\min_{U\in\mathbb{R}^{L\times r},V\in\mathbb{R}^{K\times r},X\in\mathcal{H}} f(X) := \frac{1}{2}\|W\circ(X-Y)\|^2 + \frac{\lambda}{2}(\|U\|_F^2+\|V\|_F^2) \quad \text{s.t. } UV^T = X \tag{2.15}$$

It worth noting that Problem (2.15) is still non-convex because of the bilinear nature of the parametrizations, so there are still challenges to tackle this problem. A popular approach is to introduce the alternating directions method of multiples (ADMM) framework. The augmented Lagrangian of (2.15) is

$$\begin{aligned}\mathcal{L}(X,U,V,D) := &\frac{1}{2}\|W\circ(X-Y)\|^2 + \frac{\lambda}{2}(\|U\|_F^2+\|V\|_F^2) + \langle D, X-UV^T\rangle \\ &+ \frac{\beta}{2}\|X-UV^T\|_F^2\end{aligned} \tag{2.16}$$

where $D\in\mathcal{M}$ is the dual variable. The implementation of ADMM to solve (2.16) is proposed in the following Alg.3

The convergence property of ADMM is well studied in many researches when the optimization is convex. However in this case, the objective function is non-convex due to the product of two variables. So the convergence results of ADMM can not be extended to Alg.3, although it works fine in the numerical experiments.

Algorithm 3: Algorithm: Matrix Factorization via ADMM approach

Result: Approximated low rank matrix $\hat{X}$

Initialization: Given time series $\mathbf{x}\in\mathbb{R}^n$ and the weight vector $\mathbf{w}\in\mathbb{R}^n$. Choose the window length l. Compute $Y := \mathcal{H}(\mathbf{x})$ and matrix W by weight vector $\mathbf{w}$. Start with $X^0 = Y$ and set $\nu := 0$;

while *certain stopping criterion is not met* **do**

- Solve $X^{\nu+1} = \arg\min_{X\in\mathcal{H}} \mathcal{L}(X, U^\nu, V^\nu, D^\nu)$;
- Solve $U^{\nu+1} = \arg\min_{U} \mathcal{L}(X^{\nu+1}, U, V^\nu, D^\nu)$;
- Solve $V^{\nu+1} = \arg\min_{V} \mathcal{L}(X^{\nu+1}, U^\nu, V, D^\nu)$;
- Solve $D^{\nu+1} = D^\nu + (X^{\nu+1} - U^{\nu+1}(V^{\nu+1})^T)$;
- $\nu = \nu + 1$;

2.2.3 Alternating Projection Based Methods

Finally we discuss the alternating projection (AP) technique, which has many successful implementations such as matrix completion [Jain et al., 2013], tensor decompositions [Huang et al., 2015] and robust principle analysis [Netrapalli et al., 2014]. The motivation of using the alternating projection technique is the fact that the analytical solution exists for both of the low rank least square problem and some structure constrained least square problems [Eckart and Young, 1936, Golyandina and Korobeynikov, 2014]. As a result, this approach enjoys low computation cost and thus has the potential to deal with large scale optimization problems comparing with convex relaxation or matrix factorization. This approach has been introduced to solve unweighted low rank Hankel matrix approximation problem (e.g., Condat and Hirabayashi [2015]), and its performance has been tested in several empirical studies [e.g. Zabalza et al., 2015a, Xu et al., 2018, Shukla and Yadav, 2017]. Here we summarized the methods of alternating projection in Alg.4.

Algorithm 4: Algorithm: Alternating Projection Method(AP)

Result: Approximated low rank matrix $\hat{X}$

Initialization: Given time series $\mathbf{x} \in \mathbb{R}^n$ and the weight matrix W. Choose the window length L. Compute $Y := \mathcal{T}(\mathbf{x})$. Start with $X^0 = Y$ and set $\nu := 0$;

while *certain stopping criterion is not met* **do**

Compute the weighted projection on r-rank matrix set

$$\widehat{X^\nu} := \Pi^W_{\mathcal{M}_r}(X^\nu)$$

Compute the weighted projection on Hankel matrix set

$$X^{\nu+1} = \Pi^W_{\mathcal{H}}(\widehat{X^\nu})$$

$\nu = \nu + 1$;

The convergence behaviour of alternating minimization method has been well established when both subset are convex. If two convex sets have intersections, then the alternating projection method will converge to a point in the intersection sets. If the intersection

is empty between two convex sets, the sequence will converge to the periodic iteration between two points where the distance between two points are the minimal distance between two sets [Fazel, 2003]. However, it would be a challenge to build similar results when non-convex subset exists. For the basically alternating projection (Alg.4), we have the following property:

Theorem 2.9. *[Zvonarev and Golyandina, 2015, Theorem 1]*

Let the sequence X^ν generated by the Alg.4. Then we have

$$\|X^\nu - \widehat{X^\nu}\| \to 0 \quad \textit{and} \quad \|X^{\nu+1} - \widehat{X^\nu}\| \to 0, \qquad \textit{as} \quad \nu \to 0.$$

Also, there exists a convergent subsequence of points such that its limits X^* belongs to $\mathcal{M} \cap \mathcal{H}$.

Although this AP method provide a framework which is easy to implement and has some convergence property, we have several question to tackle when employing it to tackle the WLRH problems:

- Theorem 2.9 demonstrates that alternating projection between Hankel matrix and low rank matrix set will converge to a point that belong to the intersections of two sets. However, there is no theoretical guarantee that whether this point is a global or local optimal point, or even just a stationary point to the original problem.
- When more generalised norm is used in the objective function rather than the Frobenius norm, such as in Problem (1.2), the low rank approximation operator has no closed form solution as we already discussed in Chapter 1. In fact it doesn't exist an efficient and provable solver for weighted low rank approximation problem. In this case, it is not easy to implement Alg.4 unless some approximation approaches are used [Gillard and Zhigljavsky, 2016].
- As a result of the second point, the Theorem 2.9 may not hold any more in tackling WLRH because it requires both projection to be exactly orthogonal at each iteration.

Another most recent and powerful solver was proposed by Cai et al. [2019], known as fast iterative hard thresholding (FIHT). This solver is enhanced by subspace of r-rank matrix manifold optimization techniques as demonstrated in Alg.5

FIHT admits a computational complexity of $O(r^3)$ which is much smaller than the SVD based AP methods. It also guarantees the exact recovery of incomplete signal with probability once there are enough observations. However, there are two drawbacks for FIHT. One is that FHIT may fail to converge (an example can be seen in [Ying et al., 2018, Fig.3]) if some assumption are not satisfied. At the same time, it does not allow arbitrary weight matrix choice.

Algorithm 5: Algorithm: Fast Iterative Hard Thresholding(FIHT)

Result: Approximated low rank matrix $\hat{X}$

Initialization: X^0 and set $x^0 = \mathcal{H}^{-1}(X^0)$. p is the percentage of known values in a signal.

Set $\nu := 0$;

while *certain stopping criterion is not met* **do**

1. $g^\nu = \Pi_\Omega(x - x^\nu)$;
2. $W^\nu = \Pi_{\mathcal{S}^\nu}\mathcal{H}(x^\nu + p^{-1}g^\nu)$;
3. $X^{\nu+1} = \Pi_{\mathcal{M}_r}(W^\nu)$;
4. $x^{\nu+1} = \mathcal{H}^{-1}X^{\nu+1}$;
5. $\nu \to \nu + 1$

Operator Π_Ω and $\Pi_{\mathcal{S}^\nu}$ in Alg.5 are defined in [Cai et al., 2019, Equation (3) and Equation (7)], denote projection to signal completion and subspace respectively.

To tackle this NP-hard problem, many other methods are proposed in latest researches, for example, variable projection method [Usevich and Markovsky, 2014], alternating direction method of multipliers [Ying et al., 2018], fast iterative hard thresholding [Cai et al., 2019], projected gradient descent [Cai et al., 2018] and Gauss-Newton method [Zvonarev and Golyandina, 2018]. Although there are still some issues to be tackled such as optimality and convergence results, all these works inspired us to employ non-convex techniques for WLRH problem.

Chapter 3

A Sequential Majorization Method

In Chapter 1 we have reviewed the weighted Hankel structured low rank problems and their applications. Existing algorithms are discussed in the second chapter including both advantages and drawbacks. Our purpose of this study is to investigate reliable algorithms which can tackle the weighted Hankel structured low rank problem (1.2). Two guiding principles for developing such an approach are (i) the Hankel matrix optimization should be computationally tractable, and (ii) the objective in the optimization should be a close approximation to the original weighted least-squares.

In this chapter we tackle this non-convex optimization problem via a sequential majorization approach. Rather than approximating the hard problem (1.2) once like done in [Gillard and Zhigljavsky, 2016, Zvonarev and Golyandina, 2015], the new scheme yields a sequential approximation, which are hoped to provide more and more accurate approximation each step. Each approximation subproblem of our scheme enjoys the form of (2.8) and hence it is relatively easier to solve.

This chapter is arranged as following. In Section 3.1 we will firstly discuss the approach of sequential majorization minimization method to solve the weighted low rank Hankel matrix optimization problem and the main solver. Then in Section 3.2 we will further

introduce some techniques to improve the performance of the weighted norm approximation. Numerical results will be shown in Section 3.3 where we conduct several real-life time series analysis and forecasting problems to compare the performance of our proposed solver with some state-of-the-art solvers. Conclusions can be found in Section 3.4.

3.1 Sequential Majorization Method

In this section, we will describe our new approximation scheme and draw connections whenever possible to that studied in [Zvonarev and Golyandina, 2015, Gillard and Zhigljavsky, 2016], which also handle arbitrarily given weights in (1.2).

3.1.1 Framework of Sequential Majorization Method

For a given weight vector $\mathbf{w} \in \mathbb{R}^N$ with $w_t \geq 0$, denote $\sqrt{\mathbf{w}} = (\sqrt{w_1}, \sqrt{w_2}, .., \sqrt{w_N})$. We also define vector $\mathbf{v} \in \mathbb{R}^N$ by

$$v_t := \begin{cases} 1/t & \text{for } t = 1, \ldots, l-1 \\ 1/l & \text{for } t = l, \ldots, k \\ 1/(N-t+1) & \text{for } t = k+1, \ldots, N. \end{cases}$$

where $N = l + k - 1$. The Hadamard product between two matrices of same size is defined similarly. Let

$$W := \mathcal{H}(\sqrt{\mathbf{v}} \circ \sqrt{\mathbf{w}}). \tag{3.1}$$

Recall the WLRH problem we aims to solve is

$$\min \ f(X) := \frac{1}{2}\|W \circ (X - Y)\|^2, \qquad \text{s.t.} \ \ X \in \mathcal{H} \cap \mathcal{M}_r. \tag{3.2}$$

The first step is to propose a suitable surrogate function for $f(X)$. Define the new function $f_m(X, Z)$ as

$$f_m(X,Z) := f(Z)+\langle \nabla f(Z),\ X-Z\rangle+\frac{1}{2}\|(\sqrt{\mathbf{p}}\sqrt{\mathbf{q}}^T)\circ(X-Z)\|^2, \qquad \forall\ Z, X \in \mathcal{M}. \tag{3.3}$$

where we choose $\mathbf{p}$ and $\mathbf{q}$ such that

$$\|W \circ X\| \leq \|(\sqrt{\mathbf{p}}\sqrt{\mathbf{q}}^T) \circ X\| \qquad \text{for all}\ \ X \in \mathcal{M}. \tag{3.4}$$

We have the following properties

Proposition 3.1. *It holds that*

$$f_m(X, X) = f(X) \qquad \forall\ X \in \mathcal{M} \tag{3.5}$$

and

$$f(X) \leq f_m(X, Z) \qquad \forall\ X, Z \in \mathcal{M}. \tag{3.6}$$

Moreover, we have for any given $Z \in \mathcal{M}$

$$\arg\min_{X\in\mathcal{M}}\ f_m(X, Z) = \arg\min_{X\in\mathcal{M}}\ \frac{1}{2}\|P(X - \Delta_Z)Q\|^2, \tag{3.7}$$

where $P := diag(\sqrt{\mathbf{p}})$ and $Q := diag(\sqrt{\mathbf{q}})$, and the matrix $\Delta_Z \in \mathcal{M}$ is given by

$$\Delta_Z := Z - P^{-2}(W \circ W \circ (Z - Y))Q^{-2}. \tag{3.8}$$

Proof.

$$\begin{aligned} f_m(X, X) &= f(X) + \langle \nabla f(X),\ X - X\rangle + \frac{1}{2}\|(\sqrt{\mathbf{p}}\sqrt{\mathbf{q}}^T) \circ (X - X)\|^2 \\ &= f(X) \end{aligned}$$

The equality (3.5) holds. As for the inequality (3.6), we have

$$\begin{aligned} f_m(X,Z) &= f(Z) + \langle \nabla f(Z),\ X - Z\rangle + \frac{1}{2}\|W \circ (X-Z)\|^2 \\ &\quad + \underbrace{\frac{1}{2}\|(\sqrt{\mathbf{p}}\sqrt{\mathbf{q}}^T) \circ (X-Z)\|^2 - \frac{1}{2}\|W \circ (X-Z)\|^2}_{\geq 0 \ \text{ because of (3.4)}} \\ &\geq f(Z) + \langle \nabla f(Z),\ X - Z\rangle + \frac{1}{2}\|W \circ (X-Z)\|^2 \\ &= f(X). \end{aligned}$$

The last equality holds because $f(\cdot)$ is quadratic and its second order Taylor expansion is exact.

We now prove (3.7). We note that

$$\|(\sqrt{\mathbf{p}}\sqrt{\mathbf{q}}^T) \circ X\| = \|PXQ\|, \qquad \forall\ X \in \mathcal{M},$$

Using this observation, we have

$$\begin{aligned} \arg\min\ f_m(X,Z) &= \arg\min\ \langle \nabla f(Z),\ X - Z\rangle + \frac{1}{2}\|(\sqrt{\mathbf{p}}\sqrt{\mathbf{q}}^T) \circ (X-Z)\|^2 \\ &= \arg\min \langle W \circ W \circ (Z-Y),\ X - Z\rangle + \frac{1}{2}\|P(X-Z)Q\|^2 \\ &= \arg\min\ \frac{1}{2}\|P(X-Z)Q + P^{-1}(W \circ W \circ (Z-Y))Q^{-1}\|^2 \\ &= \arg\min\ \frac{1}{2}\left\| P\Big(X - \underbrace{[Z - P^{-2}(W \circ W \circ (Z-Y))Q^{-2}]}_{=:\Delta_Z}\Big)Q \right\|^2 \\ &= \arg\min \frac{1}{2}\|P(X-\Delta_Z)Q\|^2. \end{aligned}$$

This proved the claim in (3.7). □

Because of the properties in Proposition 3.1, $f_m(Z,X)$ is known as a majorization of $f(X)$. This new function provides a rather accurate (local) approximation of $f(\cdot)$ at any given point X. The computational implication is that we may minimize this new function instead of the original function provided that the new function is easier to

minimize. This approximation procedure can be repeated until convergence is observed. We formally state this computational procedure below.

Let X^ν be the current iterate. We try to find the next iterate by

$$X^{\nu+1} \in \arg\min \ f_m(X, X^\nu), \qquad \text{s.t.} \ \ X \in \mathcal{H} \cap \mathcal{M}_r. \tag{3.9}$$

We note that the problem may have multiple solutions. Suppose $X^\nu \in \mathcal{H} \cap \mathcal{M}_r$. We immediately have

$$f(X^{\nu+1}) \leq f_m(X^{\nu+1}, X^\nu) \leq f_m(X^\nu, X^\nu) = f(X^\nu), \tag{3.10}$$

where the first inequality follows from (3.6); the second inequality is because of (3.9); and the last equality follows from (3.5). This means that the majorization procedure generates a sequence $\{X^\nu\}$ with decreasing objective function values in the original function $f(X)$. The inequality in (3.10) is known as the Sandwich inequality in using the majorization technique [De Leeuw, 1993].

It is difficult to obtain the optimal solution for the optimization problem (3.9) because it is nonconvex. Fortunately, it is enough to just compute a point $X^{\nu+1}$ such that

$$f_m(X^{\nu+1}, X^\nu) \leq f_m(X^\nu, X^\nu). \tag{3.11}$$

As long as this condition holds, the sandwich inequality will hold and the functional value sequence $\{f(X^\nu)\}$ will be nonincreasing. This property provides a justification for using the method of SSA or the Cadzow method, which do not enforce the constraint be strictly satisfied.

3.1.2 Relationship with Previous Research

In fact problem (2.7) and (2.8) that we mentioned before are also included in our approximation. Our approximation is equivalent to problems when choosing $M = E$ (the matrix of all ones) and $\mathbf{p} = \mathbf{1} \in \mathbb{R}^l$, $\mathbf{q} = \mathbf{1} \in \mathbb{R}^k$. This immediately suggests that we

may use the diagonally weighted version of the SSA method or Cadzow's method to solve the subproblem (3.12) . Moreover, if we choose $W = \mathbf{p}\mathbf{q}^T$, then the subproblem (3.12) reduces to

$$\min \ \frac{1}{2}\|P(X-Y)Q\|^2, \qquad \text{s.t.} \ \ X \in \mathcal{H} \cap \mathcal{M}_r,$$

which is exactly the approximation problem of (2.8) considered by Gillard and Zhigljavsky [2016].

At the same time, our subproblem (3.9) is the type of (Q, R)-norm problem (2.8) studied by Gillard and Zhigljavsky [2016]. It follows from (3.7) that the optimization problem (3.9) is equivalent to

$$\min f^{\nu}(X) := \frac{1}{2}\|P(X-\Delta^{\nu})Q\|^2, \qquad \text{s.t.} \ \ X \in \mathcal{H} \cap \mathcal{M}_r, \tag{3.12}$$

where Δ^{ν} is obtained from (3.8) by replacing Z by X^{ν}:

$$\Delta^{\nu} := X^{\nu} - P^{-2}(W \circ W \circ (X^{\nu} - Y))Q^{-2}.$$

We further note that

$$\begin{aligned} \|P(X-\Delta^{\nu})Q\|^2 &= \mathrm{Tr}\Big(P(X-\Delta^{\nu})QQ(X_{\Delta}^{\nu})^T P\Big) \\ &= \mathrm{Tr}\Big(P^2(X-\Delta^{\nu})Q^2(X-\Delta^{\nu})^T\Big) \\ &= \|X-\Delta^{\nu}\|^2_{(P^2,Q^2)}, \end{aligned}$$

which is exactly the type of the (Q, R)-norm defined by [Gillard and Zhigljavsky, 2016, Eq. (9)] (see also (2.8)). Therefore, our subproblem is the type of the approximation problem considered by Gillard and Zhigljavsky [2016]. Consequently, the method of alternating projection proposed by Gillard and Zhigljavsky [2016] can be used to solve (3.12). The essential difference from Gillard and Zhigljavsky [2016] is how we have derived the sequential approximations by defining Δ^{ν}.

In summary, we developed a computational scheme for arbitrarily weighted problem

(1.2). The scheme amounts to solving a sequence of approximation problems of (3.12). It includes both (2.7) and (2.8) as special cases and it is essentially different from that of [Gillard and Zhigljavsky, 2016, Zvonarev and Golyandina, 2015] in the way how Δ^ν is being defined. We put the scheme in the following algorithm framework. We call it Sequential Majorization Method (SMM).

Algorithm 6: Algorithm: Sequential Majorization Method (SMM)

Result: Approximated low rank matrix $\hat{X}$

Initialization: Given time series $\mathbf{x} \in \mathbb{R}^N$ and the weight vector $\mathbf{w} \in \mathbb{R}^N$. Choose the window length l. Compute $Y := \mathcal{H}(\mathbf{x})$ and matrix W by weight vector $\mathbf{w}$. Start with $X^0 = Y$ and set $\nu := 0$;

while *certain stopping criterion is not met* **do**

Computing the vectors $(\mathbf{p}, \mathbf{q})$ to satisfy the inequality (3.4) ;

Computing the next iterate $X^{\nu+1}$ as an approximate solution of the problem (3.9) with Δ^ν defined by

$$\Delta^\nu := X^\nu - P^{-2}\Big(W \circ W \circ (X^\nu - Y)\Big)Q^{-2},$$

where $P := \mathrm{diag}(\sqrt{\mathbf{p}})$ and $Q := \mathrm{diag}(\sqrt{\mathbf{q}})$;

$\nu = \nu + 1$;

We already mentioned that $X^{\nu+1}$ can be computed by the diagonally weighted SSA or the diagonally weighted Cadzow's method in the remark above. We will address how to compute $(\mathbf{p}, \mathbf{q})$ in the next section. We apply the method of alternating projection proposed in Gillard and Zhigljavsky [2016]) to solve (3.12), so the algorithm applied in numerical part is defined as SMM-Cadzow method. We will leave it to our numerical part.

3.2 Improving the Approximation

The quality of our approximation is governed by the inequality (3.4), which replies on the two vectors $\mathbf{p}$ and $\mathbf{q}$. A measurement of quality of the approximation is that the tighter

the inequality is, the better the approximation would be. In this section, we propose two schemes for generating a pair of $(\mathbf{p}, \mathbf{q})$. The rationale behind the two schemes is that the computation should be very fast. As a matter of fact, both can be done by solving a linear programming problem.

3.2.1 A simple choice of (p, q) and its improvement

A particular choice of the pair $(\mathbf{p}, \mathbf{q})$ satisfying (3.4) is as follows. We denote the pair by $(\overline{\mathbf{p}}, \overline{\mathbf{q}})$:

$$\begin{cases} \overline{p}_i & := & \max\{w_{i,j} \mid j = 1, \ldots, k\}, & i = 1, \ldots, l \\ \overline{q}_j & := & \max\{w_{i,j} \mid i = 1, \ldots, l\}, & j = 1, \ldots, k. \end{cases} \tag{3.13}$$

It is easy to check that the choice of $(\overline{\mathbf{p}}, \overline{\mathbf{q}})$ satisfies (3.4) by referring to the W matrix (3.1).

Our purpose below is to reduce $(\overline{\mathbf{p}}, \overline{\mathbf{q}})$ as much as we can under the constraint that it still satisfies (3.4). We note that a necessary and sufficient condition for $(\mathbf{p}, \mathbf{q})$ to satisfy (3.4) is

$$\sum_{i=1}^{l} \sum_{j=1:\ i+j=t+1}^{k} (p_i q_j) \geq w_t, \quad t = 1, \ldots, N. \tag{3.14}$$

Suppose $(\mathbf{p}, \mathbf{q})$ takes the following form:

$$\mathbf{p} := \overline{\mathbf{p}} - \mathbf{s}, \quad \mathbf{q} := \overline{\mathbf{q}} - \mathbf{t}, \quad 0 \leq \mathbf{s} \leq \overline{\mathbf{p}}, \quad 0 \leq \mathbf{t} \leq \overline{\mathbf{q}}. \tag{3.15}$$

From all such representations, we would like to find a best pair that minimizes the following problem:

$$\begin{array}{ll} \min & \sum_{i=1}^{l} \sum_{j=1}^{k} p_i q_j \\ \text{s.t.} & \text{Constraints in (3.14).} \end{array} \tag{3.16}$$

It follows from (3.15) that

$$\begin{aligned} p_i q_j &= (\overline{p}_i - s_i)(\overline{q}_j - t_j) \\ &= \overline{p}_i \overline{q}_j - (\overline{p}_i t_j + \overline{q}_j s_i) + s_i t_j \end{aligned}$$

$$\geq \quad \overline{p}_i\overline{q}_j - (\overline{p}_i t_j + \overline{q}_j s_i),$$

which implies

$$\sum_{i+j=t+1}(p_i q_j) - w_t \geq \sum_{i+j=t+1}\overline{p}_i\overline{q}_j - \sum_{i+j=t+1}(\overline{p}_i t_j + \overline{q}_j s_i) - w_t.$$

Hence, the constraints in (3.16) are satisfied if

$$\sum_{i+j=t+1}(\overline{p}_i t_j + \overline{q}_j s_i) \leq \sum_{i+j=t+1}\overline{p}_i\overline{q}_j - w_t, \qquad t = 1, \ldots, N. \tag{3.17}$$

On the other hand, we have for the objective that

$$\begin{aligned}\sum_{i=1}^{l}\sum_{j=1}^{k} p_i q_j &= \mathbf{1}_l^T(\mathbf{p}\mathbf{q}^T)\mathbf{1}_k \\ &= \mathbf{1}_l^T((\overline{\mathbf{p}} - \mathbf{s})(\overline{\mathbf{q}} - \mathbf{t})^T)\mathbf{1}_k \\ &= (\mathbf{1}_l^T\mathbf{s})(\mathbf{1}_k^T\mathbf{t}) - \left[(\mathbf{1}_l^T\mathbf{s})(\mathbf{1}_k^T\overline{\mathbf{q}}) + (\mathbf{1}_l^T\overline{\mathbf{p}})(\mathbf{1}_k^T\mathbf{t})\right] \\ &\quad +(\mathbf{1}_l^T\overline{\mathbf{p}})(\mathbf{1}_k^T\overline{\mathbf{q}}).\end{aligned} \tag{3.18}$$

Define

$$\alpha := \mathbf{1}_l^T\mathbf{s}, \quad \beta := \mathbf{1}_k^T\mathbf{t}, \quad \lambda := \mathbf{1}_l^T\overline{\mathbf{p}}, \quad \gamma := \mathbf{1}_k^K\overline{\mathbf{q}}.$$

The objective becomes

$$\sum_{i=1}^{l}\sum_{j=1}^{k} p_i q_j = \alpha\beta - (\alpha\gamma + \beta\lambda) + \lambda\gamma = (\lambda - \alpha)(\gamma - \beta),$$

and because of (3.15)

$$0 \leq \alpha \leq \lambda \qquad \text{and} \qquad 0 \leq \beta \leq \gamma.$$

It is easy to verify that

$$\alpha\beta - (\alpha\gamma + \beta\lambda) + \lambda\gamma \leq \left(\sqrt{\lambda\gamma} - \frac{1}{2\sqrt{\lambda\gamma}}(\alpha\gamma + \beta\lambda)\right)^2. \tag{3.19}$$

We replace the objective function by the right hand quantity of (4.38) and replace the constraints in (3.16) by (3.17) to derive a new optimization problem:

$$\begin{array}{ll} \min_{\alpha,\beta} & \left(\sqrt{\lambda\gamma} - \frac{1}{2\sqrt{\lambda\gamma}}(\alpha\gamma + \beta\lambda)\right)^2 \\ \text{s.t.} & \sum_{i+j=t+1}(\overline{p}_i t_j + \overline{q}_j s_i) \le \sum_{i+j=t+1}\overline{p}_i\overline{q}_j - w_t, \quad t = 1,\ldots,N. \\ & 0 \le \mathbf{s} \le \overline{\mathbf{p}}, \quad 0 \le \mathbf{t} \le \overline{\mathbf{q}}. \end{array} \tag{3.20}$$

It follows from the inequality

$$\sqrt{\lambda\gamma} \ge \frac{1}{2\sqrt{\lambda\gamma}}(\alpha\gamma + \beta\lambda)$$

that the problem (3.20) is equivalent to

$$\begin{array}{ll} \max_{\mathbf{s},\mathbf{t}} & \alpha\gamma + \beta\lambda = (\mathbf{1}_L^T\mathbf{s})(\mathbf{1}_K^T\overline{\mathbf{q}}) + (\mathbf{1}_L^T\overline{\mathbf{p}})(\mathbf{1}_K^T\mathbf{t}) \\ \text{s.t.} & \sum_{i+j=t+1}(\overline{p}_i t_j + \overline{q}_j s_i) \le \sum_{i+j=t+1}\overline{p}_i\overline{q}_j - w_t, \quad t = 1,\ldots,N. \\ & 0 \le \mathbf{s} \le \overline{\mathbf{p}}, \quad 0 \le \mathbf{t} \le \overline{\mathbf{q}}. \end{array} \tag{3.21}$$

The benefit of all those calculations is that the problem (3.21) is a linear programming problem and it can be efficiently solved by any standard linear programming solver. A side note is that the above technique leading to (3.21) is known as relaxation in optimization. We now formally state our algorithm for improving the pair $(\overline{\mathbf{p}}, \overline{\mathbf{q}})$.

Algorithm 7: Algorithm: LP$(\overline{\mathbf{p}}, \overline{\mathbf{q}})$

Result: Approximated $(\overline{\mathbf{p}}, \overline{\mathbf{q}})$

[S.1]:Input a pair of positive vectors $(\overline{\mathbf{p}}, \overline{\mathbf{q}})$ satisfying (3.4); weight vector $\mathbf{w} \in \mathbb{R}^N$ and the widow length l and $k = N - l + 1$;

[S.2] Use any standard Linear Programming solver to the problem (3.21) for the optimal $(\mathbf{s}, \mathbf{t})$.

[S.3] Output: Let

$$\mathbf{p} := \overline{\mathbf{p}} - \mathbf{s} \qquad \text{and} \qquad \mathbf{q} := \overline{\mathbf{q}} - \mathbf{t}.$$

3.2.2 Quality of the Approximation of the Weight Vector

In this part, we demonstrate how good is the $(\mathbf{p}, \mathbf{q})$-approximation to a given weight vector $\mathbf{w} \in \mathbb{R}^N$. We consider the following type of the weight vector, which was extensively used by Gillard and Zhigljavsky [2016]:

$$\mathbf{w} = (w_1, w_2, \ldots, w_{N-l}, w_{N-l+1}, \ldots, w_N),$$

where $l \geq 0$ is a given integer and for a given $\beta \geq 1$,

$$w_t := \beta^t, \qquad t = 1, \ldots, N - l.$$

and

$$w_t := w_{N-l} - \frac{w_{N-l}}{l+1}(t - (N-l)), \qquad \text{for } \; t = N - l + 1, \ldots, N.$$

Two particular choices of β that were used in Gillard and Zhigljavsky [2016] are $\beta = 1$ and $\beta = 1.01$. To follow the reference in Gillard and Zhigljavsky [2016], we label the weight vector $\mathbf{w}$ from $\beta = 1$ by $\mathbf{w}_1$ and $\mathbf{w}_2$ for $\beta = 1.01$.

For a given pair $(\mathbf{p}, \mathbf{q})$, the corresponding weight vector $\widetilde{\mathbf{w}} \in \mathbb{R}^N$ is given by

$$\widetilde{w}_t := \sum_{i=1}^{l} \sum_{j=1:\, i+j=t+1}^{k} (p_i p_j), \qquad t = 1, \ldots, N.$$

Because of the majorization inequality (3.4), we must have

$$\widetilde{w}_i \geq w_i, \qquad i = 1, \ldots, N. \tag{3.22}$$

We consider the following pairs of $(\mathbf{p}, \mathbf{q})$.

Case 1:	$(\overline{\mathbf{p}}, \overline{\mathbf{q}})$ by (3.13)
Case 2:	$(\mathbf{p}, \mathbf{q})$ by LP$(\overline{\mathbf{p}}, \overline{\mathbf{q}})$
Case 3:	$(\mathbf{1}, \widehat{\mathbf{c}})$ with $\widehat{\mathbf{c}}$ given by (3.13)
Case 4:	$(\mathbf{1}, \mathbf{c})$ with $\mathbf{c}$ given by LP$(\widehat{\mathbf{c}})$

TABLE 3.1: Choices of $(\overline{\mathbf{p}}, \overline{\mathbf{q}})$

We also consider the choice $(\mathbf{1}, \widehat{\mathbf{c}})$ with $\widehat{\mathbf{c}}$ given by used in Zvonarev and Golyandina [2015]. The corresponding weights with the original ones are plotted in Fig. 3.1.

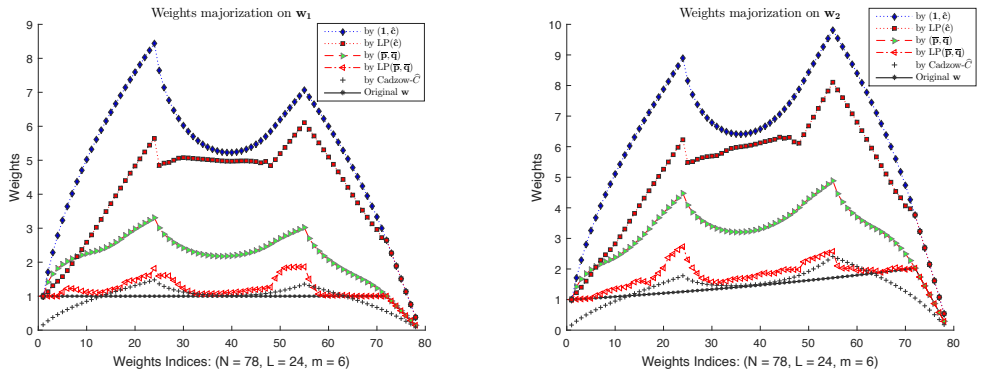

(a) Five weight vector approximations to $\mathbf{w}_1$ (b) Five weight vector approximations to $\mathbf{w}_2$

FIGURE 3.1: Five approximations of the weight vector $\mathbf{w}_1$ in Fig. 3.1(a) and of $\mathbf{w}_2$ in Fig. 3.1(b).

It is not surprising to see that all approximations from our 4 cases are above the original weights. In other words, the inequality (3.22) holds. However, for the choice of Zvonarev and Golyandina [2015], the weights on both ends are below the original weights and the weights in the middle part are above the original weights. Hence, the choice does not give a majorized weight approximation. We would also like to point out the approximation by $\mathrm{LP}(\overline{\mathbf{p}}, \overline{\mathbf{q}})$ closely follows the original weights. In theory, the closer the approximation is, the better the numerical performance should be for `SMM` provided that its subproblems can be solved globally. However, the subproblems are of nonconvex nature. This echoes the need of global techniques in low-rank matrix approximation through optimization raised in a recent paper [Chu et al., 2014]. Therefore, different choice of $(\mathbf{p}, \mathbf{q})$ may have its own advantages depending on the actual applications. We will see the dependence in our numerical experiments below.

We finish this section by pointing out that there are other ways to generate $(\mathbf{p}, \mathbf{q})$. For example, the inequality (3.4) that $(\mathbf{p}, \mathbf{q})$ has to satisfy can be cast as a rank-one nonnegative matrix factorization such that

$$W \approx \sqrt{\mathbf{p}}\sqrt{\mathbf{q}}^T$$

and $(\mathbf{p}, \mathbf{q})$ satisfies the inequalities in (3.14). Nonnegative matrix factorization has many applications and hence has many algorithms, depending on the problem in hand, see and the references therein.

3.3 Numerical Experiments

In this part, we report our preliminary numerical results on a widely researched real life example. We first describe the implementation issues of our Alg. 6.

3.3.1 Solving the Subproblem

The major computational part in Alg. 6 is on solving its subproblem (3.12) in (S.3). We propose to use the Cadzow method for the subproblem. For easy reference, we name the resulting method as `SMM-Cadzow` method, which runs as follows: Start with X^0, $\nu := 0$, compute the next iterate $X^{\nu+1}$ as the final iterate if the following iterative procedure (Cadzow's method applied to the subproblem (3.12)):

$$\widetilde{X}^{j+1} = \Pi_{\mathcal{H}}^{(\mathbf{p},\mathbf{q})}\Big(\Pi_{\mathcal{M}_r}^{(\mathbf{p},\mathbf{q})}(\widetilde{X}^j)\Big), \quad \widetilde{X}^0 := \Delta^\nu, \quad j = 0, 1, \tag{3.23}$$

We terminate (3.23) if the following conditions are met

$$\frac{|f^\nu(\widetilde{X}^{j+1}) - f^\nu(\widetilde{X}^j)|}{\max\{1, f^\nu(\widetilde{X}^j\}} \leq \texttt{tol} \qquad \text{or} \qquad \frac{\|\widetilde{X}^{j+1} - \widetilde{X}^j\|}{\|\widetilde{X}^j\|} \leq \texttt{tol},$$

where `tol` is the tolerance level set by the user. In this part, we used $\texttt{tol} = 10^{-3}$. We terminate Alg. 6 if

$$\frac{|f(X^{\nu+1}) - f(X^\nu)|}{\max\{1, f(X^\nu)\}} \leq \texttt{tol} \qquad \text{or} \qquad \frac{\|X^{\nu+1} - X^\nu\|}{\|X^\nu\|} \leq \texttt{tol}.$$

The convergence of Alg. 6 relies on the sandwich inequality (3.10), which essentially requires computing $X^{\nu+1} \in \mathcal{H}$ that satisfies (3.11). However, the subproblem (3.12) is non-convex and `Cadzow`'s method is not of global method, the sufficient condition (3.11) is not theoretically guaranteed. Surprisingly, when Cadzow's method is used to

the subproblem (3.12), the inequality (3.11) is often observed. We will demonstrate this feature when we come to reporting the numerical results.

3.3.2 USA Death Time Series

This is a widely used test data Golyandina et al. [2001] and comprehensive results based on the two weight vectors $\mathbf{w}_1$ and $\mathbf{w}_2$ in Subsect. 3.2.2 were reported in Gillard and Zhigljavsky [2016], which provides a basis for our comparison. The data set can be easily obtained online and contains the monthly accidental deaths in the USA between 1973 and 1978. The time series contains a total of $N = 78$ observations. Our task is to use the first 72 data points to forecast the remaining 6 observations (hence $m = 6$ in defining $\mathbf{w}_1$ and $\mathbf{w}_2$ in Subsect. 3.2.2). We will use the same parameters as those given in Hassani [2007], Gillard and Zhigljavsky [2016] and follow the suggestion in Gillard and Zhigljavsky [2016] that there are several forecasting available to start with for further improvement. Those forecasts (for the last 6 data points) as well as their corresponding methods are included in Table 3.2, where 5 forecasting methods are included. In particular, Model I and Model II are examples of SARIMA models as described in Box et al. [2015]. HWS represents the model as fitted by the Holt-Winter seasonal algorithm. ARAR represent the model as fitted by transforming the data prior to fitting an autoregressive model. Forecaster values by `SSA` is taken from Hassani [2007]. More details about those 5 methods can be found in [Gillard and Zhigljavsky, 2016, Sect. 7.3].

Models	**1**	**2**	**3**	**4**	**5**	**6**
Original data	7798	7406	8363	8460	9217	9316
Model I	8441	7704	8549	8885	9843	10279
Model II	8345	7619	8356	8742	9795	10179
HWS	8039	7077	7750	7941	8824	9329
ARAR	8168	7196	7982	8284	9144	9465
SSA	7782	7428	7804	8081	9302	9333

TABLE 3.2: Forecasts from five different models.

In our experiments below, we will use them as our initial guess for the last 6 data points. In other words, we have a data series $\mathbf{y} \in \mathbb{R}^N$ with the first 72 data being the first 72 data in the USA time series, which is denoted as $\mathbf{x}^*$ and the last 6 points in $\mathbf{y}$ being

one of the forecast values in Table 3.2. We use $\mathbf{x}$ to denote the obtained time series by Alg. 6. The root of squared mean error is then defined as

$$\texttt{RMSE} := \sqrt{\sum_{i=1}^{6}(x_{72+i} - x^*_{72+i})^2},$$

which is often used to quantify how good the estimated values are to the original data. Obviously, the smaller is the `RMSE`, the better the forecasting is.

(a) Demonstration of convergence. We implemented Alg. 6 in `Matlab` and run it in `Matlab` 2015b. We would like to take this opportunity to demonstrate the convergence of Alg. 6 in terms of the objective values. For this experiments, we set $\texttt{tol} = 10^{-5}$ and the maximum number of iterations allowed for the subproblem is 100. The choice of this higher accuracy allows us to observe the trend of the objective values in many steps (lower accuracy would require a less number of iterations).

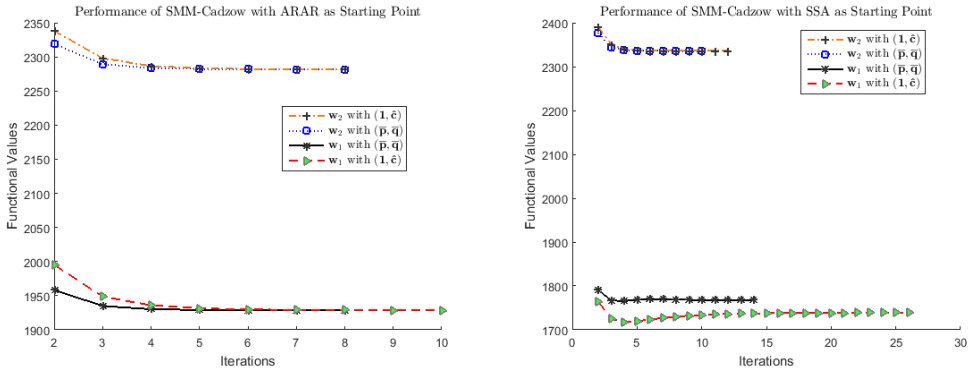

(a) Convergence in the objective of `SMM-Cadzow` (b) Convergence in the objective of `SMM-Cadzow`

FIGURE 3.2: Similar convergence was observed in both Fig. 3.2(a) and Fig. 3.2(b), in terms of functional values respectively starting from `ARAR` and `SSA` point in Table 3.2.

The functional sequence generated by our method are plotted in Fig. 3.2 from two starting points (ARAR and SSA respectively). `SMM-Cadzow` solved the subproblem iteratively by (3.23) and it can be observed in in both figures in Fig. 3.2 that the functional sequence is decreasing and converges. This is because that the sufficient condition (3.11) is more often to be met than otherwise in `SMM-Cadzow`. This behaviour of convergence appears consistence for other test problems. Hence, we will not repeat the demonstration for

other examples.

(b) RMSE comparison. We will report the `RMSE` obtained by `SMM-Cadzow` with the 5 starting points from Table 3.2. The approximation weights $(\mathbf{p}, \mathbf{q})$ used are from Table 3.1. We will compare the obtained `RMSE` with those by the 5 starting points, the (Q, R)-norm approximation Gillard and Zhigljavsky [2016] and the Cadzow-$\widehat{C}$ method in Zvonarev and Golyandina [2015] (based on our own implementation).

The RMSE results are reported in Table 3.3 for the two weight vectors $\mathbf{w}_1$ ($\beta = 1$) and $\mathbf{w}_2$ ($\beta = 1.01$). The first row (Initial RMSE) of the table includes the RMSE from the 5 initial points in Table 3.2. We first note that for many cases, there have been significant reductions in RMSE from each of the starting point. The numbers in bold indicate they are the best RMSE obtained by all the methods for $\mathbf{w}_1$ and $\mathbf{w}_2$ respectively, from a given starting point. It can be observed that for both weighting schemes, the Cadzow-$\widehat{C}$ method of Zvonarev and Golyandina [2015] worked very well. In particular, the Cadzow-$\widehat{C}$ achieved the 2 best RMSE for $\mathbf{w}_1$ and 3 best RMSE for $\mathbf{w}_2$. The `SMM-Cadzow` with $(\mathbf{1}, \widehat{\mathbf{c}})$ closely followed the Cadzow-$\widehat{C}$ and achieved the overall best RMSE (217.40). This trend can be clearly seen in the Fig. 3.3, where we only plotted `SMM-Cadzow` with $(\overline{\mathbf{p}}, \overline{\mathbf{q}})$ and LP$(\overline{\mathbf{p}}, \overline{\mathbf{q}})$ for the case $\mathbf{w}_1$, and `SMM-Cadzow` with $(\mathbf{1}, \widehat{\mathbf{c}})$ and LP$(\mathbf{1}, \widehat{\mathbf{c}})$ for the case $\mathbf{w}_2$ for a better visualization. It can also be seen that the (Q, R) approximation method of Gillard and Zhigljavsky [2016] did well for the ARAR starting point. For both $\mathbf{w}_1$ and $\mathbf{w}_2$, it achieved the best RMSE (247.56 and 244.61 respectively). Therefore, our purpose below is to improve `SMM-Cadzow` to outperform both (Q, R) method and the Cadzow-$\widehat{C}$ method.

The number of iterations are reported in Table 3.4, where `It` is the number of subproblems solved in `SMM` and `Iter` is the total number of Cadzow iterations. For example, the first pair 4(126) in Table 3.4 means that for $\mathbf{w}_1$ and $(\overline{\mathbf{p}}, \overline{\mathbf{q}})$, `SMM-Cadzow` solved 4 subproblems by a total of 126 iterations of (3.23). In this experiment, the computing cost for both `SMM` and Cadzow-$\widehat{C}$ is around 1.2 milliseconds per `Iter` on a 16GB-ram laptop. In our experiments, we set the maximum number of subproblems to be solved to

20. As we can see, there are a few cases where the maximum number (20) was reached and the numbers for `Iter` in some cases are large. Below we propose a strategy that would improve `SMM-Cadzow` both in quality of RMSE and in the number of total `Iter`.

β	$(\mathbf{p}, \mathbf{q})$	5 starting points				
		Model I	Model II	HWS	ARAR	SSA
Initial	RMSE	582.63	500.5	401.26	253.20	278.20
	$(\overline{\mathbf{p}}, \overline{\mathbf{q}})$	508.83	413.73	**234.25**	253.45	302.72
	LP$(\overline{\mathbf{p}}, \overline{\mathbf{q}})$	512.15	414.02	347.09	271.70	278.24
$\beta = 1$	$(\mathbf{1}, \hat{\mathbf{c}})$	497.46	402.13	410.61	252.27	313.71
$(\mathbf{w}_1)$	LP$(\hat{\mathbf{c}})$	**495.26**	400.36	347.27	282.22	283.82
	(Q,R)	582.20	486.03	385.81	**247.56**	276.28
	Cadzow-$\widehat{C}$	557.92	**374.32**	234.63	257.09	**220.11**
	$(\overline{\mathbf{p}}, \overline{\mathbf{q}})$	492.38	427.66	252.02	260.65	218.17
$\beta = 1.01$	LP$(\overline{\mathbf{p}}, \overline{\mathbf{q}})$	493.60	426.94	354.83	250.48	280.99
$(\mathbf{w}_2)$	$(\mathbf{1}, \hat{\mathbf{c}})$	492.60	427.46	251.95	259.50	**217.40**
	LP$(\hat{\mathbf{c}})$	475.43	426.95	350.02	258.20	279.45
	(Q,R)	559.55	481.91	380.79	**244.61**	275.68
	Cadzow-$\widehat{C}$	**461.48**	**404.78**	**249.75**	267.71	227.56

TABLE 3.3: RSME comparison between the method `SMM-Cadzow` and (Q, R)-approximation Gillard and Zhigljavsky [2016], Cadzow-$\widehat{C}$ method in Zvonarev and Golyandina [2015]

β	$(\mathbf{p}, \mathbf{q})$	5 starting points				
		Model I	Model II	HWS	ARAR	SSA
		It (iter)	It (iter)	It (iter)	It (iter)	It (iter)
	$(\overline{\mathbf{p}}, \overline{\mathbf{q}})$	4(126)	5(166)	4(72)	4(68)	8(724)
	LP$(\overline{\mathbf{p}}, \overline{\mathbf{q}})$	20(343)	20(352)	5(81)	20(343)	6(104)
$\beta = 1$	$(\mathbf{1}, \hat{\mathbf{c}})$	5(130)	7(183)	4(281)	5(89)	4(186)
$(\mathbf{w}_1)$	LP$(\hat{\mathbf{c}})$	20(422)	20(433)	5(121)	20(403)	5(123)
	$(\overline{\mathbf{p}}, \overline{\mathbf{q}})$	4(60)	4(61)	4(71)	4(68)	4(68)
$\beta = 1.01$	LP$(\overline{\mathbf{p}}, \overline{\mathbf{q}})$	5(85)	5(86)	9(121)	5(101)	3(49)
$(\mathbf{w}_2)$	$(\mathbf{1}, \hat{\mathbf{c}})$	5(82)	5(82)	5(91)	5(86)	5(86)
	LP$(\hat{\mathbf{c}})$	20(385)	20(392)	4(75)	20(381)	3(63)

TABLE 3.4: Number of iterations used by `SMM-Cadzow` starting with the 5 points from Table 3.2.

(c) Improving `SMM-Cadzow` via warmstart. It follows from both Table 3.3 and Table 3.4 that the `SMM-Cadozw` method has already shown its potential in finding the best RMSE (217.40) among all the method tested. In this part, we will show that its quality and efficiency can be further improved by incorporating a warm start strategy, which is often used in a sequential optimization setting. For example, it has been successfully

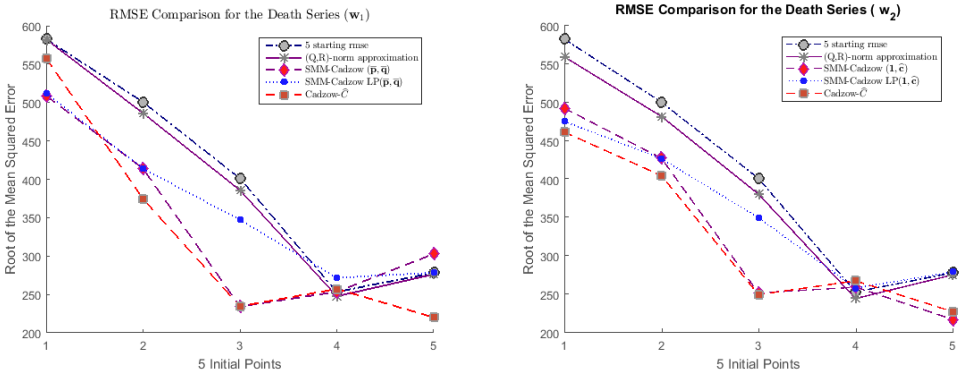

(a) RMSE: $(\mathbf{p},\mathbf{q}) = (\overline{\mathbf{p}},\overline{\mathbf{q}})$ or LP$(\overline{\mathbf{p}},\overline{\mathbf{q}})$ (b) RMSE: $(\mathbf{p},\mathbf{q}) = (\mathbf{1},\widehat{\mathbf{c}})$ or LP$(\widehat{\mathbf{c}})$

FIGURE 3.3: RMSE comparison in Fig. 3.3(a) for $\mathbf{w}_1$ and Fig. 3.3(b) for $\mathbf{w}_2$. Data were obtained by `SMM-Cadzow` with the 5 initial points given in Table 3.2.

used in the sequential matrix optimization for computing a low-rank correlation matrix Sun [2010], Li et al. [2016]. We describe this simple strategy below.

At the νth iteration with X^ν obtained, we compute

$$\widetilde{\mathbf{x}}^\nu := \mathcal{H}^{-1}(X^\nu)$$

and we replace the first 72 data points of $\widetilde{\mathbf{x}}^\nu$ by the original ones in $\mathbf{y}$ to get $\widehat{\mathbf{x}}^\nu$:

$$\widehat{\mathbf{x}}^\nu := \widetilde{\mathbf{x}}^\nu, \qquad \widehat{\mathbf{x}}^k(1:72) = \mathbf{y}(1:72).$$

Finally, we replace X^ν by $\widehat{X}^\nu$:

$$\widehat{X}^\nu := \mathcal{H}(\widehat{\mathbf{x}}^\nu).$$

This warm start strategy uses the original 72 data (known) and the latest prediction for the last 6 missing values in $\mathbf{y}$ to define $\widehat{X}^\nu$. The subproblem is still solved by the Cadzow's method (3.23). Hence, it is still convergent with this choice.

Under our stopping criterion (see Subsect. 3.3.1), only 2 subproblems were solved for each case. The results on RMSE and the iteration information are reported in Table 3.5 and Table 3.6, where $It = 2$ for all cases. It can be observed that not only the number of iterations (iter) has been reduced, the RMSE has also seen significant reduction. Moreover, 4 out of 5 best cases were obtained by our method for $\mathbf{w}_2$. The remaining

β	$(\mathbf{p},\mathbf{q})$	5 starting points				
		Model I	Model II	HWS	ARAR	SSA
Initial	RMSE	582.63	500.5	401.26	253.20	278.20
	$(\overline{\mathbf{p}},\overline{\mathbf{q}})$	469.15	359.47	**226.50**	247.60	296.33
	LP$(\overline{\mathbf{p}},\overline{\mathbf{q}})$	**454.72**	398.84	362.96	253.60	292.74
$\beta = 1$	$(\mathbf{1},\hat{\mathbf{c}})$	466.84	**344.75**	354.38	**231.21**	317.39
$(\mathbf{w}_1)$	LP$(\hat{\mathbf{c}})$	490.74	375.18	345.66	243.68	295.72
	(Q,R)	582.20	486.03	385.81	247.56	276.28
	Cadzow-$\widehat{C}$	557.92	374.32	234.63	257.09	**220.11**
	$(\overline{\mathbf{p}},\overline{\mathbf{q}})$	433.37	381.81	238.70	257.48	219.31
$\beta = 1.01$	LP$(\overline{\mathbf{p}},\overline{\mathbf{q}})$	482.98	422.39	256.95	269.15	227.29
$(\mathbf{w}_2)$	$(\mathbf{1},\hat{\mathbf{c}})$	**408.76**	**360.75**	**238.08**	247.98	**218.89**
	LP$(\hat{\mathbf{c}})$	506.88	404.73	346.59	255.93	285.34
	(Q,R)	559.55	481.91	380.79	**244.61**	275.68
	Cadzow-$\widehat{C}$	461.48	404.78	249.75	267.71	227.56

TABLE 3.5: RSME comparison between the method `SMM-Cadzow` with the warm-start and (Q,R)-approximation [Gillard and Zhigljavsky, 2016], Cadzow-$\widehat{C}$ method in [Zvonarev and Golyandina, 2015]

RMSE (247.98 for ARAR starting point) is not far from the best RMSE (244.61 for ARAR starting point). This is clearly demonstrated in Fig. 3.4(a), where the both lines for `SMM-Cadzow` with $(\overline{\mathbf{p}},\overline{\mathbf{q}})$ and $(\mathbf{1},\hat{\mathbf{c}})$ are below the others.

β	$(\mathbf{p},\mathbf{q})$	5 starting points				
		Model I	Model II	HWS	ARAR	SSA
		It (iter)	It (iter)	It (iter)	It (iter)	It (iter)
	$(\overline{\mathbf{p}},\overline{\mathbf{q}})$	2(38)	2(36)	2(36)	2(34)	2(46)
	LP$(\overline{\mathbf{p}},\overline{\mathbf{q}})$	2(44)	2(44)	2(40)	2(48)	2(44)
$\beta = 1$	$(\mathbf{1},\hat{\mathbf{c}})$	2(38)	2(30)	2(34)	2(42)	2(40)
$(\mathbf{w}_1)$	LP$(\hat{\mathbf{c}})$	2(50)	2(48)	2(64)	2(48)	2(62)
	$(\overline{\mathbf{p}},\overline{\mathbf{q}})$	2(30)	2(32)	2(34)	2(34)	2(34)
$\beta = 1.01$	LP$(\overline{\mathbf{p}},\overline{\mathbf{q}})$	2(42)	2(44)	2(52)	2(50)	2(50)
$(\mathbf{w}_2)$	$(\mathbf{1},\hat{\mathbf{c}})$	2(36)	2(36)	2(38)	2(36)	2(36)
	LP$(\hat{\mathbf{c}})$	2(46)	2(44)	2(48)	2(46)	2(50)

TABLE 3.6: Number of iterations used by `SMM-Cadzow` starting with the 5 points from Table 3.2.

If we were even more "aggressive" in the sense that we apply the warm start strategy at every iteration. That is, we replace $\widetilde{X}^{j+1}$ in (3.23) by $\widehat{\widetilde{X}}^{j+1}$, we may achieve even more reduction RMSE. Fig. 3.4(b) plotted two cases of `SMM-Cadzow` with LP$(\overline{\mathbf{p}},\overline{\mathbf{q}})$ and LP$(\hat{\mathbf{c}})$. It is observed that the line for LP$(\hat{\mathbf{c}})$ is well below all other lines and in fact achieved

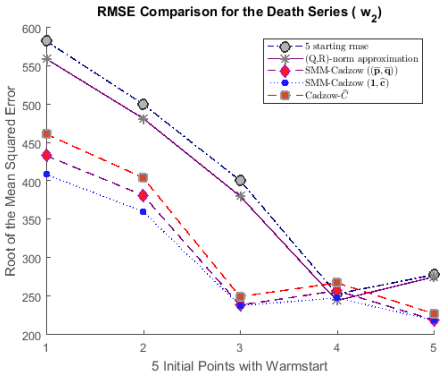

(a) RMSE: $(\mathbf{p}, \mathbf{q}) = (\overline{\mathbf{p}}, \overline{\mathbf{q}})$ or LP$(\overline{\mathbf{p}}, \overline{\mathbf{q}})$

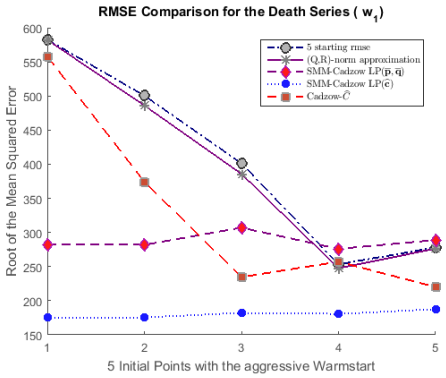

(b) RMSE: $(\mathbf{p}, \mathbf{q}) = (\mathbf{1}, \widehat{\mathbf{c}})$ or LP$(\widehat{\mathbf{c}})$

FIGURE 3.4: RMSE comparison in Fig. 3.4(a) for $\mathbf{w}_2$ with the warm-start once and Fig. 3.4(b) for $\mathbf{w}_1$ with the warm-start always. Data were obtained by `SMM-Cadzow` with the 5 initial points given in Table 3.2.

the best RMSE for all 5 starting points. The corresponding values of RMSE are:

$$(175.53,\ 175.47,\ 182.13,\ 180.68,\ 187.47).$$

While we note that it may yield better RMSE in some cases, however, the big question for this "aggressive" use of the warm start strategy is that the resulting algorithm may suffer non-convergence. Hence, we choose not to report any further result for this choice and leave it to our future research.

3.3.3 Energy Prices Forecasting

a. Introduction. This experiment uses the daily price series of crude and several petroleum products including conventional gasoline, No.2 heating oil, ultra-low-sulfur (ULS) No.2 diesel fuel and Kerosene-type jet fuel. The price series of crude oil is chosen as the daily contract price of West Texas Intermediate (WTI) from Cushing, Oklahoma. Daily price series of conventional gasoline, No.2 heating oil and ultra-low-sulfur No.2 diesel fuel is obtained from New York Harbor. Daily trading prices of kerosene-type jet fuel is collected from U.S. Gulf Coast [1]. Time period for each price series is from 16th May, 2016 to 19th May, 2017 so that we have total 252 observations for each series.

[1] All the data used in this paper can be found from https://www.eia.gov/dnav/pet/pet_pri_spt_s1_d.htm

We plot the daily price series of these products in Figure 3.5 and summarize descriptive statistics for these five time series in Table 3.7. The skewness and kurtosis statistic indicates the distributions of all five time series of daily spot price are left-skewed and platykurtic. We further note that price volatilities of No.2 heating oil, ultra-low-sulfur No.2 diesel fuel and Kerosene-type jet fuel were consistent during this period. By contrast, the probabilities of extreme value in the price series of conventional gasoline and crude oil were comparably high with a smaller Kurtosis value. This phenomenon can be observed from Figure. 3.5(b) as well.

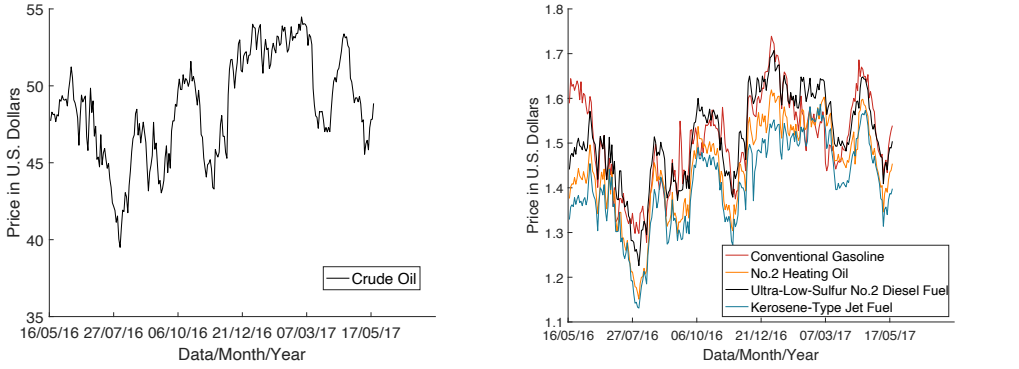

(a) Daily spot price series of crude oil

(b) Daily spot price series of four petroleum products

FIGURE 3.5: The actual spot price series of crude oil in Figure. 3.5(a) and four petroleum products in Figure. 3.5(b), from 16th May 2016 to 19th May 2017.

TABLE 3.7: Descriptive Statistics: Daily prices of crude oil and petroleum products, from 16th May 2016 to 19th May 2017

Series	Mean	Median	Min.	Max.	Std.Dev	Skew.	Kurtosis
Crude Oil	48.66	48.78	39.50	54.48	3.38	-0.27	2.34
Conventional Gasoline	1.51	1.51	1.28	1.74	0.10	-0.10	2.33
No.2 Heating Oil	1.44	1.45	1.15	1.62	0.10	-0.59	2.92
Ultra-Low-Sulfur No.2 Diesel Fuel	1.51	1.51	1.23	1.71	0.10	-0.43	2.75
Kerosene-Type Jet Fuel	1.41	1.41	1.13	1.59	0.10	-0.48	2.81

b. Parameter Selection. Two important parameters need to be determined before the implementation of Alg.6 are the window length l and the rank of objective Hankel matrix r. In this experiment we follow the suggestions by [Hassani et al., 2011, Section 2.3] through introducing the concept of separability to determine the choices of parameters.

Setting window length $l = N/2$, results of parameter selections for all five time series are listed in Table 3.8.

TABLE 3.8: Parameter Choices for Window Length l and Objective Rank r for the daily price series of crude oil and petroleum products.

Series	Crude Oil Crude Oil	Conventional Gasoline	No.2 Heating Oil	ULS No.2 Diesel Fuel	Kerosene Type Jet Fuel
m	100	100	100	100	100
r	12	25	11	9	7

c. Numerical Result. The estimating components of crude oil daily prices are plotted in Figure 3.6 as well as the actual observed data.

$$W_{i,j} = \frac{1}{i+j-1} \qquad \text{for } 1 \le i \le l \text{ and } 1 \le j \le k \tag{3.24}$$

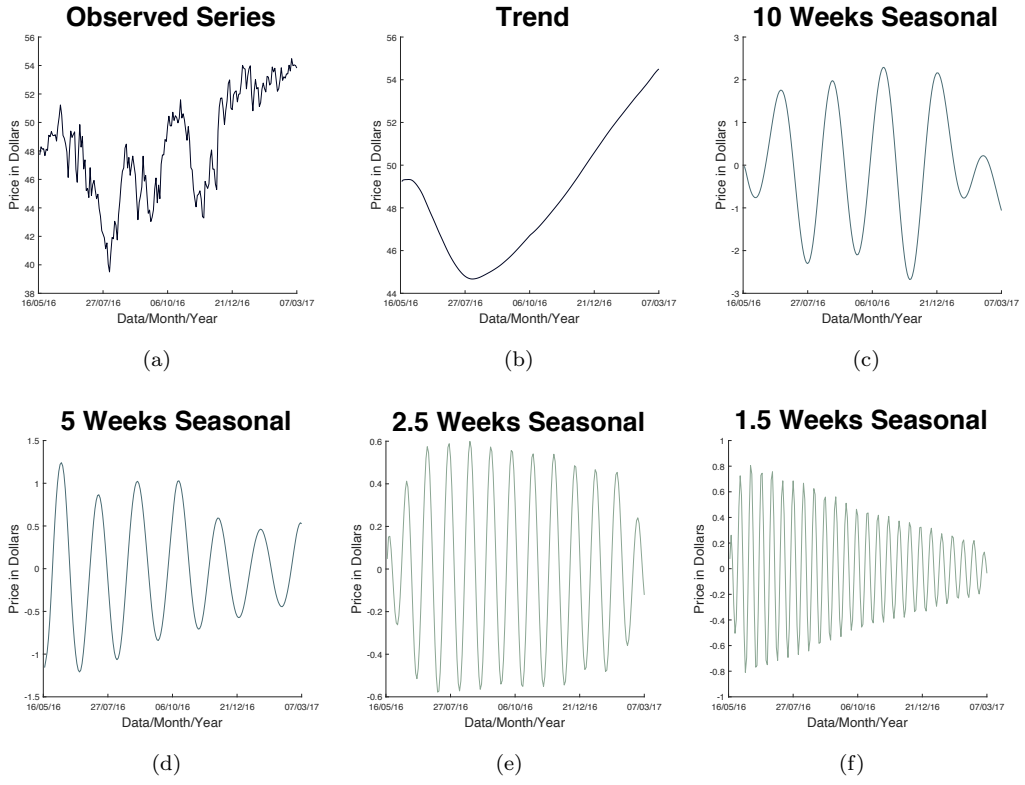

FIGURE 3.6: Decomposition Result of Crude Oil WTI Daily Prices Series by SMM Algorithm.

The trend series in Figure. 3.6(b) is constructed by the first and second singular values and this series the largest part of crude oil daily price volatility, as we can observed from the vertical axis of this figure. This trend decreased from the beginning to the end

of July 2016, then inverted to be increasing for the rest of the period. The 10 weeks seasonal component (Figure. 3.6(c)) is constructed by the 3rd to 5th singular values and it fluctuates between within (-2.5 , 2.5). The 5, 2.5 and 1.5 weeks seasonal components are constructed by 7th to 8th (Figure. 3.6(d)), 9th to 10th (Figure. 3.6(e)) and 11th to 12th (Figure. 3.6(f)) singular values respectively.

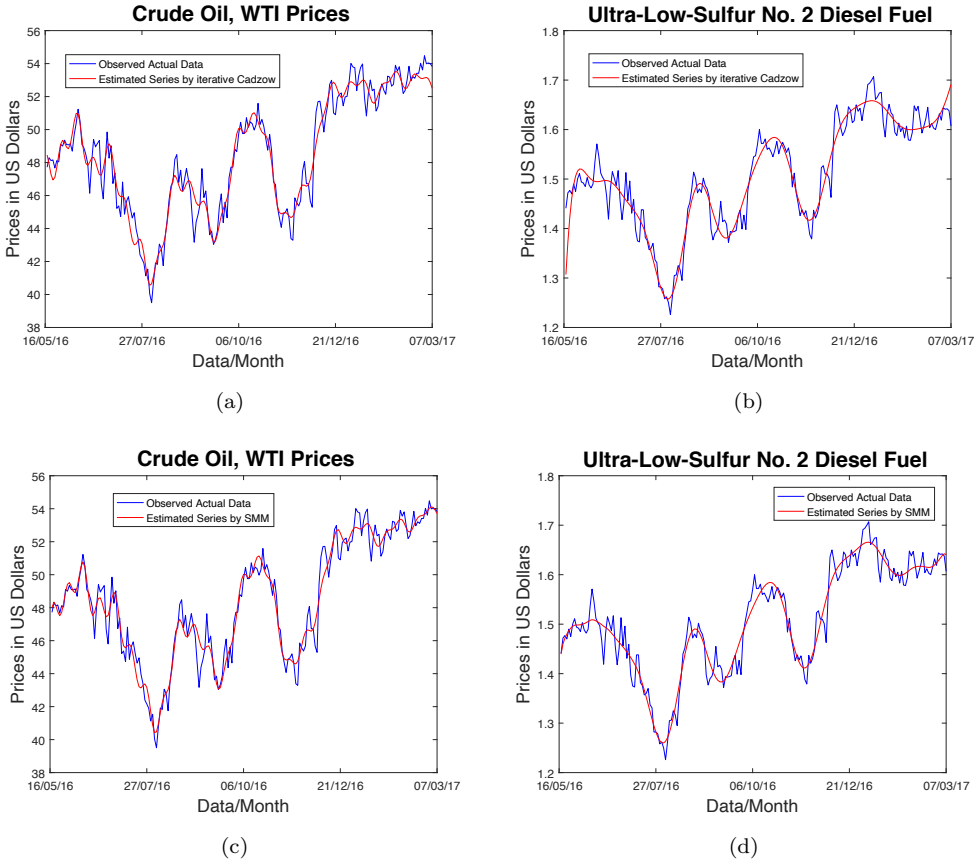

FIGURE 3.7: Estimated series comparison between iterative Cadzow method and SMM.

Figure.3.7(a) and 3.7(c) compare the estimation result between Cadzow method and SMM. At both ends of time series, it is easily observed that SMM provides better data approximations compared with Cadzow method by fitting the input observed time series better.

We further include five candidate models are in forecasting the future energy prices including SMM, Cadzow, SSA and other two benchmarking models, ARIMA and GARCH. We will consider three forecasting scenarios as 10 steps forecasting ($h = 10$), 15 steps forecasting ($h = 15$) and 20 steps forecasting ($h = 20$). Root mean square error (RMSE)

is again introduced to measure the forecasting accuracy. We further apply Diebold-Mariano tests to examine if SMM outperforms other models at a certain significant level. The weight matrox W used in SMM is defined as Equation (3.25) so that training set data has equal weights and the starting value of forecasted data are assigned by linearly decreasing weights because we have less information to forecast the long-step-ahead future data:

$$W_{i,j} := \begin{cases} \frac{1}{i+j-1} & \text{for } (i+j-1) \leq N \\ 1 - \frac{i-N}{(h+1)(i+j-1)} & \text{for } N+1 \leq (i+j-1) \leq N+h \end{cases} \tag{3.25}$$

Stopping criteria for iterative Cadzow method and SMM are defined as:

- Iteration stops when
$$tol = \frac{\|X^{\nu+1} - X^{\nu}\|}{\|X^{\nu}\|} \leq 10^{-3}$$
- The maximum step of iterations is set as 100.

Iteration algorithms stop when any one of above two criteria is met. Forecasting results by five candidate models are listed in Table 3.9. For comparison purpose, the RMSE ratios (RRMSE) of SMM to other four models are presented in Table 3.9, while RRMSE smaller than 1 indicates that SMM algorithm provide better forecasting data compared with candidate model.

Table 3.9 shows that SMM outperforms all other four models in 8 cases over 15, as indicated by the result of Diebold-Mariano test at 5% significant level. There are three scenarios that ARIMA or Cadzow provides a slightly better forecasting results comparing with SMM, however, the improvement is not significant at 5% level. There is only 1 case that candidate models generating more accurate forecasting data significantly, which is the 10-step conventional gasoline prices forecasting by ARIMA and GARCH.

We further note from Table 3.9 that with longer forecasting steps, RMSE ratios of SMM to ARIMA or GARCH become smaller in most cases. For example in the Kerosene-Type Jet Fuel forecasting, 10-step prediction errors between of ARIMA and SMM are

TABLE 3.9: RSME comparison of estimation result by five different models

Price Series	Forecasting Steps	SMM	$\frac{\text{SMM}}{\text{ARIMA}}$	$\frac{\text{SMM}}{\text{GARCH}}$	$\frac{\text{SMM}}{\text{SSA}}$	$\frac{\text{SMM}}{\text{Cadzow}}$
Crude Oil	h = 10	2.4177	1.01	0.99	0.60**	0.63**
	h = 15	2.5399	0.83**	0.82**	0.45**	0.90**
	h = 20	2.4600	0.72**	0.70**	0.35**	0.86**
Conventional Gasoline	h = 10	0.0999	1.55	1.53	0.89**	0.66**
	h = 15	0.0853	0.97	0.95	0.48**	1.03
	h = 20	0.0947	0.92**	0.85**	0.51**	1.00
No.2 Heating Oil	h = 10	0.0631	1.03	1.00	0.59**	0.86**
	h = 15	0.0666	0.87*	0.84*	0.51**	0.87**
	h = 20	0.0724	0.86*	0.82**	0.51**	0.97**
Ultra-Low-Sulfur No. 2 Diesel Fuel	h = 10	0.0496	0.87*	0.87	0.40**	0.78**
	h = 15	0.0529	0.69**	0.68**	0.33**	0.75**
	h = 20	0.0612	0.72**	0.69**	0.33**	0.82**
Kerosene-Type Jet Fuel	h = 10	0.0637	0.95	0.92	0.40**	0.75**
	h = 15	0.0682	0.80*	0.77**	0.38**	0.75**
	h = 20	0.0757	0.79**	0.76**	0.41**	0.78**

Notes: **/* represents the results of Diebold-Mariano test. ** indicates SMM provides more accurate results than another model at 5% significant level. * indicates SMM provides more accurate results than another model at 10% significant level.

not significant since the RMSE ratio is just 0.95. While in the 15-step forecasting experiment, SMM generates more accurate forecasting result at 10% significant level than ARIMA model. Then in the 20-step ahead forecasting, RMSE ratio of SMM to ARIMA decreased continuously to 0.79 and forecasting date estimated by SMM is more accurate than data estimated by ARIMA at even 5% significant level. We can observe this phenomenon for other time series cases as well.

On the other hand, although Cadzow failed to generate better predictions than SMM, its forecasting result do not get worse when the forecasting steps extended from 10 steps to 20 steps. For all five daily price series used in this paper, RMSE ratio of SMM to Cadzow actually imporved from 10 steps forecasting to 20 steps forecasting, e.g., increased from 0.63 to 0.86 in the case of crude oil daily prices forecasting. This result shows the advantage of the rank-minimization based methods in capturing both short term cyclical fluctuations and long term trend of a series.

3.4 Conclusions

In this chapter, we proposed a method to tackle the weighted low rank Hankel matrix approximation problem. We demonstrated the advantages of the proposed method, named as SMM-Cadzow due to the fact that the subproblem is solved by the Cadzow method by [Gillard, 2010]. For example, the latest gradient information was used to construct the new approximation once a new iterate was obtained. The approximation can be improved through a smaller $(\mathbf{p}, \mathbf{q})$ weights, which can be refined by linear programming (cheap computational cost). The method was guaranteed to converge if the sandwich inequality is satisfied at each iterate. Moreover, its numerical performance was demonstrated against several popular test problem and a thorough comparison with the two existing methods were conducted to show its improvement. We also introduce a real life time series as oil price forecasting to compare the performance of our proposed SMM with several classical time series models.

Chapter 4

A Majorization Penalty Method

In this chapter, we still target to solve the low rank Hankel matrix approximation problem under weighted norm. A majorized penalty method is proposed to tackle this problem so that it enjoys the advantage of majorization minimization. This chapter is arranged as follows. Section 4.1 provides a very brief motivation for this new scheme. In Section 4.2 we introduce the majorized penalty method to tackle the WLRH problem and provide our main convergence result. Then we will further prove that the properties of our approach can be further extended to the case of complex valued matrix in Section 4.3. The performances of majorized penalty method in time series analysis and signal completions are compared with other WLRH solvers in Section 4.4 by conducting some synthetic numerical experiments. In Section 4.5, we will compare the difference between SMM-Cadzow and the solver proposed in this chapter and discuss the improvement we achieved by introducing the majorized penalty approach. Finally in Section 4.6 we summarize the conclusions of this chapter.

4.1 Introduction

In the last chapter we have introduced the Sequential Majorization Method (SMM) to tackle the weighted low rank Hankel matrix approximation problem. Several numerical experiments are conducted to show that SMM outperforms some of the state-of-art

solvers. However, it is worth noting that the framework of SMM still has some drawbacks. In SMM we introduced the inequality (3.4) to obtain the surrogate majorization of original objective function. As a result, the weight matrix introduced in SMM via the approximation approach would be slightly different from the original weight matrix W. At the same time, we notice that SMM still implements alternating projection method at each iteration to get the next iterate $X^{\nu+1}$. It may lead to 1) heavy computational cost and 2) the convergence framework may not hold because the inequalities (3.11) may not hold.

In this chapter, we try to tackle the weighted low rank Hankel matrix approximation problem from a new approach which is known as the penalty approach. This approach has been widely employed to tackle non-convex rank constraint minimization problem because it turns out that the penalty approach can help to develop the globally convergence algorithms for such problems. For example, Yan [2010] and Sun [2010] used this approach to solve the calibrating rank constrained correlation matrix problems. They established the following corresponding relationship that:

$$\operatorname{rank}(X) \leq r \qquad \Longleftrightarrow \qquad \sum_{i=r+1} \sigma_i(X) = 0$$

Liu et al. [2018] also applied the similar penalty approach to solve the semidefinite-box constrained low-rank matrix optimization problems, provided that the established algorithm will converge to a first order stationary point. Some other recent relevant publications including Shen and Mitchell [2018] and Lu et al. [2015]. However, these introduced methods have nothing to do with MAP and their implementations are not trivial.

4.2 A Majorized Penalty Method

4.2.1 A Majorized Surrogate Function

Recall the weighted low rank Hankel matrix approximation problem:

$$\begin{aligned} &\min \frac{1}{2}\|X-Y\|_W^2 \\ &\text{s.t.} X \in \mathcal{H} \cap \mathcal{M}_r \end{aligned} \tag{4.1}$$

We now introduce a majorization approach to handle the low rank constraint in (4.1). Firstly we define the quadratic function $h_r(A)$ as the squared sum of first r singular values of A:

$$\begin{aligned} h_r(A) &= \frac{1}{2}\|\Pi_{\mathcal{M}_r}(A)\|^2 \\ &= \frac{1}{2}\|U_A\Sigma_r(A)V_A^T\|^2 \\ &= \frac{1}{2}\sum_{i=1}^{r}\sigma_i^2(A), \qquad \forall A \in \mathcal{M} \end{aligned} \tag{4.2}$$

where A has the singular value decomposition $A = U_A\Sigma(A)V_A^T$ and $\sigma_i(A)$ in the non-increasing order denotes the singular value of A, i.e., $\sigma_i(A) = \Sigma(A)_{i,i}$. $\Sigma_r(A)$ is defined as following:

$$\Sigma_r(A)_{i,j} = \begin{cases} \Sigma(A)_{i,j} & \text{if } \ i=j\le r \\ 0 & \text{otherwise.} \end{cases}$$

$\Pi_{\mathcal{M}_r}(A)$ is computed through (2.6) as an analytical solution to the unweighted low rank approximations of matrix A. The third equality in (4.2) holds because we have $UU^T = I_{l\times l}$ and $V^TV = I_{k\times k}$, while $I_{n\times n}$ is the $n\times n$ identity matrix. We further note that $h_r(A)$ is a differentiable quadratic function, therefore for all $A, Z \in \mathcal{M}$ we have

$$\begin{aligned} h_r(A) &= h_r(Z) + < \partial h_r(Z), A-Z > \\ &\quad +(A-Z)^T\partial^2 h_r(Z)(A-Z) \\ &\ge h_r(Z) + < \partial h_r(Z), A-Z > \end{aligned}$$

$$= \quad h_r(Z) + < \Pi_{\mathcal{M}_r}(Z), A - Z > \tag{4.3}$$

The last equality holds because $\Pi_{\mathcal{M}_r}(A) \in \partial h_r(A)$. To show this, we introduce the following proposition:

Proposition 4.1. *[Yan, 2010, Proposition 2.16] Let matrix $A \in R^{l\times k}$ has above singular value decomposition. Define the function $h_r(A)$ as Equation (4.2). Then we have that $h_r(A)$ is convex and subdifferentials of $h_r(A)$ is given as:*

$$\Pi_{\mathcal{M}_r}(A) \in \partial h_r(A). \tag{4.4}$$

We further note that by computing $\Pi_{\mathcal{M}_r}(A)$ through (2.6), the Euclidean distance between A and its projection on r-rank matrix set $\mathcal{M}_r$, denoted as $g_r(A)$, can be computed as

$$\begin{aligned} g_r(A) &= \frac{1}{2}\|A - \Pi_{M_r}(A)\|^2 \\ &= \frac{1}{2}\|U_A[\Sigma(A) - \Sigma_r(A)]V_A^T\|^2 \\ &= \sum_{i=r+1}^{l} \sigma_i^2(A) \\ &= \sum_{i=1}^{l} \sigma_i^2(A) - \sum_{i=1}^{r} \sigma_i^2(A) \\ &= \frac{1}{2}\|A\|^2 - h_r(A) \end{aligned} \tag{4.5}$$

Given the fact that for any $A \in \mathcal{M}$, $\text{rank}(A) \leq r$ if and only if $\sigma_{i+1}(A) = ... = \sigma_L(A) = 0$, we rewrite Problem (4.1) by replacing the rank constraint ($X \in \mathcal{M}_r$):

$$\begin{aligned} \min \quad & f(X) := \frac{1}{2}\|W \circ (X - Y)\|^2 \\ \text{s.t.} \quad & X \in \mathcal{H} \\ & g_r(X) = 0 \end{aligned} \tag{4.6}$$

In fact, Problem (4.6) is equivalent to (4.1) because when $rank(X) \leq r$, we have $g_r(X) = \sum_{i=r+1}^{l} \sigma_i^2(X) = 0$. For any $A, Z \in \mathcal{M}$, defining $g_r^m(A, Z)$ as

$$g_r^m(A, Z) := \frac{1}{2}\|A\|^2 - h_r(Z) - < \Pi_{\mathcal{M}_r}(Z), A - Z > \tag{4.7}$$

then we have following properties.

Proposition 4.2. *Given $g_r(A)$ and $g_r^m(A, Z)$ defined in (4.5) and (4.7), we have*

$$g_r^m(A, A) = g_r(A) \tag{4.8}$$

$$g_r^m(A, Z) \geq g_r(A) \tag{4.9}$$

Proof. Equality (4.8) holds because we have

$$\begin{aligned} g_r^m(A, A) &= \frac{1}{2}\|A\|^2 - h_r(A) - < \Pi_{\mathcal{M}_r}(A), A - A > \\ &= \frac{1}{2}\|A\|^2 - h_r(A) \\ &= g_r(A) \end{aligned}$$

Using Equation (4.3) and (4.5), it is enough to prove (4.9):

$$\begin{aligned} g_r^m(A, Z) &= \frac{1}{2}\|A\|^2 - h_r(Z) - < \Pi_{\mathcal{M}_r}(Z), A - Z > \\ &\geq \frac{1}{2}\|A\|^2 - h_r(A) \\ &= g_r(A) \end{aligned}$$

This completes our proof. □

When Proposition 4.2 holds, $g_r^m(A, Z)$ is known as a majorization function of $g_r(A)$.

4.2.2 The Majorized Penalty Method

In previous discussion we mentioned that the rank constraint in (4.1) causes the difficulties in handling these problems through alternating projection method. Now we consider to use the penalty method to rewrite (4.6) by taking the trade-off between the rank constraint and weighted least square distance as

$$\begin{aligned} \min \quad & f_\rho(X) := \frac{1}{2}\|W \circ (X - Y)\|^2 + \rho g_r(X) \\ \text{s.t.} \quad & X \in \mathcal{H} \end{aligned} \tag{4.10}$$

where $\rho > 0$ is the penalty parameter. A larger choice of ρ means we penalise the rank constraint violations with more severity. We note that Problem (4.10) is not equivalent to Problem (4.6) because the rank of optimal solution to (4.10) may not be smaller than r, especially when the penalty parameters ρ is not large enough. Here we illustrate the relationship between the global optimal solutions to (4.6) and (4.10) by introducing two propositions.

Proposition 4.3. *Let $X_r^* \in \mathcal{M}$ be the global solution to problem (4.10). If the rank of X_r^* is not larger than r, then X_r^* is a global optimal solution to problem (4.6).*

Proof. Let $X_r \in \mathcal{M}$ to be any feasible solution to problem (4.6). Because X_r^* is the global solution to (4.10) and its rank is not larger than r, we have $g_r(X_r^*) = 0$ and

$$\begin{aligned} f(X_r^*) &= f(X_r^*) + \rho g_r(X_r^*) \\ &= f_\rho(X_r^*) \leq f(X_r) + \rho g_r(X_r) = f(X_r) \end{aligned}$$

So X_r^* is also the global optimal solution to (4.6). □

Proposition 4.4. *Let $\varepsilon > 0$ be a given positive number and $X^* \in \mathcal{M}$ a optimal solution to least square problem:*

$$\begin{aligned} \min \quad & \frac{1}{2}\|W \circ (X - Y)\|^2 \\ s.t. \quad & X \in \mathcal{H} \end{aligned}$$

Assume $\rho > 0$ is chosen such that $(f(X_r) - f(X_r^*))/\rho \leq \varepsilon$ and let $\overline{X}_r$ be a global optimal solution to (4.6). Then we have

$$g_r(X_r^*) \leq \varepsilon \qquad \text{and} \qquad f(X_r^*) \leq f(\overline{X}_r) - \rho g_r(X_r^*) \leq f(\overline{X}_r) \tag{4.11}$$

Proof. From the proof of Proposition (4.3) we have

$$f(X_r) \geq f(X_r^*) + \rho g_r(X_r^*) \geq f(X^*) + \rho g_r(X_r^*)$$

It indicates

$$g_r(X_r^*) \leq \frac{f(X_r) - f(X^*)}{\rho} \leq \varepsilon$$

Because $\overline{X}_r$ is a global optimal solution to (4.6), then we have $g_r(\overline{X}_r) = 0$. So at the same time, the following inequality holds:

$$f(\overline{X}_r) + \rho g_r(\overline{X}_r) = f_\rho(\overline{X}_r) \geq f_\rho(X_r^*) = f(X_r^*) + \rho g_r(X_r^*)$$

As a result,

$$f(X_r^*) \leq f(\overline{X}_r) - \rho g_r(X_r^*) \leq f(\overline{X}_r)$$

□

Proposition 4.3 and 4.4 has also been proved in a similar case by Sun [2010]. These two propositions support us to solve the penalized problem (4.10) instead of (4.6). Next we consider to tackle (4.10) by introducing the majorization approaches since we have found a majorization function $g_r^m(X, Z)$. Define the new function:

$$f_\rho^m(X, Z) := \frac{1}{2}\|W \circ (X - Y)\|^2 + \rho g_r^m(X, Z) \tag{4.12}$$

we have the following lemma:

Lemma 4.5. *Given $f_\rho(X)$ and $f_\rho^m(X,Z)$ defined in (4.10) and (4.12), we have*

$$\begin{aligned} f_\rho^m(X,X) &= f_\rho(X) \\ f_\rho^m(X,Z) &\geq f_\rho(X) \end{aligned}$$

The proof of Lemma 4.5 is straightforward using Proposition 4.2. In this case $f_\rho^m(X,Z)$ is thought to be the majorization function of $f_\rho(X)$ as well. We now consider solving the following majorization problem so that it enjoys the properties of majorization scheme

$$\begin{aligned} \min \quad & f_\rho^m(X,Z) = \frac{1}{2}\|W \circ (X-Y)\|^2 + \rho g_r^m(X,Z) \\ \text{s.t.} \quad & X \in \mathcal{H} \end{aligned} \tag{4.13}$$

Set $X^0 = Y$ and suppose we have current iterate X^ν, the next iterate $X^{\nu+1}$ is computed by solving the minimization problem:

$$X^{\nu+1} \in \arg\min f_\rho^m(X, X^\nu) \qquad \text{s.t. } X \in \mathcal{H} \tag{4.14}$$

Note when Lemma 4.5 holds, we have the following proposition for the sequence $\{X^\nu\}$ generated through (4.14).

Proposition 4.6. *Let the sequence $\{X^\nu\}$ be the iterate computed through (4.14), we have*

$$f_\rho(X^{\nu+1}) \leq f_\rho(X^\nu) \qquad \text{for } \nu = 0, 1, \ldots \tag{4.15}$$

That is to say, the function value $f_\rho(X^\nu)$ is non-increasing to ν.

Proof. From Proposition 4.5 we easily have

$$f_\rho(X^\nu) = f_\rho^m(X^\nu, X^\nu) \tag{4.16}$$

$$f_\rho(X^{\nu+1}) \leq f_\rho^m(X^{\nu+1}, X^\nu) \tag{4.17}$$

Then by solving Problem (4.14) , we have

$$f_\rho^m(X^{\nu+1}, X^\nu) \leq f_\rho^m(X^\nu, X^\nu) \tag{4.18}$$

As a result,

$$f_\rho(X^{\nu+1}) \leq f_\rho^m(X^{\nu+1}, X^\nu) \leq f_\rho^m(X^\nu, X^\nu) = f_\rho(X^\nu) \tag{4.19}$$

□

4.2.3 Convergence of quadratic penalty approach

The classical quadratic penalty methods try to solve a sequence of penalty problems:

$$X^\nu = \arg\min \; F_{\rho_\nu}(X), \quad \text{s.t.} \quad X \in \mathcal{H}, \tag{4.20}$$

where the sequence $\rho_\nu > 0$ is increasing and goes to ∞. By following the standard argument (e.g., [Nocedal and Wright, 2006, Thm. 17.1]), one can establish that every limit of $\{X^\nu\}$ is also a global solution of (1.2). However, in practice, it is probably as difficult to find a global solution for (4.20) as for the original problem (1.2). Therefore, only an approximate solution of (4.20) is possible. To quantify the approximation, we recall the optimality conditions relating to both the original and penalized problems.

It follows from the optimality theorem [Rockafellar and Wets, 2009, Thm. 8.15] that we say $\widehat{X} \in \mathcal{H}$ satisfies the first-order optimality condition of (1.2) if

$$0 \in \nabla f(\widehat{X}) + \widehat{\lambda} \partial d_{\mathcal{M}_r}(\widehat{X}) + \mathcal{H}^\perp, \tag{4.21}$$

where $\widehat{\lambda}$ is the Lagrangian multiplier and $d_{\mathcal{M}_r}$ denotes the distance function to low rank space, i.e., $d_{\mathcal{M}_r} = \min\{\|X - Z\| \mid Z \in \mathcal{M}_r\}$. Similarly, we say $X^\nu \in \mathcal{H}$ satisfies the first-order optimality condition of the penalty problem (4.10) if

$$0 \in \nabla f(X^\nu) + \rho_\nu \, \partial g_r(X^\nu) + \mathcal{H}^\perp. \tag{4.22}$$

We generate $X^\nu \in \mathcal{H}$ such that the condition (4.22) is approximately satisfied:

$$\|P_{\mathcal{H}}(\nabla f(X^\nu) + \rho_\nu(X^\nu - \Pi_{\mathcal{M}_r}(X^\nu)))\| \le \epsilon_\nu, \tag{4.23}$$

where $\epsilon_\nu \downarrow 0$. We can establish the following convergence result.

Theorem 4.7. *We assume the sequence $\{\rho_\nu\}$ goes to ∞ and $\{\epsilon_\nu\}$ decreases to 0. Suppose each approximate solution X^ν is generated to satisfy (4.23). Let $\widehat{X}$ be an accumulation point of $\{X^\nu\}$ and we assume*

$$\partial d_{\mathcal{M}_r}(\widehat{X}) \cap \mathcal{H}^\perp = \emptyset. \tag{4.24}$$

Then $\widehat{X}$ satisfies the first-order optimality condition (4.21).

Proof. Suppose $\widehat{X}$ is the limiting point of the subsequence $\{X^\nu\}_{\mathcal{K}}$. We consider the following two cases.

Case 1. There exists an infinite subsequence $\mathcal{K}_1$ of $\mathcal{K}$ such that $\operatorname{rank}(X^\nu) \le r$ for $\nu \in \mathcal{K}_1$. This would imply $\partial g_r(X^\nu) = \{0\}$, which with (4.23) implies $\|\mathcal{P}_{\mathcal{H}}(\nabla f(X^\nu))\| \to 0$. Hence (4.21) holds at $\widehat{X}$ with the choice $\widehat{\lambda} = 0$.

Case 2. There exists an index ν_0 such that $X^\nu \notin \mathcal{M}_r$ for all $\nu_0 \le \nu \in \mathcal{K}$. In this case, we assume that there exists an infinite subsequence $\mathcal{K}_2$ of $\mathcal{K}$ such that $\{(X^\nu - \Pi_{\mathcal{M}_r}(X^\nu))/d_{\mathcal{M}_r}(X^\nu)\}$ has the limit $\mathbf{v}$. We note that $(X^\nu - \Pi_{\mathcal{M}_r}(X^\nu))/d_{\mathcal{M}_r}(X^\nu) \in \partial d_{\mathcal{M}_r}(X^\nu)$ for $\nu \ge \nu_0$ by [Rockafellar and Wets, 2009, (8.53)]. Therefore, its limit $\mathbf{v} \in \partial d_{\mathcal{M}_r}(\widehat{X})$ by the upper semicontinuity. By the assumption (4.24), we have $\mathbf{v} \notin \mathcal{H}^\perp$. Since $\mathcal{H}$ is a subspace, $\mathcal{P}_{\mathcal{H}}(\cdot)$ is a linear operator. It follows from (4.23) that

$$\rho_\nu\|P_{\mathcal{H}}(X^\nu - \Pi_{\mathcal{M}_r}(X^\nu))\| - \|P_{\mathcal{H}}(\nabla f(X^\nu))\| \le \|P_{\mathcal{H}}(\nabla f(X^\nu) + \rho_\nu(X^\nu - \Pi_{\mathcal{M}_r}(X^\nu))\| \le \epsilon_\nu.$$

Hence

$$\|P_{\mathcal{H}}(X^\nu - \Pi_{\mathcal{M}_r}(X^\nu))\| \le \frac{1}{\rho_\nu}\Big(\epsilon_\nu + \|P_{\mathcal{H}}(\nabla f(X^\nu))\|\Big),$$

which, for $\nu \geq \nu_0$, is equivalent to

$$d_{\mathcal{M}_r}(X^\nu)\|P_{\mathcal{H}}(X^\nu - X_r^\nu)/d_{\mathcal{M}_r}(X^\nu)\| \leq \frac{1}{\rho_\nu}\Big(\epsilon_\nu + \|P_{\mathcal{H}}(\nabla f(X^\nu))\|\Big).$$

Taking limits on $\{X^\nu\}_{\nu\in\mathcal{K}_2}$ and using the fact $\rho_\nu \to \infty$ leads to $d_{\mathcal{M}_r}(X^*)\|P_{\mathcal{H}}(\mathbf{v})\| = 0$. Since $\mathbf{v} \notin \mathcal{H}^\perp$, we have $\|P_{\mathcal{H}}(\mathbf{v})\| > 0$, which implies $d_{\mathcal{M}_r}(X^*) = 0$. That is, X^* is a feasible point of (1.2). Now let $\lambda_\nu := \rho_\nu d_{\mathcal{M}_r}(X^\nu)$, we then have

$$\lambda_\nu \frac{X^\nu - \Pi_{\mathcal{M}_r}(X^\nu)}{d_{\mathcal{M}_r}(X^\nu)} = -\nabla f(X^\nu) + \xi^\nu, \quad \xi^\nu := \nabla f(X^\nu) + \rho_\nu(X^\nu - \Pi_{\mathcal{M}_r}(X^\nu)).$$

Projecting on both sides to $\mathcal{H}$ yields

$$\lambda_\nu P_{\mathcal{H}}\left(\frac{X^\nu - \Pi_{\mathcal{M}_r}(X^\nu)}{d_{\mathcal{M}_r}(X^\nu)}\right) = P_{\mathcal{H}}(-\nabla f(X^\nu)) + P_{\mathcal{H}}(\xi^\nu). \tag{4.25}$$

Computing the inner product on both sides with $P_{\mathcal{H}}((X^\nu - \Pi_{\mathcal{M}_r}(X^\nu))/d_{\mathcal{M}_r}(X^\nu))$, taking limits on on the sequence indexed by $\mathcal{K}_2$, and using the fact $P_{\mathcal{H}}(\xi^\nu) \to 0$ due to (4.23), we obtain

$$\lim_{\nu\in\mathcal{K}_2} \lambda_\nu \|\mathbf{v}\|^2 = \langle \mathbf{v},\ P_{\mathcal{H}}(\nabla f(\widehat{X}))\rangle.$$

We then have

$$\widehat{\lambda} = \lim_{\nu\in\mathcal{K}_2} \lambda_\nu = \frac{1}{\|\mathbf{v}\|^2}\langle \mathbf{v},\ P_{\mathcal{H}}(\nabla f(\widehat{X}))\rangle.$$

Taking limits on both sides of (4.25) yields

$$P_{\mathcal{H}}(\nabla f(\widehat{X}) + \widehat{\lambda}\mathbf{v}) = 0,$$

which is sufficient for

$$0 \in \nabla f(\widehat{X}) + \widehat{\lambda}\partial d_{\mathcal{M}_r}(\widehat{X}) + \mathcal{H}^\perp.$$

This completes our result. □

Remark 1. Condition (4.24) can be equivalently interpreted as that any $0 \neq \mathbf{v} \in \partial d_{\mathcal{M}_r}(\widehat{X})$ is linearly independent of any set of basis of $\mathcal{H}^\perp$. Therefore, (4.24) can be seen as a generalization of the linear independence assumption required in the classical

quadratic penalty method for a similar convergence result with all the functions involved being assumed continuously differentiable, see [Nocedal and Wright, 2006, Thm. 17.2]. In fact, what we really needed in our proof is that there exists a subsequence $\{(X^\nu - \Pi_{\mathcal{M}_r}(X^\nu))/d_{\mathcal{M}_r}(X^\nu)\}$ in Case (ii) such that its limit $\mathbf{v}$ does not belong to $\mathcal{H}^\perp$. That could be much weaker than the sufficient condition (4.24).

Thm. 4.7 establishes the global convergence of quadratic penalty method when the penalty parameter approaches infinity, which drives $g_r(X^\nu)$ to become smaller and smaller. In practice, however, we often fix ρ and solve for X^ν. We are interested how far X^ν is from being a first-order optimal point of the original problem. For this purpose, we introduce the approximate KKT point, which keeps in the first-order optimality condition (4.22) with an additional requirement that $g_r(X)$ is small enough.

Definition 4.8. (ϵ-approximate KKT point) Consider the penalty problem (4.10) and $\epsilon > 0$ is given. We say a point $\widehat{X} \in \mathcal{H}$ is an ϵ-approximate KKT point of (1.2) if

$$0 \in \nabla f(\widehat{X}) + \rho\, \partial g_r(\widehat{X}) + \mathcal{H}^\perp \qquad \text{and} \qquad g_r(\widehat{X}) \leq \epsilon.$$

4.2.4 Solving the Subproblem

Until now we proposed the framework of majorized penalty method that approximating the result of Problem (4.1) sequentially with convergent results. One remaining question is how to solve the Sub-Problem (4.14) to make sure the inequalities (4.19) holds. Firstly we have following proposition:

Proposition 4.9. *We have the following equivalent minimization problem to Problem (4.14)*

$$\arg\min_X \; f_\rho^m(X, X_\rho^\nu) = \arg\min_X \; \frac{1}{2}\|W_\rho \circ (X - X_\rho^\nu)\|^2 \tag{4.26}$$

where $W_\rho := \sqrt{\rho E + W \circ W}$ *and matrix* $E = \mathbf{1_{m,n}}$ *with all entities equal to 1; "*$\sqrt{\ }$*" represents the componentwise root, e.g.,* $(\sqrt{A})_{i,j} = \sqrt{A_{i,j}}$ *for* $i = 1, ..., m$ *and* $j = 1, ..., n$. X_ρ^ν *is computed by:*

$$X_\rho^\nu := W_\rho^{(-1)} \circ (W \circ W \circ Y + \rho \Pi_{\mathcal{M}_r}(X^\nu)) \tag{4.27}$$

Proof. Taking Equation (4.7) into the objective function of Problem (4.14) we can easily get

$$\begin{aligned}
f_\rho^m(X, X^\nu) &= \frac{1}{2}\|W \circ (X - Y)\|^2 + \rho g_r^m(X, X^\nu) \\
&= \frac{1}{2}\|W \circ (X - Y)\|^2 + \frac{\rho}{2}\|X\|^2 - \rho h_r(X^\nu) - \rho < \Pi_{M_r}(X^\nu), X - X^\nu > \\
&= \frac{\rho}{2}\|X\|^2 + \frac{1}{2}\|W \circ X\|^2 - < X, W \circ W \circ Y > - < X, \rho\Pi_{\mathcal{M}_r}(X^\nu) > \\
&\quad \underbrace{+ \frac{1}{2}\|W \circ Y\|^2 - \rho h_r(X^\nu) + \rho < X^\nu, \Pi_{\mathcal{M}_r}(X^\nu) >}_{:=\Delta_1} \\
&= \frac{1}{2}\| \underbrace{\sqrt{\rho E + W \circ W}}_{=:W_\rho} \circ X\|^2 - \langle X, W \circ W \circ Y + \rho\Pi_{\mathcal{M}_r}(X^\nu)\rangle + \Delta_1 \\
&= \frac{1}{2}\|W_\rho \circ X\|^2 - \langle W_\rho \circ X, W_\rho^{(-1)} \circ (W \circ W \circ Y + \rho\Pi_{\mathcal{M}_r}(X^\nu))\rangle + \Delta_1 \\
&= \frac{1}{2}\|W_\rho \circ (X - W_\rho^{(-1)} \circ (W \circ W \circ Y + \rho\Pi_{\mathcal{M}_r}(X^\nu)))\|^2 \\
&\quad \underbrace{-\frac{1}{2}\|W_\rho^{(-1)} \circ (W \circ W \circ Y + \rho\Pi_{\mathcal{M}_r}(X^\nu))\|^2 + \Delta_1}_{:=\Delta_2} \\
&= \frac{1}{2}\|W_\rho \circ (X - \underbrace{W_\rho^{(-1)} \circ (W \circ W \circ Y + \rho\Pi_{\mathcal{M}_r}(X^\nu))}_{:=X_\rho^\nu})\|^2 + \Delta_2 \\
&= \frac{1}{2}\|W_\rho \circ (X - X_\rho^\nu)\|^2 + \Delta_2
\end{aligned} \tag{4.28}$$

where we define Δ_1, Δ_2 and X_ρ^ν as following

$$\begin{aligned}
\Delta_1 &= \frac{1}{2}\|W \circ Y\|^2 - \rho h_r(X^\nu) + \rho < X^k, \Pi_{\mathcal{M}_r}(X^k) > \\
\Delta_2 &= \frac{1}{2}\|W_\rho^{(-1)} \circ (W \circ W \circ Y + \rho\Pi_{\mathcal{M}_r}(X^\nu))\|^2 + \Delta_1 \\
X_\rho^\nu &= W_\rho^{(-1)} \circ (W \circ W \circ Y + \rho\Pi_{\mathcal{M}_r}(X^\nu)
\end{aligned}$$

Then the Proposition 4.9 is proved because Δ_2 is a constant item that is independent with variable X. □

According to Proposition 4.5 and 4.9, we compute $X^{\nu+1}$ iteratively by solving the following problem to get the estimated low rank Hankel matrix:

$$X^{\nu+1} \in \arg\min \frac{1}{2}\|W_\rho \circ (X - X_\rho^\nu)\|^2 \qquad \text{s.t. } X \in \mathcal{H} \tag{4.29}$$

while Problem (4.29) can be easily solved through the weighted diagonal averaging (2.4). The algorithm of majorized penalty method to solving Problem (4.1) is summarized as following:

Algorithm 8: Algorithm: Penalised Method of Alternating Projection (pMAP)

Result: Approximated low rank Hankel matrix $\hat{X}$ and estimated finite rank time series $\widehat{\mathbf{x}} = \mathcal{H}^{-1}(X^{\nu+1})$

Initialization: Trajectory matrix Y, rank constraint r, penalty parameter ρ, $W_\rho = \sqrt{\rho E + W \circ W}$ and stop criterion $STOP$. Construct $X^0 = Y$ and set $\nu = 0$.;

while *The stop condition STOP is not met* **do**

Compute X_ρ^ν

$$X_\rho^\nu := W_\rho^{-1} \circ (W \circ W \circ Y + \rho \Pi_{\mathcal{M}_r}(X^\nu))$$

Compute $X^{\nu+1}$ by solving Problem (4.29)

$$X^{\nu+1} \in \arg\min \frac{1}{2}\|W_\rho \circ (X - X_\rho^\nu)\|^2 \qquad \text{s.t. } X \in \mathcal{H}$$

$\nu \to \nu + 1$

Alg.8 indicates at each iterate of pMAP, the current solution $X^{\nu+1}$ is in fact obtained by the following update:

$$X^{\nu+1} = \frac{W^{(2)}}{\rho + W^{(2)}} \circ A + \frac{\rho}{\rho + W^{(2)}} \circ \Pi_{\mathcal{H}}(\Pi_{\mathcal{M}_r}(X^\nu)), \tag{4.30}$$

where $W^{(2)} := W \circ W$ and the division $W^{(2)}/(\rho + W^{(2)})$ is taken componentwise. Compared with the method of alternating projection, this update is just a convex combination of the observation matrix A and the MAP iterate in the method of alternating projection. In the special case that $W = 0$ (which completely ignores the objective in Problem (4.1)) or $\rho = \infty$, (4.30) reduces to MAP.

4.2.5 Convergence Analysis

Proposition.4.6 shows that the functional value $f_\rho(X^{\nu+1})$ is non-increasing to ν. In this section we establish the convergence for pMAP.

Theorem 4.10. *Let the function $f_\rho(X)$ be defined in (4.10) and $\{X^\nu\}$ be the sequence generated by Alg.8.*

1. *We have*

$$f_\rho(X^{\nu+1}) - f_\rho(X^\nu) \leq -\frac{\rho}{2}\|X^{\nu+1} - X^\nu\|^2, \qquad \nu = 1, 2, ...$$

2. *Let $\widehat{X}$ be ab accumulation point of $\{X^\nu\}$, then for any $X \in \mathcal{H}$, we have*

$$\langle \nabla f(\widehat{X}) + \rho\widehat{X} + \rho\Pi_{\mathcal{M}_r}(-\widehat{X}), X - \widehat{X}\rangle \geq 0$$

That is, $\widehat{X}$ is a stationary point of the problem (4.10). Moreover, for a given $\epsilon > 0$, if $X^0 \in \mathcal{M}_r \cap \mathcal{H}$ and

$$\rho \geq \rho_\epsilon := \frac{f(X^0)}{\epsilon},$$

then $\widehat{X}$ is an ϵ-approximate KKT point of (4.1).

Proof. 1. Firstly we have

$$f(X^\nu) - f(X^{\nu+1}) \geq \langle \nabla f(X^{\nu+1}), X^\nu - X^{\nu+1}\rangle \tag{4.31}$$

This is because the convexity of cost function $f(X)$. The second fact is

$$\|X^{\nu+1}\|^2 - \|X^\nu\|^2 = 2\langle X^{\nu+1} - X^\nu, X^{\nu+1}\rangle - \|X^{\nu+1} - X^\nu\|^2 \tag{4.32}$$

Let $A = X^{\nu+1}$ and $Z = X^\nu$, from (4.3) we have

$$h_r(X^{\nu+1}) - h_r(X^\nu) \geq \langle \Pi_{\mathcal{M}_r}(X^\nu), X^{\nu+1} - X^\nu\rangle \tag{4.33}$$

The last fact is the optimality condition of problem (4.29) that, $\forall X \in \mathcal{H}$ we have

$$\langle \nabla f(X^{\nu+1}) + \rho(X^{\nu+1} - \Pi_{\mathcal{M}_r}(X^{\nu})), X - X^{\nu+1} \rangle \geq 0 \tag{4.34}$$

Combining all facts discussed above, we can deduce the upper bond of functional error for $f_\rho(X^\nu)$ as

$$\begin{aligned}
& f_\rho(X^{\nu+1}) - f_\rho(X^\nu) \\
&= f(X^{\nu+1}) - f(X^\nu) + \rho g_r(X^{\nu+1}) - \rho g_r(X^\nu) \\
&\overset{(4.31)}{\leq} \langle \nabla f(X^{\nu+1}), X^{\nu+1} - X^\nu \rangle + \rho g_r(X^{\nu+1}) - \rho g_r(X^\nu) \\
&= \langle \nabla(X^{\nu+1}), X^{\nu+1} - X^\nu \rangle \\
&\quad + \frac{\rho}{2}(\|X^{\nu+1}\|^2 - \|X^\nu\|^2) - \rho(h_r(X^{\nu+1}) - h_r(X^\nu)) \\
&\overset{(4.32)}{=} \langle \nabla(X^{\nu+1}) + \rho X^{\nu+1}, X^{\nu+1} - X^\nu \rangle \\
&\quad - \frac{\rho}{2}(\|X^{\nu+1} - X^\nu\|^2) - \rho(h_r(X^{\nu+1}) - h_r(X^\nu)) \\
&\overset{(4.33)}{\leq} \langle \nabla(X^{\nu+1}) + \rho X^{\nu+1} - \rho \Pi_{\mathcal{M}_r}(X^\nu), X^{\nu+1} - X^\nu \rangle \\
&\quad - \frac{\rho}{2}\|X^{\nu+1} - X^\nu\|^2 \\
&\overset{(4.34)}{\leq} -\frac{\rho}{2}\|X^{\nu+1} - X^\nu\|^2
\end{aligned}$$

From Proposition 4.6 we have the sequence $\{f_\rho(X^\nu)\}$ converges to a unknown constant, hence we have $\|X^{\nu+1} - X^\nu\|^2 \to 0$ and $(X^{\nu+1} - X^\nu) \to 0$ as well.

2. Let $\widehat{X}$ be the accumulation point of $\{X^\nu\}$. From (i) we have $(X^{\nu+1} - X^\nu) \to 0$, which means $\widehat{X}$ is the accumulation point of sequence $\{X^{\nu+1}\}$ as well. Then by taking the limits on the both side of inequality (4.34), we have

$$\langle \nabla f(\widehat{X}) + \rho\widehat{X} + \rho\Pi_{\mathcal{M}_r}(-\widehat{X}), X - \widehat{X} \rangle \geq 0$$

The condition of ϵ-approximate KKT point is proposed in [Zhou et al., 2018, Definition 3.1]. For a given point $\widehat{X}$ and the Lagrangian function $f_\rho(X)$, $\widehat{X}$ is said to be the ϵ-approximate KKT point if $\widehat{X} \in \mathcal{H}$, $g_r(\widehat{X}) \leq \epsilon$ and

$$\langle \partial f_\rho(X), X - \widehat{X} \rangle \geq 0 \tag{4.35}$$

It is straightforward that $\widehat{X} \in \mathcal{H}$ because each entry in sequence $\{X^\nu\}$ is calculated through weighted Hankel projection, so any X^ν is a Hankel matrix. (4.35) also holds because we have $\nabla f(\widehat{X}) + \rho\widehat{X} + \rho\Pi_{\mathcal{M}_r}(-\widehat{X}) \in \partial f_\rho(X)$. From Proposition.4.6 we have $f_\rho(X^0) \geq f_\rho(X^1) \geq ... \geq f_\rho(\widehat{X})$, which means

$$\begin{aligned} f(X^0) &= f(X^0) + \rho g_r(X^0) = f_\rho(X^0) \\ &\geq f_\rho(\widehat{X}) = f(\widehat{X}) + \rho g_r(\widehat{X}) \geq \rho g_r(\widehat{X}) \end{aligned}$$

The first equality holds because $g_r(X^0) = 0$ when $X^0 \in \mathcal{M}_r$. As a result,

$$g_r(\widehat{X}) \leq \frac{f(X^0)}{\rho} \leq \frac{f(X^0)}{\rho_\epsilon} = \epsilon. \tag{4.36}$$

With all three condition being satisfied, $\widehat{X}$ is an ϵ-approximate KKT point of (4.6).

□

4.2.6 Final rank and linear convergence

This part reports two results. One is on the final rank of the output of pMAP and the rank is always bigger than the desired rank r unless A is already an optimal solution of (1.2). The other is on the conditions that ensure a linear convergence rate of pMAP. For this purpose, we need the following result.

Proposition 4.11. *[Feppon and Lermusiaux, 2018, Thm. 25] Given the integer $r > 0$ and consider $\widehat{X} \in \mathbb{R}^{k\times\ell}$ of rank $(r+p)$ with $p \geq 0$. Suppose the SVD of $\widehat{X}$ is represented as $\widehat{X} = \sum_{i=1}^{r+p} \sigma_i \mathbf{u}_i \mathbf{v}_i^T$, where $\sigma_1(\widehat{X}) \geq \sigma_2(\widehat{X}) \geq \cdots \geq \sigma_{r+p}(\widehat{X})$ are the singular values of $\widehat{X}$ and $\mathbf{u}_i, \mathbf{v}_i$, $i = 1, \ldots, r+p$ are the left and right (normalized) eigenvectors. We assume $\sigma_r(\widehat{X}) > \sigma_{r+1}(\widehat{X})$ so that the projection operator $\Pi_{\mathcal{M}_r}(X)$ is uniquely defined in a neighbourhood of $\widehat{X}$. Then $\Pi_{\mathcal{M}_r}(X)$ is differentiable at $\widehat{X}$ and the directional derivative*

along the direction Y is given by

$$\nabla\Pi_{\mathcal{M}_r}(\widehat{X})(Y) = \Pi_{\mathcal{T}_{\mathcal{M}_r}(\widehat{X})}(Y) + \sum_{\substack{1\le i\le r\\ 1\le j\le p}} \left[\frac{\sigma_{r+j}}{\sigma_i - \sigma_{r+j}} \langle Y,\ \Phi^+_{i,r+j}\rangle \Phi^+_{i,r+j} \right.$$

$$\left. - \frac{\sigma_{r+j}}{\sigma_i - \sigma_{r+j}} \langle Y,\ \Phi^-_{i,r+j}\rangle \Phi^-_{i,r+j} \right]$$

where $\mathcal{T}_{\mathcal{M}_r}(\widehat{X})$ is the tangent subspace of $\mathcal{M}_r$ at $\widehat{X}$ and

$$\Phi^{\pm}_{i,r+j} = \frac{1}{\sqrt{2}} \left(\mathbf{u}_{r+j}\mathbf{v}_i^T \pm \mathbf{u}_i\mathbf{v}_{r+j}^T \right).$$

Theorem 4.12. *Assume that $W > 0$ and $\widehat{X}$ be an accumulation point of $\{X^\nu\}$. The following hold.*

(i) rank$(\widehat{X}) > r$ unless A is already the optimal solution of (1.2).

(ii) Suppose $\widehat{X}$ has rank $(r+p)$ with $p > 0$. Let $\sigma_1 \ge \sigma_2 \ge \cdots \ge \sigma_k$ be the singular values of $\widehat{X}$. Define

$$w_0 := \min\{W_{ij}\} > 0, \qquad \epsilon_0 := \frac{w_0}{\rho}, \qquad \epsilon_1 := \frac{\epsilon_0}{4+3\epsilon_0}, \qquad c := \frac{1}{1+\epsilon_1} < 1.$$

Under the condition

$$\frac{\sigma_r}{\sigma_{r+1}} \ge \frac{8p}{\epsilon_0} + 1,$$

it holds

$$\|X^{\nu+1} - \widehat{X}\| \le c\|X^\nu - \widehat{X}\| \qquad \text{for } \nu \text{ sufficiently large.}$$

Consequently, the whole sequence $\{X^\nu\}$ converges linearly to $\widehat{X}$.

Proof. (i) Suppose $\widehat{X}$ is the limit of the subsequence $\{X^\nu\}_{k\in\mathcal{K}}$. We assume rank$(\widehat{X}) \le r$. It follows from Thm. 4.10 that

$$\{X^{\nu+1}\}_{k\in\mathcal{K}} \to \widehat{X} \quad \text{and} \quad \lim_{k\in\mathcal{K}} \Pi_{\mathcal{M}_r}(X^\nu) = \Pi_{\mathcal{M}_r}(\widehat{X}) = \widehat{X}.$$

Taking limits on both sides of (4.30) and using the fact that $\widehat{X}$ is Hankel, we get

$$\widehat{X} = \frac{W^{(2)}}{\rho + W^{(2)}} \circ A + \frac{\rho}{\rho + W^{(2)}} \circ \Pi_{\mathcal{H}}(\Pi_{\mathcal{M}_r}(\widehat{X})) = \frac{W^{(2)}}{\rho + W^{(2)}} \circ A + \frac{\rho}{\rho + W^{(2)}} \circ \widehat{X}.$$

Under the assumption $W > 0$, we have $\widehat{X} = A$. Consequently, $\mathrm{rank}(A) \le r$, implying that A is the optimal solution of (1.2). Therefore, we must have $\mathrm{rank}(\widehat{X}) > r$.

(ii) Let $\phi(X) := \Pi_{\mathcal{H}}(\Pi_{\mathcal{M}_r}(X))$. Since $\Pi_{\mathcal{M}_r}(X)$ is differentiable at $\widehat{X}$, so is $\phi(X)$. Moreover, the directional derivative of $\phi(X)$ at $\widehat{X}$ along the direction Y is given by

$$\nabla\phi(\widehat{X})Y = \Pi_{\mathcal{H}}(\nabla\Pi_{\mathcal{M}_r}(\widehat{X})Y) \qquad \text{and} \qquad \|\nabla\phi(\widehat{X})Y\| \le \|\nabla\Pi_{\mathcal{M}_r}(\widehat{X})Y\|. \tag{4.37}$$

The inequality above holds because $\Pi_{\mathcal{H}}(\cdot)$ is an orthogonal projection operation to a subspace and its operator norm is 1. The matrix in Prop. 4.11 have the following bounds.

$$\|\Phi^{\pm}_{i,r+j}\| \le \frac{1}{\sqrt{2}}\Big(\|\mathbf{u}_{r+j}\mathbf{v}_i^T\| + \|\mathbf{u}_i\mathbf{v}_{r+j}^T\|\Big) \le \frac{1}{\sqrt{2}}(1+1) = \sqrt{2},$$

$$\|\langle Y,\ \Phi^{\pm}_{i,r+j}\rangle\Phi^{\pm}_{i,r+j}\| \le \|\Phi^{\pm}_{i,r+j}\|^2\|Y\| \le 2\|Y\|.$$

Therefore,

$$\begin{aligned} & \left\| \sum_{\substack{1\le i\le r\\ 1\le j\le p}} \left[\frac{\sigma_{r+j}}{\sigma_i - \sigma_{r+j}}\langle Y,\ \Phi^{+}_{i,r+j}\rangle\Phi^{+}_{i,r+j} - \frac{\sigma_{r+j}}{\sigma_i - \sigma_{r+j}}\langle Y,\ \Phi^{-}_{i,r+j}\rangle\Phi^{-}_{i,r+j} \right] \right\| \\ \le\ & 4 \sum_{\substack{1\le i\le r\\ 1\le j\le p}} \frac{\sigma_{r+j}}{\sigma_i - \sigma_{r+j}}\|Y\| \le 4p\frac{\sigma_{r+1}}{\sigma_r - \sigma_{r+1}} = \frac{w_0}{2\rho} = \frac{1}{2}\epsilon_0\|Y\|. \end{aligned} \tag{4.38}$$

In the above, we used the fact that $\psi(t) := t/(\sigma_r - t)$ is an increasing function of t for $t < \sigma_r$. Prop. 4.11, (4.37) and (4.38) imply

$$\|\nabla\phi(\widehat{X})Y\| \le \|\Pi_{\mathcal{T}_{\mathcal{M}_r}(\widehat{X})}(Y)\| + \epsilon_0/2\|Y\| \le \|Y\| + \epsilon_0/2\|Y\| \le (1+\epsilon_0/2)\|Y\|.$$

The second equality above used the fact that the operator norm of $\Pi_{\mathcal{T}_{\mathcal{M}_r}(\widehat{X})}$ is not greater than 1 due to $\mathcal{T}_{\mathcal{M}_r}(\widehat{X})$ being a subspace. Since $\phi(\cdot)$ is differentiable at $\widehat{X}$, there exists

$\epsilon > 0$ such that

$$\|\phi(X) - \phi(\widehat{X}) - \nabla\phi(\widehat{X})(X - \widehat{X})\| \leq \frac{1}{4}\epsilon_0\|X - \widehat{X}\|, \qquad \forall \;\; X \in \mathcal{B}_\epsilon(\widehat{X}).$$

Therefore,

$$\begin{aligned}\|\phi(X) - \phi(\widehat{X})\| &\leq \|\phi(X) - \phi(\widehat{X}) - \nabla\phi(\widehat{X})(X - \widehat{X})\| + \|\nabla\phi(\widehat{X})(X - \widehat{X})\\ &\leq \frac{1}{4}\epsilon\|X - \widehat{X}\| + (1 + \epsilon_0/2)\|X - \widehat{X}\| = (1 + 3\epsilon/4)\|X - \widehat{X}\|.\end{aligned}$$

Now we are ready to quantify the error between X^ν and $\widehat{X}$ whenever $X^\nu \in \mathcal{B}_\epsilon(\widehat{X})$.

$$\begin{aligned}\|X^{\nu+1} - \widehat{X}\| &= \left\|\frac{\rho}{\rho + W^{(2)}} \circ (\phi(X^\nu) - \phi(\widehat{X}))\right\| \leq \frac{\rho}{\rho + w_0}\|\phi(X^\nu) - \phi(\widehat{X})\|\\ &\leq \frac{1 + 3\epsilon_0/4}{1 + \epsilon_0}\|X^\nu - \widehat{X}\| = c\|X^\nu - \widehat{X}\|.\end{aligned}$$

Consequently, $X^{\nu+1} \in \mathcal{B}_\epsilon(\widehat{X})$. Since $\{X^\nu\}_{\nu\in\mathcal{K}}$ converges to $\widehat{X}$, X^ν will eventually falls in $\mathcal{B}_\epsilon(\widehat{X})$, which implies that the whole sequence $\{X^\nu\}$ will converge to $\widehat{X}$ and eventually converges at a linear rate. □

Remark 3. (Implication on MAP) When the weight matrix $W = 0$, pMAP reduces to MAP according to (4.30). Thm. 4.10(i) implies

$$\|X^{\nu+1} - \Pi_{\mathcal{M}_r}(X^{\nu+1})\|^2 - \|X^\nu - \Pi_{\mathcal{M}_r}(X^\nu)\|^2 \leq -\|X^{\nu+1} - X^\nu\|^2, \tag{4.39}$$

which obviously implies

$$\|X^{\nu+1} - \Pi_{\mathcal{M}_r}(X^{\nu+1})\| \leq \|X^\nu - \Pi_{\mathcal{M}_r}(X^\nu)\|. \tag{4.40}$$

The decrease property (4.40) was known in [Chu et al., 2003, Eq.(4.1)] and was used there to ascertain that MAP is a descent algorithm. Our improvement bound (4.39) says a lightly more that the decrease each step in the function $\|X - \Pi_{\mathcal{M}_r}(X)\|$ is strict unless the update becomes unchanged. In this case ($W = 0$), the penalty parameter is just a scaling factor in the objective, hence the approximation KKT result in Thm. 4.10(ii)

does not apply to MAP. This probably explains why it is difficult to establish similar results for MAP.

Remark 4. (On linear convergence) In the general context of matrix completion, Lai and Varghese [2017] established a local linear convergence of MAP under the following two assumptions. We describe them in terms of the Hankel matrix completion. (i) The partially observed data $\mathbf{a}$ can be completed to a rank r Hankel matrix M. (ii) A transversality condition (see [Lai and Varghese, 2017, Thm. 2]) holds at M. We emphasize that the result of Lai and Varghese [2017] is a local result that requires the initial point of MAP is close enough to M and the rank r assumption of M is also crucial to their analysis, which also motivated our proof. In contrast, our result is a global one and enjoys a linear convergence rate near the limit under a more realistic assumption $\sigma_r \gg \sigma_{r+1}$. One may have noticed that the convergence rate c though strictly less than 1 may be close to 1. This is also practically expected as MAP often converges slowly. But the more important point here is that in such a situation it ensures that the whole sequence converges. This global convergence justifies the widely used stopping criterion $\|X^{\nu+1} - X^{\nu}\| \leq \epsilon$.

4.3 Extension to complex-valued matrix

The results obtained in the previous sections are for real-valued matrix and they can be extended to complex-valued matrix by employing what is known as the Wirtinger calculus Wirtinger [1927]. We note that not all algorithms for Hankel matrix optimization have a straightforward extension from the real case to the complex case, see Condat and Hirabayashi [2015] for comments on some algorithms. We explain our extension below.

Suppose $f : \mathbb{C}^n \mapsto \mathbb{R}$ is a real-valued function in the complex domain. We write $\mathbf{z} \in \mathbb{C}^n$ as $\mathbf{z} = \mathbf{x} + j\mathbf{y}$ with $\mathbf{x}, \mathbf{y} \in \mathbb{R}^n$. The conjugate $\bar{\mathbf{z}} := \mathbf{x} - j\mathbf{y}$. Then we can write the function $f(\mathbf{z})$ in terms of its real variables $\mathbf{x}$ and $\mathbf{y}$. With a slight abuse of notation, we still denote it as $f(\mathbf{x}, \mathbf{y})$. In the case where the optimization of $f(\mathbf{z})$ can be equivalently represented as optimization of f in terms of its real variables, the partial derivatives $\partial f(\mathbf{x}, \mathbf{y})/\partial \mathbf{x}$ and $\partial f(\mathbf{x}, \mathbf{y})/\partial \mathbf{y}$ would be sufficient. For other cases where algorithms are

preferred to be executed in the complex domain, then the Wirtinger calculus Wirtinger [1927] is more convenient to use and it is well explained (and derived) in Kreutz-Delgado [2009]. The $\mathbb{R}$-derivative and the conjugate $\mathbb{R}$-derivative of f in the complex domain are defined respectively by

$$\frac{\partial f}{\partial \mathbf{z}} = \frac{1}{2}\left(\frac{\partial f}{\partial \mathbf{x}} - \mathbf{j}\frac{\partial f}{\partial \mathbf{y}}\right), \qquad \frac{\partial f}{\partial \bar{\mathbf{z}}} = \frac{1}{2}\left(\frac{\partial f}{\partial \mathbf{x}} + \mathbf{j}\frac{\partial f}{\partial \mathbf{y}}\right).$$

The $\mathbb{R}$-derivatives in the complex domain play the same role as the derivatives in the real domain because the following two first-order expansions are equivalent:

$$\begin{aligned} f(\mathbf{x}+\Delta\mathbf{x}, \mathbf{y}+\Delta\mathbf{y}) &= f(\mathbf{x},\mathbf{y}) + \langle \partial f/\partial \mathbf{x},\ \Delta\mathbf{x}\rangle + \langle \partial f/\partial \mathbf{y},\ \Delta\mathbf{y}\rangle + o(\|\Delta\mathbf{x}\| + \Delta\mathbf{y}\|) \\ f(\mathbf{z}+\Delta\mathbf{z}) &= f(\mathbf{z}) + 2\mathbf{Re}(\langle \partial \mathrm{f}/\partial \bar{\mathbf{z}},\ \Delta\mathbf{z}\rangle) + \mathrm{o}(\|\Delta\mathbf{z}\|). \end{aligned} \tag{4.41}$$

Here, we treat the partial derivatives as column vectors and $\mathbf{Re}(\mathbf{x})$ is the real part of $\mathbf{x}$. Note that in the first-order expansion in $f(\mathbf{z}+\Delta\mathbf{z})$ used the conjugate $\mathbb{R}$-derivative. Hence, we define the complex gradient to be $\nabla f(\mathbf{z}) := 2\partial f/\partial \bar{\mathbf{z}}$, when it exists. When f is not differentiable, we can extend the subdifferntial of f from the real case to the complex case by generalizing (4.41).

In order to extend Thm. 4.7, we need to characterize $\partial d_{\mathcal{M}_r}(X)$ in the complex domain. We may follow the route of Rockafellar and Wets [2009] to conduct the extension. For example, we may define the regular subgradient of $d_{\mathcal{M}_r}(X)$ [Rockafellar and Wets, 2009, Def. 8.3] to its complex counterpart by replacing the conjugate-gradient in the first-order expansion in (4.41) by a regular subgradient. We then define subdifferential through regular subgradients. With this definition in the complex domain, we may extend [Rockafellar and Wets, 2009, (8.53]) to derive formulae for $\partial d_{\mathcal{M}_r}(X)$. What we needed in the proof of Thm. 4.7 is $(X - \Pi_{\mathcal{M}_r}(X))/d_{\mathcal{M}_r}(X) \in \partial d_{\mathcal{M}_r}(X)$ when $X \notin \mathcal{M}_r$. The proof of this result follows a straightforward extension of the corresponding part in [Rockafellar and Wets, 2009, (8.53]) and if reproduced here would take up much space. Hence we omit it.

In order to extend the results in Sect. 4.2, we need the subdifferential of $h_r(X)$ in order to majorize $g_r(X)$. Since $h_r(X)$ is convex, its subdifferenial is easy to define.

Definition 4.13. The subdifferential $\partial h_r(X)$ is defined as

$$\partial h_r(X) = \Big\{ S \in \mathbb{C}^{k\times\ell} \mid h_r(Z) \geq h_r(X) + \mathbf{Re}\Big(\langle \overline{\mathrm{S}},\ \mathrm{Z}-\mathrm{X}\rangle\Big) \Big\}.$$

The following result is really what we needed in order to extend the results in Sect. 4.2 to the complex domain.

Proposition 4.14. *For any $X \in \mathbb{C}^{k\times\ell}$, we have $\mathcal{P}_{\mathcal{M}_r}(X) \subset \partial h_r(X)$.*

Proof. Let $\Pi_{\mathcal{M}_r}(X)$ stand for any element in $\mathcal{P}_{\mathcal{M}_r}(X)$. It is easy to verify the following identities:

$$\|X-Z\|^2 = \|X\|^2 + \|Z\|^2 - 2\mathbf{Re}\Big(\langle \overline{\mathrm{X}},\ \mathrm{Z}\rangle\Big) = \|\mathrm{X}\|^2 + \|\mathrm{Z}\|^2 - 2\mathbf{Re}\Big(\langle \overline{\mathrm{Z}},\ \mathrm{X}\rangle\Big). \tag{4.42}$$

We use (4.42) to compute

$$\begin{aligned}
& h_r(Z) - h_r(X) - \mathbf{Re}\Big(\langle \overline{\Pi_{\mathcal{M}_r}(\mathrm{X})},\ \mathrm{Z}-\mathrm{X}\rangle\Big) \\
= \ & \frac{1}{2}\|\Pi_{\mathcal{M}_r}(Z)\|^2 - \frac{1}{2}\|\Pi_{\mathcal{M}_r}(X)\|^2 + \underbrace{\frac{1}{2}\|\Pi_{\mathcal{M}_r}(X)-Z\|^2 - \frac{1}{2}\|\Pi_{\mathcal{M}_r}(X)\|^2 - \frac{1}{2}\|Z\|^2}_{\mathbf{Re}(\langle \overline{\Pi_{\mathcal{M}_r}(\mathrm{X})},\ \mathrm{Z}\rangle)} \\
& \underbrace{+\frac{1}{2}\|\Pi_{\mathcal{M}_r}(X)\|^2 + \frac{1}{2}\|X\|^2 - \frac{1}{2}\|\Pi_{\mathcal{M}_r}(X)-X\|^2}_{\mathbf{Re}(\langle \overline{\Pi_{\mathcal{M}_r}(\mathrm{X})},\ \mathrm{X}\rangle)} \\
= \ & \frac{1}{2}\|\Pi_{\mathcal{M}_r}(Z)\|^2 - \frac{1}{2}\|Z\|^2 + \frac{1}{2}\|\Pi_{\mathcal{M}_r}(X)-Z\|^2 \\
& \underbrace{-\left(\frac{1}{2}\|\Pi_{\mathcal{M}_r}(X)\|^2 - \frac{1}{2}\|X\|^2 + \frac{1}{2}\|\Pi_{\mathcal{M}_r}(X)-X\|^2\right)}_{=0} \\
= \ & \frac{1}{2}\|\Pi_{\mathcal{M}_r}(Z)\|^2 - \frac{1}{2}\|Z\|^2 + \frac{1}{2}\|\Pi_{\mathcal{M}_r}(X)-Z\|^2 \\
\geq \ & \frac{1}{2}\|\Pi_{\mathcal{M}_r}(Z)\|^2 - \frac{1}{2}\|Z\|^2 + \frac{1}{2}\|\Pi_{\mathcal{M}_r}(Z)-Z\|^2 = 0.
\end{aligned}$$

This proves the claim. □

A direct consequence is that

$$\partial g_r(X) = X - \partial h_r(X) \supset \mathcal{P}_{\mathcal{M}_r}(X)$$

and the majorization $g_r(X)$ through the subdifferential of $h_r(X)$ holds. The rest of the extension is straightforward and we do not repeat it here.

4.4 Numerical experiments

In this section we conduct two popular test problems, time series denoising and incomplete signal completion, to demonstrate the numerical performance of pMAP. The time series denoising problem aims to extract the noiseless data from polluted observations by removing the noise component, while incomplete signal completion problem tries to approximate the missing data in a incomplete complex valued signal.

In both numerical experiments, a solver is terminated when any of the following conditions is met

$$\frac{|F_\rho(X^{\nu+1}) - F_\rho(X^\nu)|}{\max\{1, F_\rho(X^\nu)\}} \leq ftol, \quad g_r(X^{\nu+1}) \leq gtol \quad \text{or} \quad \frac{\|X^{\nu+1} - X^\nu\|}{\|X^\nu\|} \leq tol.$$

here tol, $ftol$, $gtol$ are set as $1.0e-5$, $1.0e-7$ and $1.0e-8$ in both experiments. A solver will also be terminated if it reaches the maximum iteration steps upper-bound, which is set as 200. All codes used in below test are written in MATLAB and run on a laptop with a 16GB memory card, equipped with MATLAB 2019a.

4.4.1 Time Series Denoising

4.4.1.1 Experiment Introduction

In the first experiment we implement the proposed pMAP and some leading solvers including Structured Low Rank Approximation (SLRA, Usevich and Markovsky [2014]),

Cadzow iterations (Cadzow, Gillard [2010]) and Douglas-Rachford iterations (DRI, Condat and Hirabayashi [2015]) for real-valued time series de-noising. In this test we randomly generate noiseless time series $\mathbf{a} = (a_1, a_2, ..., a_n)$ via the following process:

$$a_t = \sum_{s=1}^{r} d_s(1+\alpha_s)^t cos(\frac{2\pi t}{\beta_s} - \tau_s), \qquad \text{for } t = 1, 2, ..., n$$

where all d_s, α_s, β_s and τ_s follow uniform distribution as $d_s \sim U[0, 10^3)$, $\alpha_s \sim U[-10^{-3}, 10^{-3})$, $\beta_s \sim U[6, 18)$ and $\tau_s \sim U[-\pi, \pi)$. It is known that for any $\{l, k\}$ such that $l + k - 1 = n$, the rank of Hankel matrix $A = \mathcal{T}(\mathbf{a}) \in \mathbb{R}^{l\times k}$ must be $2r$ when both l and k are no smaller than $2r$. We then construct the noisy time series $\mathbf{y}$ by adding the noise series ϵ to $\mathbf{a}$ as $\mathbf{y} = \mathbf{a} + \boldsymbol{\epsilon}$, where $\boldsymbol{\epsilon} = \{\epsilon_1, \epsilon_2, ..., \epsilon_n\}$ is the noise component and $\epsilon_t = \theta\frac{e_t}{\|e\|_2}\|a\|$. Here e_t is the white noise with mean 0 and variance 1. In this test, two scenarios are considered as $\{n, r\} = \{1000, 10\}$ and $\{2000, 20\}$ respectively. For each scenario we test three noise levels as $\theta = 0.1, 0.2$ and 0.5.

We further consider two weight choices in this experiment as:

1. $\{W_1\}_{i,j} = 1$, for $i = 1, ..., l$ and $j = 1, ..., k$;
2. $\{W_2\}_{i,j} = \frac{1}{i+j-1}$, for $i = 1, ..., l$ and $j = 1, ..., k$.

Both weights are standardised for comparison purpose. Note that Cadzow method do not allow the weight matrix to be selected flexibly rather than the default W_1.

4.4.1.2 Demonstration of convergence

Before coming to the numerical results, we firstly use this test to demonstrate the convergence of Alg.8 and also the updating strategy of penalty parameter ρ. The sequences of $F_\rho(X^\nu)$ at each iterate are plotted in Fig.4.1(a) for both W_1 and W_2. It can be observed that in both cases, the functional value $F_\rho(X^\nu)$ at each iterate kept decreasing and converged. This result is achieved by solving the subproblem at each iterate with the help of closed form solution (see equation chain (4.30)), hence the decreasing property (see Remark 2) always holds. We further plotted the value of $\|X^{\nu+1} - X^\nu\|$ at each

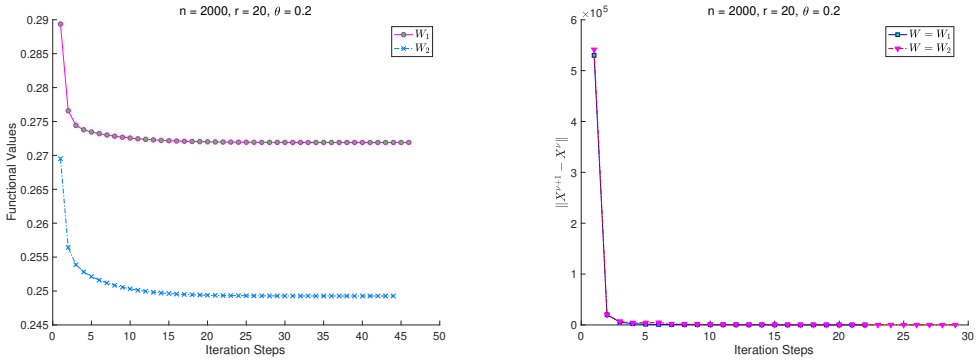

(a) $F_\rho(X^\nu)$ (b) $\|X^{\nu+1} - X^\nu\|$

FIGURE 4.1: Plot of $F_\rho(X^\nu)$ and $\|X^{\nu+1} - X^v\|$ at each iterate by pMAP. In this test we keep ρ as fixed.

iterate in Fig.4.1(b). We can find that sequence of $\|X^{\nu+1} - X^\nu\|$ is also decreasing and converges to zero, which is consistent with our proof in Theorem.4.10.

The behaviours of $\frac{\sigma_{r+1}}{\sigma_r}$ are shown in Fig.4.2 with respect to different ρ choices. In this and later experiments, ρ is initialised as $\rho^0 = 1.0e-2 \times m/n^2$ where n denotes the length of a time series or a signal and m denotes the amount of known observations which equals to n in this test. As we mentioned in Remark 1, the global convergence of quadratic penalty method can be established when ρ approaches infinity with $\frac{\sigma_{r+1}}{\sigma_r}$ approaches zero as shown in Fig.4.2(a), which means $g_r(X^\nu)$ will go to zero. However in this case, we may lose information from input matrix A because a much higher weight is given to the penalised item $g_r(X^\nu)$. By contrast if ρ is kept fixed as $\rho^\nu = \rho^0$ at each iterate, it can be seen from Fig.4.2(b) that $\frac{\sigma_{r+1}}{\sigma_r}$ fails to approach zero, which leads to output matrix with higher distances to the r-rank matrix set. Hence for all experiments in this paper, we will only update ρ by $\rho^{\nu+1} = 1.1\rho^\nu$ at each iterate when $\rho^\nu \leq n \times \min(W)$, where $\min(W)$ returns the minimal weights in W. The behaviour of convergence of Alg.8 appears consistence for other tests, so we will not repeat this demonstration for the rest experiments.

4.4.1.3 Numerical results

The numerical results are reported in Table.4.1 including the number of iterations (Iter), cpu time for computation (Time) and root of mean square error (RMSE) for each solver

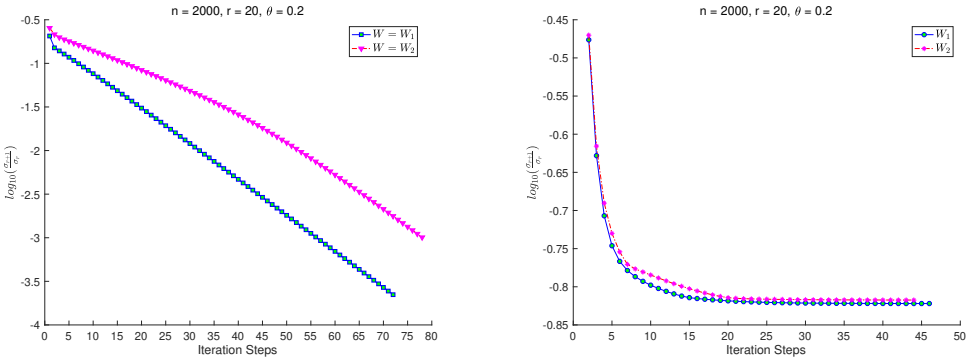

(a) $\frac{\sigma_{r+1}}{\sigma_r}$ with fixed ρ (b) $\frac{\sigma_{r+1}}{\sigma_r}$ with increasing ρ

FIGURE 4.2: Plot of $\frac{\sigma_{r+1}}{\sigma_r}$ at each iterate by pMAP. ρ is updated by $\rho^{\nu+1} = 1.1\rho^{\nu}$ in Fig.4.2(a) and fixed without updating in Fig.4.2(b).

which is calculated as

$$\text{RMSE} := \sqrt{\sum_{i\in\mathcal{I}}(\hat{x_i} - a_i)^2/|\mathcal{I}|}.$$

where $\hat{\mathbf{x}} = \{\hat{x_1}, ..., \hat{x_n}\}$ is obtained as $\hat{\mathbf{x}} = \mathcal{H}^{-1}(\widehat{X})$ and $\widehat{X}$ is the estimated result from a certain solver. $\mathcal{I}$ denotes the index set of all data to be predicted while $|\mathcal{I}|$ stands for the size of set $\mathcal{I}$. Apparently smaller RMSEs indicate better solution qualities. Because Cadzow do not allow users to select arbitrary weights apart from W_1, we will not report the numerical results of Cadzow under W_2. For any combinations of $\{n/r/\theta\}$, we conduct 50 random test and all numerical results reported in Table.4.1 are the mean values over 50 tests.

Our first observation on Table.4.1 is that SLRA always performs worse than other three solvers in terms of estimation accuracy (RMSE). This is partly because SLRA is efficient only when the inverse of W is banded ([Usevich and Markovsky, 2014, Theorem 1]), which may not hold in this test. When applying $W = W_1$, we found that pMAP reports the best results in 3 examples out of 6 while DRI performs the best in the rest 3 examples. In general, Cadzow, DRI and pMAP have very closed performance on estimation accuracy under W_1 because they are Method of Alternating Projections based algorithms.

When the weight matrix is set as W_2, a significant improvement on the estimation accuracy can be observed for SLRA, DRI and pMAP comparing using $W = W_1$. This

result matches our expectation because W_2 assumes that all data have equal importance by sharing the same weight, while using W_1 implies that data in the middle of a time series are more accurately measured than the data at both ends by having higher weights.

For all $\{n/r/\theta\}$ combinations, our proposed solver with W_2 can always generate the estimation results with lowest RMSEs. It is also important to mention that our pMAP algorithm enjoys the most robust convergence result among all candidate solvers. As a result, we conclude that our propose pMAP algorithm is very competitive and powerful in solving real-valued time series denosing problems.

4.4.2 Spectral Sparse Signal Recovery

4.4.2.1 Experiment Introduction

In this experiment, we consider the problem of recovering missing values in an incomplete spectral sparse signal. We refer to Cai et al. [2018, 2019] and the references therein for its background in recovering signals which are spectrally sparse via off-grid methodologies. We follow the suggestions in Cai et al. [2019] to generate the experiment data $\mathbf{a} = \{a_1, a_2, ...a_n\}$ where

$$a_t = \sum_{s=1}^{r} d_s e^{2\pi j \omega_s t}, \qquad \text{for} \quad t \in \{0, 1, , ..., n\}$$

where $j = \sqrt{-1}$, r is the model order, ω_s is the frequency of each sinusoid and $d_s \neq 0$ is the weight of each sinusoid. Both ω_s and d_s are randomly sampled following uniform distributions, as $\omega_s \sim U[0, 1)$ and $d_s \sim U[0, 2\pi)$. Indexes of missing data are randomly sampled following uniform distribution. In this experiment we introduce three sub-tests with different targets.

test.a) Incomplete signal recovery without noise. In this sub-test we assume only a subset Ω of the sampling points $\{1, ..., n\}$ are observed and we aim to recovery the signal by estimating the missing data. Here all observed data are noiseless. We use success rate (SR) to measure the performance of candidate methods in incomplete signal recovery.

Parameters	**W**		**Cadzow**	**SLRA**	**DRI**	**pMAP**
1000/10/0.1	W_1	Iter	7.86	136.86	115.64	60.50
		Time	0.11	14.92	4.70	1.21
		RMSE	19.81	520.21	19.81	19.80
1000/10/0.1	W_2	Iter		146.84	200	**70.90**
		Time		15.95	7.88	**1.18**
		RMSE		455.85	19.70	**17.10**
1000/10/0.2	W_1	Iter	9.30	151.28	200	65.90
		Time	0.11	16.40	7.83	1.30
		RMSE	26.68	325.94	26.67	26.62
1000/10/0.2	W_2	Iter		148.74	200	**78.64**
		Time		16.06	7.88	**1.28**
		RMSE		305.27	26.47	**22.42**
1000/10/0.5	W_1	Iter	12.50	107.78	200	79.94
		Time	0.15	11.65	7.61	1.53
		RMSE	83.97	160.84	83.81	84.49
1000/10/0.5	W_2	Iter		115.98	200	**88.80**
		Time		12.64	7.50	**1.39**
		RMSE		117.02	83.37	**73.68**
2000/20/0.1	W_1	Iter	10.16	163.30	200	58
		Time	0.97	192.74	51.87	6.80
		RMSE	89.85	1685.07	89.60	90.90
2000/20/0.1	W_2	Iter		135.56	132.88	**59.14**
		Time		160.17	35.93	**6.32**
		RMSE		1033.91	78.27	**76.30**
2000/20/0.2	W_1	Iter	10.28	165.94	200	74.00
		Time	0.96	194.05	47.19	9.61
		RMSE	139.31	942.41	139.03	140.96
2000/20/0.2	W_2	Iter		185.64	200	**81.24**
		Time		218.95	48.00	**8.25**
		RMSE		671.99	138.64	**122.19**
2000/20/0.2	W_1	Iter	14.58	166.00	200	70.14
		Time	1.32	196.08	53.63	7.15
		RMSE	654.92	2149.37	650.22	641.95
2000/20/0.2	W_2	Iter		176.02	200	**78.64**
		Time		207.31	53.53	**7.99**
		RMSE		1926.84	649.56	**622.45**

TABLE 4.1: Experiment Results for Cadzow iteration, SLRA(structured low rank approximation), DRI(Douglas-Rachford iterations) and our proposed pMAP, including iterations (Iter), CPU time in seconds (Time) and Root of mean square error (RMSE).

We say the signal is successfully recovered if

$$\frac{\|\hat{\mathbf{x}} - \mathbf{a}\|}{\|\mathbf{a}\|} \leq 1.0e-3$$

where $\hat{\mathbf{x}}$ is the estimated signal.

In this test, signal length n is set to 499, 999 or 1999, respectively. The percentage of known observations $\frac{m}{n}$ is set to 30% or 60% where m stands for the amount of known observations. All combinations of $\{n/m/r\}$ used in this test can be found in Table.4.2. To compare the performance of our proposed method, we further introduce three state-of-art solvers in spectral sparse signal recovery including Atomic Norm Minimization (ANM Tang et al. [2013]), Fast Iterative Hard Thresholding (FIHT Cai et al. [2018]) and Projected Gradient Descent (PGD Cai et al. [2018]). W for each solver is defined as

$$W_{i,j} = \begin{cases} 1/\sqrt{i+j-1} & \text{for } i+j-1 = 1,\ldots,k-1 \\ 1/\sqrt{k} & \text{for } i+j-1 = k,\ldots,n-k+1 \\ 1/\sqrt{(n-i-j+2)} & \text{for } i+j-1 = n-k+2,\ldots,n, \end{cases}$$

if a_{i+j-1} is observed, and $W_{i,j} = 0$ if it is missing.

test.b) Incomplete signal recovery with noise. This sub-test still aims to recover an incomplete spectral sparse signal, but some observed data are noisy while others are noiseless. Here we follow the signal generating process the same as it in **test.a**, however, $\frac{1}{3}m$ observations are polluted by random noise, as $y_i = a_i + \epsilon_i$ where $\epsilon_i = \theta \frac{e_t}{\|e\|_2}\|a\|$. Here e_t is a complex stranded normal random variable and the noise level θ is set as 0.2. We assume the index set of polluted observations is known in advance.

The weight matrix W is set as follows. We give polluted observations very small weights (say 1) and noiseless observations are assigned to much larger wights such as 100. The missing data in the signal are still given zero weight. It is worth noting that this weight matrix setting is for pMAP only because FIHT and PGD do not support flexible weight choices. The rest settings of this sub-test such as the definition of $\{n, m, r\}$ are consistences with **test.a**.

test.c) Recover missing data with inaccurately estimated rank. In **test.a** and **test.b**, we assume the objective rank r to be a known parameter. However, obtaining the true information of objective rank is quite challenging in many real applications. So in this sub-test we will examine the performances of candidate solvers in recovering the incomplete spectral sparse signals while the objective rank r is incorrectly estimated. Signal length n is set as 3999 and we assume that 30% data in a signal are randomly and accurately observed without noise. True rank r is set as 15 but assumed to be unknown in this test. It means for each solver, we will try different estimated rank $\hat{r}$ ranges from 6 to 30. Success rates (SR) over 50 instances are reported to measure the performance of each solver.

4.4.2.2 Numerical Results

test.a) The numerical results of this test are listed in Table 4.2 including total iterations (Iter), CPU time cost in seconds (Time), RMSE and success rate (SR) for each candidate solver. Among all solvers, ANM enjoys the best global convergence result because of its convex relaxation. However, the computational cost of ANM is much heavier than the rest solvers and it runs out of memories when n is larger than 500. At the same time, it fails to generate better results comparing with our proposed solver. Hence we do not report its performances in the rest part of this test problem. Although DRI performs slightly better than Cadzow in terms of accuracy, both of these two solvers can not successfully recovery any incomplete signals.

We further note the fact that in some cases FIHT stops within a few iteration step and this behaviour may lead to inferior solutions. Similar behaviours were also reported in another recent research (Fig. 3, Ying et al. [2018]). Also with the increasing of r, the performance of PGD declines when the ratio between m and r keeps fixed. It is because PGD has some assumptions on the lower bond of m with respected to r (Theorem 2.1, Cai et al. [2018]), which may not hold in some cases. On the other hand, pMAP performs the best in 11 cases out of 12 in terms of SR.

$n/m/r$		**Cadzow**	**DRI**	**ANM**	**FIHT**	**PGD**	**pMAP**
m/n = 30%							
499/150/10	Iter	10.36	200	-	**27.96**	54.66	46.90
	Time	9.2e-2	2.84	9.0e2	**0.01**	0.17	0.58
	RMSE	1.01	0.27	1.1e-4	**3.3e-6**	1.1e-3	1.1e-2
	SR	0.0	0.0	0.9	**1.0**	0.9	0.96
499/150/20	Iter	13.42	200	-	24.12	**123.14**	**107.22**
	Time	0.18	2.82	1.3e3	0.17	**0.58**	**1.75**
	RMSE	1.02	0.52	1.4e-3	4.9e-1	**3.2e-3**	**1.3e-1**
	SR	0.0	0.0	0.6	0.06	**0.68**	**0.68**
999/300/30	Iter	11.76	200		84.54	105.94	**85.12**
	Time	0.67	15.85		0.69	0.93	**5.55**
	RMSE	1.01	0.43		1.4e-2	1.5e-3	**4.9e-4**
	SR	0.0	0.0		0.94	0.76	**1.0**
999/300/40	Iter	14.18	200		9.92	161.20	**141.82**
	Time	1.06	15.81		1.9e-1	1.75	**12.40**
	RMSE	1.02	0.54		0.54	7.1e-3	**1.5e-1**
	SR	0.0	0.0		0.0	0.48	**0.56**
1999/600/60	Iter	13.06	200		98.24	155.06	**103.78**
	Time	7.39	140.94		2.18	3.80	**60.29**
	RMSE	1.02	0.45		1.2e-2	4.8e-3	**5.6e-4**
	SR	0.0	0.0		0.96	0.50	**1.0**
1999/600/80	Iter	14.38	200		2	191.16	**180.62**
	Time	11.32	140.44		3.6e-1	6.19	**147.11**
	RMSE	1.02	0.57		0.57	9.7e-3	**2.0e-1**
	SR	0.0	0.0		0.0	0.16	**0.40**
m/n = 60%							
499/300/20	Iter	11.02	200	**-**	**14.42**	76.56	**24.22**
	Time	0.15	2.82	**8.4e2**	**9.4e-2**	3.7e-1	**4.1e-1**
	RMSE	0.97	7.4e-2	**1.4e-5**	**8.5e-6**	1.2e-3	**3.9e-4**
	SR	0.0	0.0	**1.0**	**1.0**	0.8	**1.0**
499/300/40	Iter	14.98	200	-	**27.12**	180.56	**41.36**
	Time	0.39	2.79	1.6e3	**0.29**	1.34	**1.20**
	RMSE	0.95	0.22	4.9e-4	**2.7e-5**	8.3e-3	**5.2e-4**
	SR	0.0	0.0	0.8	**1.0**	0.18	**1.0**
999/600/60	Iter	13.42	200		**20.88**	172.22	**40.72**
	Time	1.71	15.84		**0.42**	2.51	**5.63**
	RMSE	0.96	0.17		**1.7e-5**	4.6e-3	**5.6e-4**
	SR	0.0	0.0		**1.0**	0.42	**1.0**
999/600/80	Iter	15.22	200		**27.14**	198.30	**52.58**
	Time	2.87	15.80		**0.66**	3.81	**11.07**
	RMSE	0.94	0.24		**2.5e-5**	9.6e-3	**6.3e-4**
	SR	0.0	0.0		**1.0**	0.06	**1.0**
1999/1200/120	Iter	14.10	200		**21.30**	195.94	**41.50**
	Time	18.12	190.52		**1.25**	9.72	**54.39**
	RMSE	0.96	0.19		**2.7e-5**	6.2e-3	**5.4e-4**
	SR	0.0	0.0		**1.0**	0.08	**1.0**
1999/1200/160	Iter	16.54	200		**27.52**	200	**52.74**
	Time	31.03	140.80		**2.47**	13.52	**101.57**
	RMSE	0.95	0.27		**2.7e-5**	1.2e-2	**6.3e-4**
	SR	0.0	0.0		**1.0**	0.0	**1.0**

TABLE 4.2: Numerical results for six different solvers on the incomplete signal recovery experiment including iterations (Iter), computational time (Time), estimation error (RMSE) and success recovery rate (SR). Results in this table are the average value of 50 trials. *Experiment results ANM when $n \geq 999$ are not available because they run out of memory.

We find that FIHT is more computational efficient than pMAP. This is the result of using the subspace technique in FIHT (Alg.2 in Cai et al. [2019]), which is designed to approximate the matrix projections on low rank subspace and reduces the computational time from $O(n^3)$ (SVD) to $O(nr^2)$. Although this technique can be applied in our framework to reduce the computational cost as well, it will break our convergence results. We leave this potential improvement for future researches.

In many real world applications, it is required to estimate the coefficients of a spectral sparse signal including amplitude d_s and frequency ω_s for all $s \in [1, 2, ..., r]$. After getting recovered spectral sparse signals by a specific solver, we use the method suggested by Condat and Hirabayashi [2015] to reconstruct their coefficients. We plot the coefficient reconstruction results in Fig.4.4 over two instances. It is easy to observe that In terms of $r = 20$, FIHT incorrectly estimated most of coefficients with significant errors while both PGD and FIHT can successfully recover most of them. On the other hand when r increases to 40, PGD works worse than FIHT and pMAP. There are 5 to 6 coefficients can be accurately estimated by FIHT and pMPA, but not PGD.

Because a spectrally sparse signal can be represented by a few non-zero coefficients in finite discrete bases or dictionaries, in this experiment we aim to estimate the locations and amplitude of these coefficients. Apparently the accuracy of signal coefficients estimation from incomplete observations is highly related to the accuracy of incomplete signal recovery. We follow the parameter reconstruction procedure given in [Condat and Hirabayashi, 2015, Fig.2, Step4 - Step 5] to generate our coefficients estimation results, which can reconstruct coefficients exactly for noiseless observations. Using the simulated signals and setting $N = 499$, we plot the coefficient estimation results for four methods in Fig.4.3 ($\gamma = 30\%$) and 4.4 ($\gamma = 60\%$) using some randomly selected sample.

- **Fig.4.3** In these figures we observe ANM, pMAP and PGD can all estimate the true coefficients accurately. However in this case, only 7 out of 20 coefficients can be approximated successfully by FIHT (see Fig.4.3(b)).

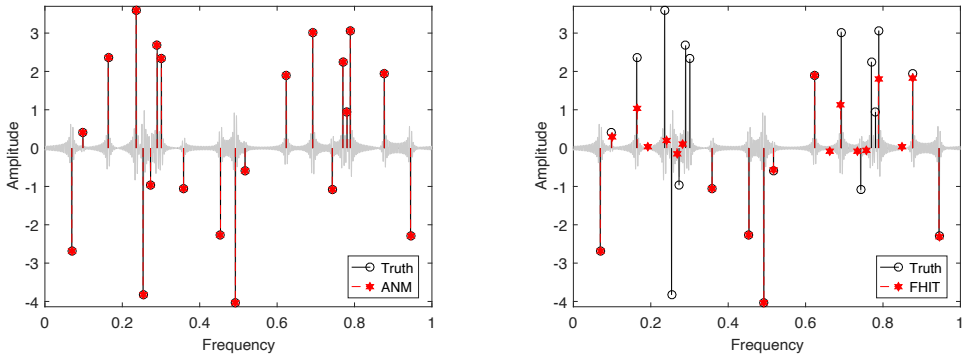

(a) ANM

(b) FIHT

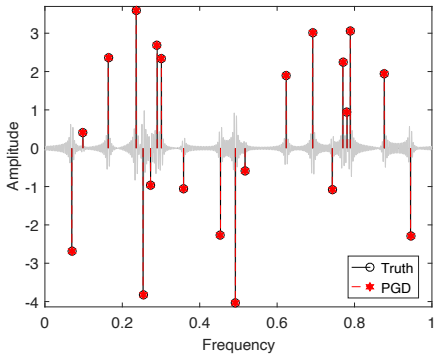

(c) PGD

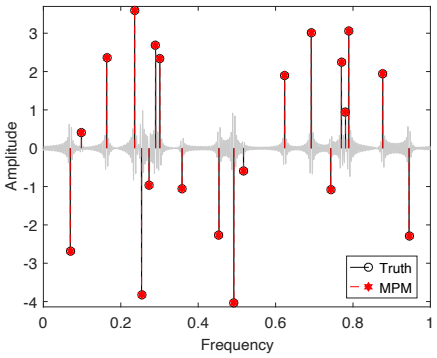

(d) pMAP

FIGURE 4.3: Spectral sparse signal coefficients reconstruction results by FIHT, PGD and pMAP, setting $\{n/m/r\} = \{499/150/20\}$. Black circles stand for the true locations of coefficients while red stars stand for the estimated locations of coefficients.

- **Fig.4.4** In this figure all these four algorithms failed to recover every coefficient exactly. But in this example, ANM, FIHT and pMAP generates very close coefficient estimation results and these results are better than the results obtained through PGD. In Fig.4.4(c) some coefficients are pointed out by arrows. These coefficients can not be accurately estimated by PGD but can be recovery through other three methods.

test.b) Table.4.3 lists the numerical results of this test including Iter, Time, RMSE and SR for five solvers. Due to the interference of noise, we arise the threshold of success rate to $1.0e-2$ to make sure the numerical results are comparable and meaningful.

Experimental results show that our proposed pMAP significantly outperforms the rest four candidate solvers in all tests. All the rest solvers fail to recover any signals successfully while in all cases, while the SR of pMAP is at least 0.94 in all cases. It is because

n/r		**Cadzow**	**FIHT**	**PGD**	**DRI**	**pMAP**
499/5	Iter	7.8	7.86	21.56	200	**20.88**
	Time	6.4e-2	2.5e-2	4.8e-2	2.84	**0.23**
	RMSE	1.00	2.5e-2	2.5e-2	2.5e-2	**2.1e-3**
	SR	0.0	0.0	0.0	0.0	**1.0**
499/10	Iter	8.92	17.32	32.64	200	**27.94**
	Time	7.9e-2	6.6e-2	0.10	2.82	**0.36**
	RMSE	0.98	3.6e-2	3.6e-2	4.4e-2	**3.2e-3**
	SR	0.0	0.0	0.0	0.0	**1.0**
499/20	Iter	10.82	30.74	79.34	200	**42.94**
	Time	7.9e-2	0.17	0.36	2.81	**0.72**
	RMSE	0.98	5.6e-2	5.6e-2	9.9e-2	**6.5e-3**
	SR	0.0	0.0	0.0	0.0	**0.96**
999/10	Iter	8.22	8.98	28.29	200	**29.58**
	Time	0.19	4.9e-2	0.12	15.89	**1.01**
	RMSE	1.00	2.6e-2	2.6e-2	3.5e-2	**1.4e-3**
	SR	0.0	0.0	0.0	0.0	**1.0**
999/20	Iter	9.26	15.76	46.70	200	**39.32**
	Time	0.35	0.11	3.1e-1	15.85	**1.82**
	RMSE	0.99	3.7e-2	3.7e-2	6.0e-2	**2.1e-3**
	SR	0.0	0.0	0.0	0.0	**1.0**
999/40	Iter	11.60	52.78	142.16	200	**60.48**
	Time	0.93	0.56	1.49	15.93	**5.29**
	RMSE	0.97	5.7e-2	5.7e-2	0.13	**4.4e-3**
	SR	0.0	0.0	0.0	0.0	**0.94**
1999/20	Iter	8.36	12.70	34.36	200	**44.86**
	Time	1.60	0.12	0.37	141.04	**9.40**
	RMSE	0.99	2.6e-2	2.6e-2	4.2e-2	**9.6e-4**
	SR	0.0	0.0	0.0	0.0	**1.0**
1999/40	Iter	9.68	19.96	69.72	200	**58.72**
	Time	3.53	0.32	1.21	140.48	**22.80**
	RMSE	0.98	3.8e-2	3.8e-2	7.2e-2	**1.6e-3**
	SR	0.0	0.0	0.0	0.0	**1.0**
1999/80	Iter	11.80	70.18	185.26	200	**86.16**
	Time	9.26	2.06	5.88	138.65	**67.73**
	RMSE	0.97	5.8e-2	5.8e-2	0.14	**3.6e-3**
	SR	0.0	0.0	0.0	0.0	**0.98**

TABLE 4.3: Numerical results for Cadzow, FIHT, PGD, DRI and our proposed pMAP on the noisy signal recovery experiment, including iterations (Iter), CPU time in seconds (Time), root of mean square error (RMSE) and success rate (SR).

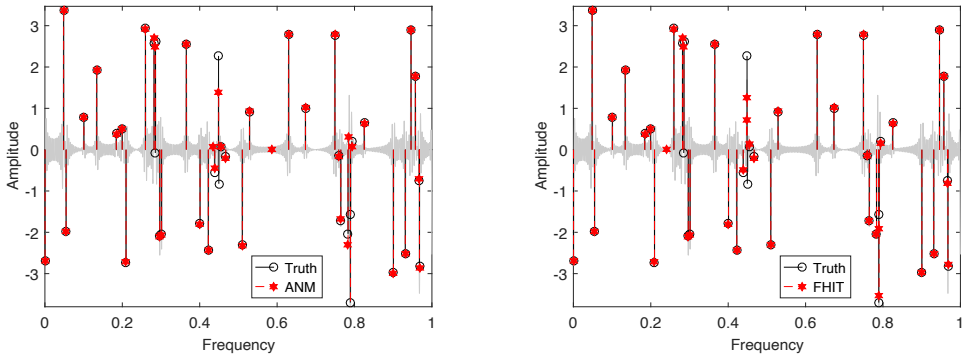

(a) ANM

(b) FIHT

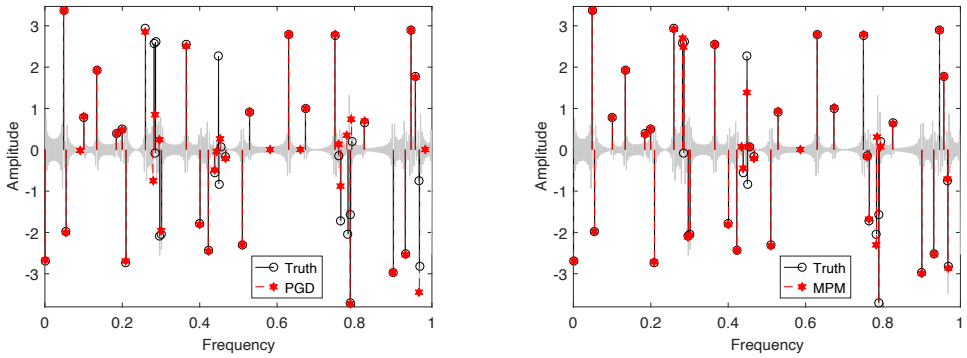

(c) PGD

(d) pMAP

FIGURE 4.4: Spectral sparse signal coefficients reconstruction results by FIHT, PGD and pMAP, setting $\{n/m/r\} = \{499/300/40\}$. Black circles stand for the true locations of coefficients while red stars stand for the estimated locations of coefficients.

in DRI, FIHT and PGD, the weight of each observations can not be customised, which means these two solvers have to give equal weights to both noisy observations and noiseless observations. As a result, their estimation results are significantly affected by noisy observations.

test.c) The numerical results of recovering missing data with inaccurately estimated rank experiment are plotted in Fig.4.5 for each solver. When $\hat{r}$ is smaller than 15, success rate for all solvers are zero. It indicates that none of these solvers can recover the incomplete signal successfully when there is a lack of coefficients information. With $\hat{r}$ exactly equals to 15, all three methods including FIHT, PGD and pMAP can achieve 100% recovery rate. However when $\hat{r} > 15$, one can expect various performances of three solvers. The success rates of both PGD and FIHT gradually decline with the increasing of $\hat{r}$ and they finally reach 35% and 25% respectively when $\hat{r} = 30$. One the other hand,

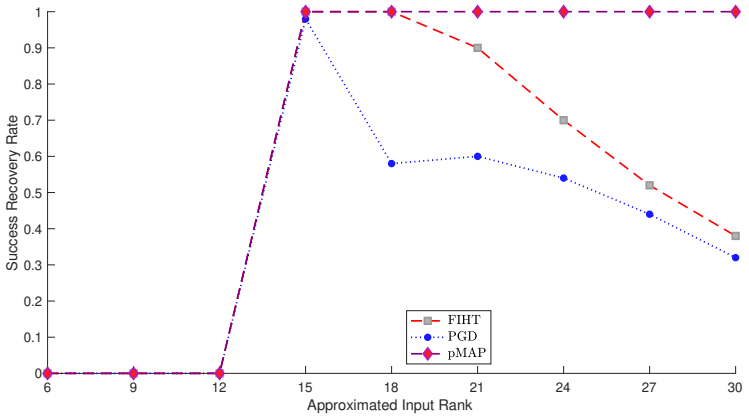

FIGURE 4.5: SR when the input rank is misappropriated for FIHT, PGD and pMAP. n is set as 3999 and 30% observations are known. True rank r is set as15.

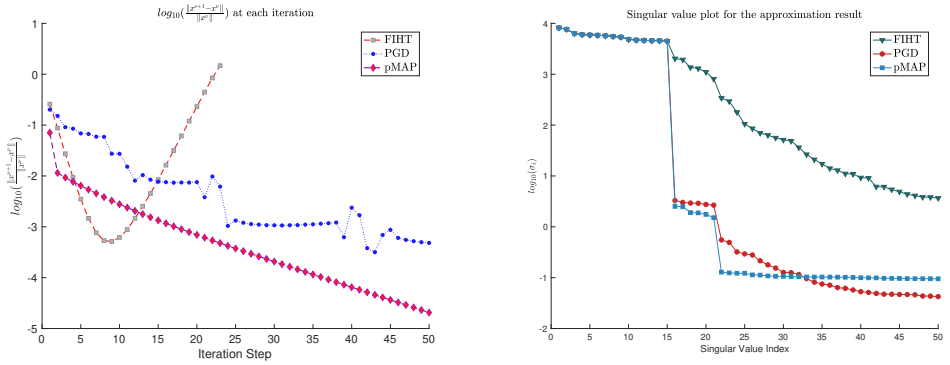

(a) Plot of $log_{10}(\frac{\|x^{\nu+1}-x^{\nu}\|}{\|x^{\nu}\|})$ ar each iteration

(b) Solution singular values

FIGURE 4.6: Performance comparison for candidate solvers in incomplete signal recovering when the input rank is incorrectly estimated. True rank is 15 and input rank is 21. Fig.4.6(a) plots the relative gap between x^{ν} and $x^{\nu+1}$ for each solver at each iteration, while Fig.4.6(b) plots the singular values of final solution by each solver.

SR of our proposed pMAP stays at 100% for any $\hat{r}$ no smaller than 15, which indicates that pMAP is more robust to the overestimation of objective rank than the rest two solvers.

Fig.4.6 compares the PGD, FIHT and pMAP using a random incomplete signal recovery example, which helps explain the performance difference. Fig.4.6(a) shows that the failures of both FIHT and PGD in recovering incomplete signal are caused by the non-convergence behaviours, which lead to inferior results as displayed in Fig.4.6(b).

4.5 Comparisons between pMAP and SMM

4.5.1 Differences between pMAP and SMM

In previous chapter we have proposed SMM to tackle the same weighted low rank Hankel matrix optimization problem. Both SMM and pMAP framework are based on the alternating minimization technique and also both implement the majorization minimization method. However, pMAP is superior than SMM in the following aspects.

1. (**Weight matrix**) The approach to deal with the weight matrix W is the first difference between SMM and pMAP. Since it is quite difficult to compute the low rank projection of a matrix under weighted norm, in SMM we introduced the $(\mathbf{p}, \mathbf{q})$-norm, where we need to find a set of $\{\mathbf{p}, \mathbf{q}\}$ such that

$$\frac{1}{2}\|(\sqrt{\mathbf{p}}\sqrt{\mathbf{q}}^T) \circ X\| \geq \frac{1}{2}\|W \circ X\| \quad \forall X \in \mathcal{M}$$

   In this way we construct the majorization surrogate function for the original objective function. However in pMAP, we kept the weight matrix W accurately. The pMAP solver can benefit from this improvement in at least two aspect. Firstly, computing the suitable $\{\mathbf{p}, \mathbf{q}\}$ to ensure the above inequality will lead to some extra computing cost. At the same time, introducing $(\mathbf{p}, \mathbf{q})$-norm changes the weight matrix W, which leads to the fact that final solution by SMM may not be a good approximation for the original matrix optimization problem.

2. (**Sub-problem solving**) The second important difference between SMM and pMAP is the sub-problem solving phase. In SMM, we introduce the alternating projection proposed in Gillard and Zhigljavsky [2016] to solve its sub-problem, i.e., Alg. (4). However, the alternating projection method is a heuristic algorithm so its solution can only be used as an approximated solution to the sub-problem.

In pMAP, by contrast, we have the closed form solution for its sub-problem. The solution updating at each iterate takes the following forms:

$$X^{k+1} = \Pi_{\mathcal{H}}^{W}(W_{\rho}^{-1} \circ (W \circ W \circ Y + \rho \Pi_{\mathcal{M}_r}(X^k)))$$

As we can see, the above solution updating process implement both Hankel matrix projection operator and low rank matrix projection operator by only once. This improvement 1) can ensure that the sandwich inequalities hold at each iterate because we solved the sub-problem using closed form solution and 2) reduce the computing cost because the alternating projection is implemented by only once.

3. (**Convergence result**) SMM and pMAP also have different convergence result. By introducing the majorization minimization framework, SMM can ensure the non-increasing of its objective function value at each iterate. Since this objective function is blow bounded by zero, we can guarantee that SMM will converge if the sandwich inequality always holds. However, majorization minimization framework can not guarantee any further convergence result, e.g., whether SMM will converge to a stationary point.

   This issue is been considered in this pMAP work. In Theorem 4.10 we proved that, if ρ is below bounded by some value then pMAP will converge to an ϵ-approximate KKT point. Then in Theorem 4.12 we further proved that, given some conditions the solution sequence generated by Alg.8 will converges linearly to the accumulation point.

4.5.2 Numerical Experiment Comparison

This section implements a synthetic incomplete spectral sparse signal recovery experiment to illustrate the performance differences between pMAP and SMM. We implement the experiment in Section.4.4.2 for both SMM and pMAPand the experimental result is shown in the following table.

$n/m/r$	**SMM**	**pMAP**
	Iter(TotalIter)/Time/RMSE/SR	Iter/Time/RMSE/SR
m/n = 30%		
499/150/10	149.8(1837)/15.4/1.00/0	**46.90/0.58/1.1e-2/0.96**
499/150/20	182.9(3465)/46.4/1.02/0	**107.22/1.75/1.3e-1/0.68**
999/300/30	188.7(2321)/31.54/1.00/0	**85.12/5.55/4.9e-4/1**
999/300/40	173.1(6916)/184.85/1.01/0	**141.82/12.40//1.5e-1/0.56**
m/n= 60%		
499/300/20	193.4(2147)/34.0/1.03/0	**24.22/4.1e-1/3.9e-4/1**
499/300/40	183.2(7694)/227.3/0.95/0	**41.36/1.20/5.2e-4/1**
999/600/60	197.8(6645)/906.7/1.00/0	**40.72/5.63/5.6e-4/1**
999/600/80	187.0(9008)/1891/0.99/0	**52.58/11.07/6.3e-4/1**

TABLE 4.4: The numerical experiment comparison between SMM and pMAP, in the experiment of incomplete spectral spare signal recovery. *Iter* of SMM denotes the total number of outer iterations implemented in SMM, while $TotalIter$ in the bracket stands for the total number of alternating projection implemented in SMM.

We have several observations from this numerical result. First of all, we may found that SMM can not recover any incomplete signal since its success rates in all instances are zeros and its RMSE is close to 1. The reason behind this result is quite straightforward. In SMM we introduce the $(\mathbf{p}, \mathbf{q})$-norm to approximate the weighted norm in objective function. As a result, the weight of unknown observations are not strictly zero, which means the result of SMM is significantly influenced by the initial guess of unobserved data.

The second observation is SMM requires much more computing cost than pMAP. The extra computational cost of SMM comes from the multiple time implementation of alternating projection at each iteration. We conclude that the pMAP scheme is superior to SMM in both approximation accuracy and computing efficiency.

4.6 Conclusions

In this section we keep focusing on the weighted low rank Hankel matrix optimization problem. Based on the SMM, we further introduced the penalised method to deal with the rank constraint, and then introduce the majorization minimization scheme so that the problem can be tackled iteratively with non-increasing objective function values.

We further showed that the subproblem enjoys a closed form solution, which can be efficiently computed. We demonstrated the global optimal convergence property of our approach pMAP by assuming that the penalty parameter goes to infinity. We also showed that this method will at least converge to an ϵ-approximate KKT point linearly if the penalty parameter ρ is above a threshold. This method can be extended to tackle complex-valued matrix because the majorization $g_r(X)$ through the subdifferential of $h_r(X)$ holds in the complex-valued case. In the computational experiments for both series denoising and signal completion problems, pMAP usually outperforms other state-of-the-art solvers in terms of approximation accuracy within reasonable computing times.

Chapter 5

Extensions of Majorized Penalty Scheme

Chapter 3 and 4 have introduced the weighted low rank Hankel matrix approximation problem and two solvers (SMM and pMAP) were proposed to tackle this NP-hard problem. In fact this problem can be considered as a specific case of low rank matrix learning which aims to find a low rank matrix while some structural constraints are satisfied. There are some other applications falling into this category, for example, matrix completion (Keshavan et al. [2010]), robust principal component analysis (Wright et al. [2009]) and multi-task feature learning (Su et al. [2015]), to name just a few. Solving these problems often faces the same difficult, i.e., they are all formulated as NP-hard optimization problem because of the low rank constraint.

A natural question is whether we can extend our proposed framework like pMAP to tackle these problems, because we have seen its outstanding performances in tackling low rank constraint in both theoretical results and numerical experiments. In this chapter we try to achieve this target by tackling another two popular problems as robust matrix completion and principle component pursuit. We will demonstrate the approach to fit pMAP in these problems and also conduct numerical experiments to illustrate the performances of pMAP when comparing with some state-of-the-art solvers.

5.1 Robust Matrix Completion

5.1.1 Introduction and Literature Review

In many practical applications, it is believed that the observed data comes from a low dimension space together with some noise. Consider a movie rating data matrix which each column represents a selected movie and each row contains the ratings from one movie customer to each movie. It is assumed that only limited factors can influence a customer's ratings on a specific movie. Also all customers can be categorised into limited sub-groups where customers in the same sub-group have similar movie preferences. These assumptions leads to the fact that this movie rating data matrix is the sum of a low rank matrix and a noise matrix (Jawanpuria and Mishra [2018]). However in real practices, it is often difficult or even impossible to get all values of a data matrix. In some circumstances one can only observe very limited data, for example in some popular movie rating dataset, the sparsity of known observations is less than 5% (e.g., in the well known Netflix database, more than 98.8% ratings are unknown).

Many researches employed low rank matrix completion techniques to recover the missing values in a low rank matrix. This problem has a variety of real applications such as video denoising [Ji et al., 2010], phase retrieval [Candes et al., 2015], image classification [Cabral et al., 2015] and wireless sensor network localization [Saeed et al., 2018]. Another famous application of matrix completion is recovering missing values in a movie rating matrix as discussed earlier such that one can make recommendations accordingly.

Consider an uncompleted matrix $Y \in \mathbb{R}^{l\times k}$ and a index set Ω including indices of all observed data, e.g., $\{i,j\} \in \Omega$ if $Y_{i,j}$ is observed and $\{i,j\} \notin \Omega$ if it is unknown. The basic low rank matrix completion problem tries to find X by solving:

$$\begin{aligned} \min \quad & \operatorname{rank}(X) \\ \text{s.t.} \quad & X_{ij} = Y_{ij} \qquad \text{for all } \{i,j\} \in \Omega \end{aligned} \tag{5.1}$$

The constraint of Problem (5.1) can be equivalently written as $P_\Omega(X) = P_\Omega(Y)$, where $P_\Omega(X)_{i,j}$ equals to $X_{i,j}$ if $\{i,j\} \in \Omega$ and 0 otherwise. This problem is highly non-convex and difficult to solve [Wright et al., 2009]. Several different approaches have been employed to tackle this problem and a popular practice is to rewrite the Problem (5.1) by replacing the non-convex rank objective function by the nuclear norm (see Liu and Vandenberghe [2009] and Toh and Yun [2010]) and solve the following problem:

$$\begin{aligned} \min_X \quad & \|X\|_* \\ \text{s.t.} \quad & X_{ij} = Y_{ij} \qquad \text{for all } \{i,j\} \in \Omega \end{aligned} \tag{5.2}$$

By introducing the convex relaxation, Problem (5.2) becomes a convex optimization problem and its global optimal solution can be guaranteed by some developed semi-definite programming solvers such as CXV (Grant et al. [2008]).

Note that Problem (5.1) and (5.2) assumes the observed data is noiseless. However, this assumption is quite strict for many real-life applications and when the observations are polluted by noise, it is often difficult to recover the matrix via these formulations. So it is important to ensure that the proposed low rank matrix recovery technique is robust to noise. Assume the object rank or its upper-bound is known, a widely considered approach (see Ngo and Saad [2012], Jiang et al. [2017]) is formulating the problem as

$$\begin{aligned} \min \quad & \|P_\Omega(X) - P_\Omega(Y)\|^2 \\ \text{s.t.} \quad & \operatorname{rank}(X) \leq r \end{aligned} \tag{5.3}$$

This problem is known as Robust Matrix Completion (RMC) which allows the observations to be noisy. One approach to solve Problem (5.3) is to introduce the nuclear norm again and rewrite the problem using penalised method:

$$\min \quad \|P_\Omega(X) - P_\Omega(Y)\|^2 + \rho\|X\|_* \tag{5.4}$$

such that the global optimal solution can be guaranteed, for example, in the work by Hsieh and Olsen [2014]. However, nuclear norm minimization technique often suffers

from heavy computational costs despite its advantage in theoretical convergence. Considering that matrix recovery is often employed in dealing with large and complex data set, a good solver should be computationally efficient as well.

Non-convex techniques such as Riemannian optimization (see Vandereycken [2013], Wei et al. [2016], Cambier and Absil [2016]) and alternating projection (Jain et al. [2010], Jiang et al. [2017]) are also introduced to tackle this problem. The numerical results show that these non-convex techniques can recover the incomplete matrix quite well in both accuracy and computing efficiency. These facts drive us to explore the potential application of our proposed non-convex framework in tackling this robust matrix completion problem.

5.1.2 The Majorization Penalty Approach

In this section we extend the pAMP framework to solve Problem (5.3). It is straightforward that (5.3) can be equivalently rewritten as:

$$\begin{aligned} \min \quad & \|W \circ (X - Y)\|^2 \\ \text{s.t.} \quad & \operatorname{rank}(X) \leq r \end{aligned} \tag{5.5}$$

where the weight matrix W is introduced to replace the fidelity projection, defined as:

$$W_{i,j} := \begin{cases} 1 & \text{if } Y_{i,j} \text{ is known} \\ 0 & \text{if } Y_{i,j} \text{ is unknown.} \end{cases}$$

Taking the advantage of pMAP framework, (5.5) can be reformulated as

$$\min \quad f_\rho(X) := \frac{1}{2}\|W \circ (X - Y)\|^2 + \rho g_r(X) \tag{5.6}$$

where $g_r(A)$ is already defined in (4.5):

$$g_r(A) = \frac{1}{2}\|A - \Pi_{M_r}(A)\|^2 = \frac{1}{2}\|A\|^2 - h_r(A), \qquad \forall A \in \mathcal{M}$$

and $h_r(A)$ is defined in (4.3):

$$h_r(A) = \frac{1}{2}\|\Pi_{\mathcal{M}_r}(A)\|^2 = \frac{1}{2}\sum_{i=1}^{r}\sigma_i^r(A), \qquad \forall A \in \mathcal{M}$$

Similarly with previous section, we have the following propositions to show that solving Problem (5.6) is equivalent to solving the original completion problem (5.5):

Proposition 5.1. *Let $X_r^* \in \mathcal{M}$ be the global solution to problem (5.6). If the rank of X_r^* is not larger than r, then X_r^* is a global optimal solution to problem (5.5).*

Proposition 5.2. *Let $\varepsilon > 0$ be a given positive number and $X^* \in \mathcal{M}$ an optimal solution to the following least square problem*

$$\min \frac{1}{2}\|W \circ (X - Y)\|^2$$

Assume $\rho > 0$ is chosen such that $(f(X_r) - f(X^*))/\rho \leq \varepsilon$ and let $\overline{X}$ be a global optimal solution to (5.5). Then we have

$$g_r(X_r^*) \leq \varepsilon \qquad \textit{and} \qquad f(X_r^*) \leq f(\overline{X}) - \rho g_r(X_r^*) \leq f(\overline{X}) \tag{5.7}$$

Proofs of Prop.5.1 and 5.2 can be easily driven from proofs of Prop.4.3 and 4.4 so we do not repeat them here. Now let's introduce the majorization minimization framework to tackled penalised problem (5.6). Let $g_r^m(A, Z)$ and $f_\rho^m(A, Z)$ be defined the same as in (4.7) and (4.10):

$$g_r^m(A, Z) := \frac{1}{2}\|A\|^2 - h_r(Z) - < \Pi_{\mathcal{M}_r}(Z), A - Z >, \qquad \forall A, Z \in \mathcal{M}$$

$$f_\rho^m(A, Z) := \frac{1}{2}\|M \circ (A - Y)\|^2 + \rho g_r^m(A, Z), \qquad \forall A, Z \in \mathcal{M}$$

Lemma 4.5 provided that $f_\rho^m(X, Z)$ is a majorization function of $f_\rho(X)$ according to Definition 2.4. This means we can introduce the majorization minimization framework to tackle (5.6). Suppose $X^0 = Y$ and we have current iterate X^ν, the majorization minimization framework suggested to find the next iterate $X^{\nu+1}$ by solving the minimization

problem:

$$X^{\nu+1} \in \arg\min f_\rho^m(X, X^\nu), \qquad \text{for } \nu = 0, 1, ... \tag{5.8}$$

As a result the sandwich inequalities must hold here:

$$f_\rho(X^{\nu+1}) \leq f_\rho(X^\nu) \qquad \text{for } \nu = 0, 1, ... \tag{5.9}$$

Inequality (5.9) can be easily driven from Theorem.2.5 and Lemma.4.5. This inequality (5.9) guarantees that the objective function value of Problem (5.6) is non-increasing at each iterate using majorization minimization framework. Because $f_\rho^m(X)$ is founded below by zero, the sequence of $f_\rho^m(X^\nu)$ will be guaranteed to converge to a certain point. At the same time, the sub-problem (5.8) can be easily solved according to Prop. (4.9) by taking the following updating at each iterate:

$$X^{\nu+1} = W_\rho^{(-1)} \circ (W \circ W \circ Y + \rho \Pi_{\mathcal{M}_r}(X^\nu)) \tag{5.10}$$

Following we summarise the algorithm of pMAP to tackle the Robust Matrix Completion problem.

Algorithm 9: Algorithm: pMAP for Robust Matrix Completion

Result: Approximated low rank matrix $\hat{X}$;

initialization: Observed incomplete matrix Y, rank constraint r, penalty parameter ρ, $W_\rho = \sqrt{\rho E + W \circ W}$, stop criterion $STOP$ and initial guess X^0. Set $\nu = 0$;

while *The stop condition STOP is not met* **do**

Compute $X^{\nu+1}$ as

$$X^{\nu+1} = W_\rho^{(-1)} \circ (W \circ W \circ Y + \rho \Pi_{\mathcal{M}_r}(X^\nu))$$

$\nu \to \nu + 1$

5.1.3 Convergence Properties

In previous section we have established the non-increasing behaviour of objective function value of $f_\rho(X^\nu)$ at each iterate using majorization minimization framework. This

section reports two more results.

Proposition 5.3. *Given X^0 and let X^ν be the sequence generated by solving Problem (5.8) iteratively. Then the following holds.*

1. *We have*

$$f_\rho(X^{\nu+1}) - f_\rho(X^\nu) \le -\frac{\rho}{2}\|X^{\nu+1} - X^\nu\|^2, \qquad \nu = 1, 2, ...$$

Furthermore, $\|X^{\nu+1} - X^\nu\| \to 0$.

2. *Let $\widehat{X}$ be ab accumulation point of $\{X^\nu\}$, then for any X we have*

$$\langle \nabla f(\widehat{X}) + \rho\widehat{X} + \rho\Pi_{\mathcal{M}_r}(-\widehat{X}), X - \widehat{X}\rangle \ge 0$$

That is, $\widehat{X}$ is a stationary point of the problem (5.6). Moreover, for a given $\epsilon > 0$, if $X^0 \in \mathcal{M}_r$ and

$$\rho \ge \rho_\epsilon := \frac{f(X^0)}{\epsilon},$$

then $\widehat{X}$ is an ϵ-approximate KKT point of (5.6).

Theorem 5.4. *Assume that $M > 0$ and $\widehat{X}$ be an accumulation point of $\{X^\nu\}$. The following hold.*

(i) rank$(\widehat{X}) > r$ unless A is already the optimal solution of (5.5).

(ii) Suppose $\widehat{X}$ has rank $(r + p)$ with $p > 0$. Let $\sigma_1 \ge \sigma_2 \ge \cdots \ge \sigma_k$ be the singular values of $\widehat{X}$. Define

$$w_0 := \min\{W_{i,j}\} > 0, \qquad \epsilon_0 := \frac{w_0}{\rho}, \qquad \epsilon_1 := \frac{\epsilon_0}{4 + 3\epsilon_0}, \qquad c := \frac{1}{1 + \epsilon_1} < 1.$$

Under the condition

$$\frac{\sigma_r}{\sigma_{r+1}} \ge \frac{8p}{\epsilon_0} + 1,$$

it holds

$$\|X^{\nu+1} - \widehat{X}\| \le c\|X^\nu - \widehat{X}\| \qquad \text{for } \nu \text{ sufficiently large.}$$

Consequently, the whole sequence $\{X^\nu\}$ *converges linearly to* $\widehat{X}$.

Proofs of Theorem 5.3 and 5.4 can be easily obtained from the proofs of Theorem 4.10 and 4.12 because WLRH problem can be seen as an extension of robust matrix completion by adding a Hankel structural constraint.

5.1.4 Numerical Experiment

In this section several experiments are conducted to demonstrate the performance of pMAP in robust matrix completion. In the first experiment, we use some synthetic dataset to check its convergence behaviour and computing efficiency. Then in the second experiment, we introduce the well-known real-life application, movie recommendation engines, which has been discussed in a lot of most recent papers (Jain et al. [2010], Ngo and Saad [2012]). We use this experiment to evaluate the performance of our proposed algorithm against several state-of-the-art solvers. All the experiments in this and following sections are implemented with Matlab 2019b, equipped with a 2.6 GHz Intel Core i7 processor with a 8 GB memory card.

5.1.4.1 Start Study

In this start study we generate r-rank matrix $X \in \mathbb{R}^{l\times k}$ by $X = AB$, where $A \in \mathbb{R}^{l\times r}$ and $B \in \mathbb{R}^{r\times k}$ are randomly generated real-valued matrices where all the elements follows independent uniform distributions $U[0, 1)$. The randomly populated locations of unknown observations in X also follow the uniform distributions to construct the initial observation matrix Y. Then we implement pMAP to recover X from Y. The parameter γ is introduce to represent the percentage of unknown observations over total amount of data in X. All unknown data will be set to zero at initial. In the following Table.5.1 we firstly list the numerical result of pMAP in this incomplete matrix recovery problem.

We have several basic observations from above table. Firstly our proposed algorithm can successfully recover the incomplete low rank matrix in most cases because most RMSEs in Table.5.1 are close to zero. However, in the case of $\gamma = 95\%$ (which means only 5%

Dimension	γ	$r = 5$	$r = 10$	$r = 15$
		RMSE/TIME	RMSE/TIME	RMSE/TIME
500 × 500	50%	5.39e-7/0.70	4.31e-7/1.85	2.82e-7/5.81
	80%	3.05e-6 /2.81	1.99e-6/6.38	1.52e-6/18.89
	90%	2.14e-5/11.62	6.34e-6/18.41	4.22e-6/46.10
	95%	6.16e-2/9.71	1.7e-3/30.82	2.57e-5/109.33
1000 × 1000	50%	9.68e-7/0.92	7.25e-7/2.38	6.24e-7/6.80
	80%	6.60e-6/4.67	3.54e-6/8.89	2.43e-6/23.88
	90%	2.50e-3/11.47	1.32e-5/28.16	7.47e-6/60.62
	95%	1.68/11.49	3.48e-2/35.92	6.06e-4/123.49
2000 × 2000	50%	1.50e-6/1.10	1.02e-6/2.72	6.79e-7/7.69
	80%	1.14e-5/6.93	5.41e-6/11.51	3.43e-6/27.54
	90%	6.05e-2/12.16	6.45e-5/39.44	1.11e-5/75.25
	95%	4.20/12.35	2.58e-1/38.67	5.30e-3/129.71

TABLE 5.1: Numerical results of synthetic incomplete low rank matrix recovery experiment for our proposed pMAP including RMSE (root mean square error) and computing time.

real observations are given in the incomplete matrix), pMAP may fail to approximate the missing values in some cases (e.g., in case $\{l, k\} = \{1000, 1000\}$ and $\{2000, 2000\}$, setting $r = 5$) because the amount of given observations are not sufficient.

We further conduct this experiment to illustrate the convergence behaviour of pMAP. Fig.5.1 plots the functional value of pMAP at each iterate using this synthetic experiment, setting rank = 10. It can be easily observed that $f_\rho(X^\nu)$ is non-increasing in all cases and converges to zero gradually. Of course the empirical convergence rate of pMAP depends on various factors, e.g., the objective rank and percentage of known observations.

Fig.5.2 further plots $\frac{\|X^{\nu+1}-X^\nu\|_F^2}{\|X^\nu\|_F^2}$, the relative gap between X^ν and $X^{\nu+1}$ at each iterate by setting rank = 10. It shows that in this experiment, the sequencing of $\|X^{\nu+1} - X^\nu\|_F$ converges to zero gradually as proved in Prop.5.3. It also shows that the sequence of $\frac{\|X^{\nu+1}-X^\nu\|_F^2}{\|X^\nu\|_F^2}$ also converges to zero in all cases.

5.1.4.2 Movie Recommendation Engines

a. Experiment Introduction This experiment conduct a popular real-life application

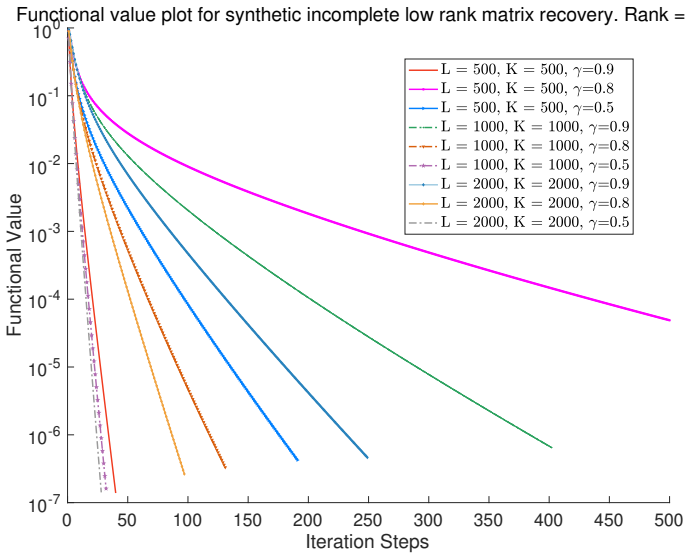

FIGURE 5.1: Plot of functional value $f_\rho(X^\nu)$ at each iterate by pMAP in robust matrix completion experiments, setting $r = 10$.

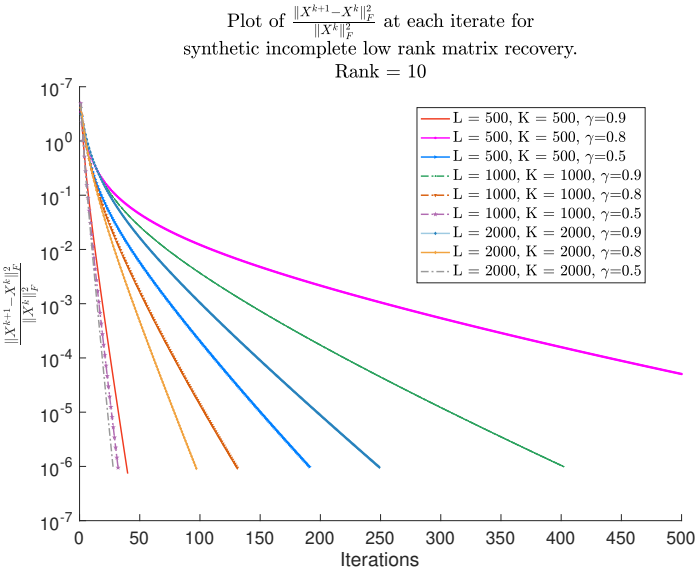

FIGURE 5.2: Plot of functional value $\frac{\|X^{\nu+1}-X^\nu\|_F^2}{\|X^\nu\|_F^2}$ at each iterate by pMAP in robust matrix completion experiments, setting $r = 10$.

of robust matrix completion problem, known as movie recommendation engines (MRE). This application has been briefly introduced in Section 1.2.2.4. Many existing researches focused on proposed on this movie recommendation engine problem by employing low rank matrix optimization methods. In this experiment we introduce several leading algorithms for benchmarking:

- Nonlinear geometric conjugate gradients (LRGeomCG, Vandereycken [2013]) tackled robust matrix completion problem (5.3). It used geometric conjugate gradients in the Riemannian manifold optimization techniques because both objective function and constraint of the problem is smooth.

- Scaled conjugate gradients on Grassmann manifolds (ScGrassMC, Ngo and Saad [2012]) also solved the robust matrix completion problem. It proved that if its initial solution is close enough to the minimal, then this method can ensure the convergence to the minimal solution and achieve exact incomplete matrix recovery.

- Combination of spectral and manifold optimization technique (OptSpace, Keshavan et al. [2010]) combined both spectral techniques and Grassman manifold optimization methods to tackle robust matrix completion problem.

- Nuclear norm minimization via active subspace selection (Active ALT, Hsieh and Olsen [2014]) tackled the nuclear norm optimization problem which tries to minimise the objective function $F(X) + \lambda\|X\|_*$ where $F(X)$ is the twice differentiable convex function, for example, $F(X) = \frac{1}{2}\|\Pi_\Omega(X) - \Pi_\Omega(A)\|_F^2$ in matrix completion problem. It provided the numerical evidences that it is superior to other state-of-art nuclear norm minimization solvers in the case of Movie recommendation engine problem.

- Accelerated proximal gradient algorithm for nuclear norm regularized linear least squares (NNLS, Toh and Yun [2010]) developed an gradient method for the general unconstrained nonsmooth convex minimization problem

$$\min_{X \in R^{L \times K}} F(X) := f(X) + P(X)$$

where both $f(X)$and $P(X)$ are convex functions. In specific, $f(X)$ should be smooth while $P(X)$ should be proper and semi-continuous at the same time. In this matrix completion case, $P(X) = \mu\|X\|_*$ and $f(X) = \|\mathcal{A}(X) - b\|_2^2$.

- Guaranteed singular value projection (SVP, Jain et al. [2010]) tried to solve the robust formulation of general affine rank minimization problem as

$$\min \|\mathcal{A}(X) - b\|_2^2, \quad s.t.\ \mathrm{rank}(X) \leq r$$

using hard singular value thresholding interatively.

There are also many novel solvers which were tested in above researches, e.g., ADMiRA (Lee and Bresler [2010]), LMAFit (Wen et al. [2012]) and RTRMC (Boumal and Absil [2011])). We will not conduct these solvers in our experiment since they have proved to be inferior than one or several solvers in the candidate solver list. We compare the performance of our proposed pMAP solver with these candidate algorithm on several movie rating data sets obtained from MovieLens [1]. Three different data set are used in this experiments as MovieLens 100K Dataset, MovieLens 1M Database and MovieLens Latest Datasets (Harper and Konstan [2016]). The detailed information for all dataset including the number of movie users, number of movies and amount of known ratings can be found in Table 5.2:

Dataset	Number of Movie Users	Number of Moives	Known Ratings	Sparsity
ML 100K	943	1 682	100 000	6.30 %
ML 1M	6 040	3 952	1 000 209	4.19 %
ML Latest	610	9 742	100 836	1.70 %

TABLE 5.2: Statistics of MovieLens rating dataset.

Ratings in these database scale from 1 star (very dissatisfied) to 5 stars (very satisfied). For all the dataset, we randomly create five different 80/20 training/testing splits. That is to say, we randomly keep 80% of known ratings for model training and left 20% known ratings for out-of-sample-testing. Some solvers may require a starting value for missing

[1] https://movielens.org/

data in the rating matrix. In these cases we will assign 3 to all unknown ratings at initial.

The stop conditions, including the maximum iterate step and stopping tolerances, are set the same as we used in the experiments of Chapter 4. Then we perform these 7 different methods to estimate the ratings in test set. For each data set, we validate the performances of all solvers by considering three rank choices as rank $= 2, 3$ and 5, respectively.

b. Experiment Result

Main numerical results of movie recommendation engines are detailed in Table.5.3. Each result in Table.5.3 is the average value over five testing instances. In this experiment we use RMSE to measure the approximation accuracy of each solver. It can be seen that pMAP performs the best in terms of estimation accuracy because it provides the smallest mean error in all experiments. To further analyse the performance of each solver in detail, the distributions of estimation errors for testing dataset is plotted in Fig.5.3. One can find that the median forecasting error of pMAP is just above zero (which is better than ALT, LRGemoCG and NNLS). At the same time, pMAP also performs better in terms of estimation variance because its first quartile, third quartile, minimum and maximum point are closer to zero comparing with other solvers.

Fig.5.4 displays the RMSE against computing time using the MovieLens 100K and 1M datasets for each solver, setting the rank as 2 and 5 respectively. We can observe that pMAP is one of the most efficient methods among all solvers since it reaches the best estimation performances using reasonable computing time. Although RMSEs of LRGeomCG and ScGrassMC decreased faster than pMAP at beginning phase in some cases, they converged to inferior results quickly. In conclusion, we observe that our proposed pMAP method enjoys competitive performance among all solvers.

r	LRGeomCG	ScGrassMC	OptSpace	Active ALT	NNLS	SVP	pMAP
Movie Lens 100K							
2	0.9494	0.9461	0.9433	0.9961	0.9294	0.9602	**0.9184**
3	0.9494	0.9637	0.9354	0.9928	0.9252	0.9485	**0.9111**
5	0.9494	1.0256	0.9230	0.9824	0.9290	0.9593	**0.9159**
Movie Lens 1M							
2	0.9136	0.8935	0.9088	0.9172	0.9053	0.9198	**0.8843**
3	0.9136	0.8889	0.9057	0.9032	0.8947	0.9176	**0.8781**
5	0.9136	0.8923	0.8966	0.8826	0.8820	0.8863	**0.8656**
Movie Lens 1M (Latest)							
2	1.0828	1.1987	1.1704	1.2572	1.1527	1.2054	**0.8851**
3	1.0828	1.2333	1.2099	1.2381	1.1503	1.1775	**0.8814**
5	1.0828	1.2860	1.2328	1.2437	1.1657	1.2343	**0.8894**

TABLE 5.3: The RMSE incurred by several methods for matrix completion problem, based on the database of Movie-Lens Database.

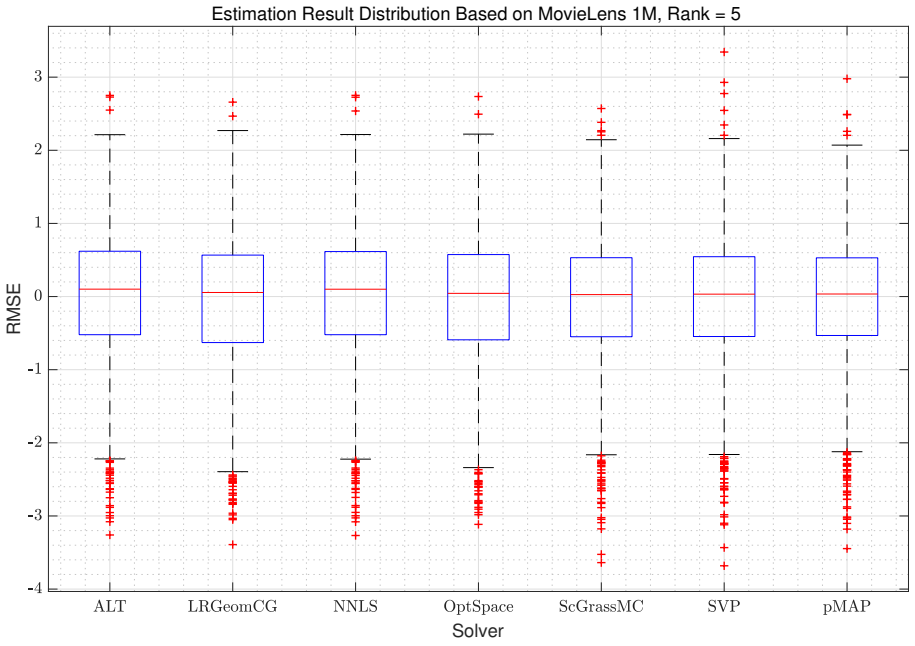

FIGURE 5.3: Distribution of estimations errors for all solvers based on the MovieLens 1M dataset, the rank is set as 5.

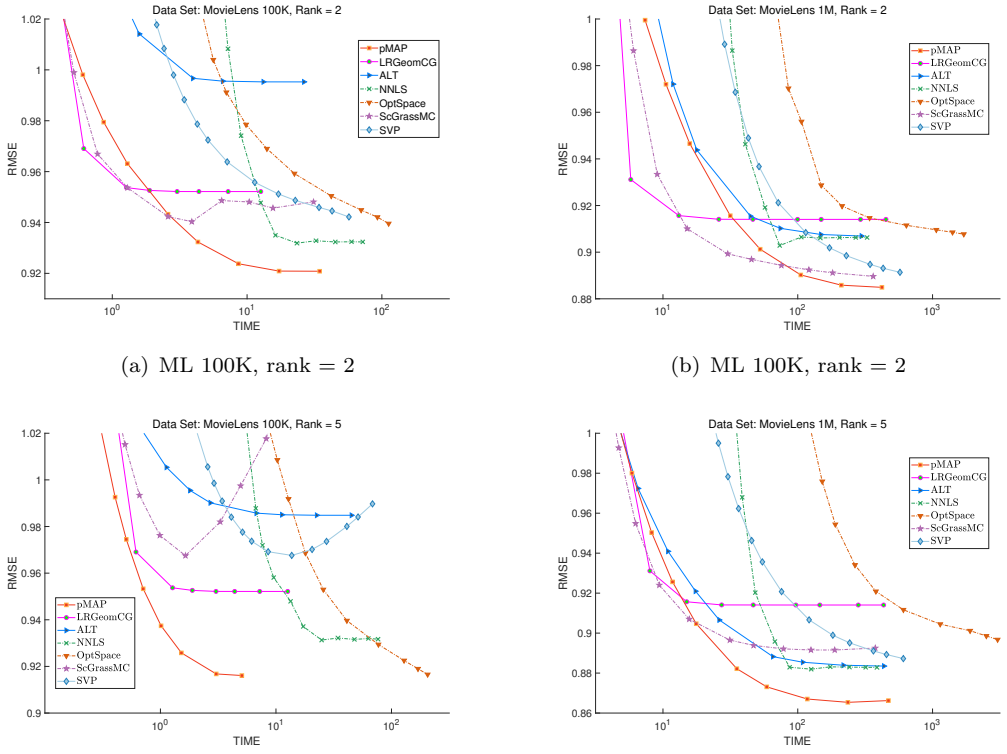

(a) ML 100K, rank = 2

(b) ML 100K, rank = 2

(c) ML M1, rank = 5

(d) ML M1, rank = 5

FIGURE 5.4: RMSE plot against computing time at each iterate for all candidate solvers.

5.2 Extension 2: Robust Principal Component Pursuit

5.2.1 Introduction and Literature Review

Principal Component Analysis (PCA) is a popular data dimensional reduction technique which is frequently employed in many areas such as video processing and data compression. This technique assumes that the high dimensional data often comes from a low dimension space with some noise, i.e., the observed data matrix $M \in \mathbb{R}^{l\times k}$ can be decomposed into two sub-matrix as $M = L + N$. Here the rank of $L \in \mathcal{M}$ is much smaller than $\min\{l, k\}$ and $N \in M$ represent the noise component. To recover the low dimension subspace from high dimensional data, PCA aims to solve the following optimization problem

$$\min \|N\|_F^2, \qquad \text{s.t. } \operatorname{rank}(L) \le r, \qquad M = L + N$$

However, it is widely believed that PCA works well only when the noise level is small and follows some certain kinds of distribution like Gaussian. In cases like video processing, there are large scaled and limited corruptions or outliers, which will lead to inferior results when using PCA. Low rank and sparse matrix decomposition (LRSMD, see [Yuan and Yang, 2009]), also known as Robust Principal Component Analysis (RPCA) is further proposed to deal with sparse and high level noise. It aims to recover a low rank matrix L from input matrix M while the noise matrix $S \in \mathcal{M}$ is sparse. This matrix separation approach has been widely employed in many applications such as subspace recovery [Liu et al., 2013], clustering [Shahid et al., 2015] and video processing [Huan et al., 2016], to name just a few. The problem of RPCA is often formulated as

$$\begin{aligned} \min_{L,S} \ & \operatorname{rank}(L) + \gamma\|S\|_0 \\ \text{s.t. } & L + S = M \end{aligned} \tag{5.11}$$

where γ is a trade-off parameter to balance the sparse and low rank components and $\|\cdot\|_0$ is ℓ_0-norm which stands for the total amount of non-zero element in a matrix.

One popular approach to solve this non-convex optimization problem is introducing the convex relaxation technique. Some researches such as Chandrasekaran et al. [2011], Lin et al. [2010] used nuclear norm as the convex relaxation of rank constraint and the ℓ_1 norm as the convex relaxation of ℓ_0-norm as

$$\begin{aligned} \min_{L,S} \quad & \|L\|_* + \lambda \|S\|_1 \\ \text{s.t.} \quad & L + S = M \end{aligned} \tag{5.12}$$

Then (5.12) can be solved by semi-definite programming solvers and a global optimal solution can be guaranteed, although the computing cost would be relatively high ([Netrapalli et al., 2014]). A more robust formulating is to taking both outliers and regular noise into consideration as

$$\begin{aligned} \min_{L} \quad & \|M - L - S\|^2 \\ \text{s.t.} \quad & \|S\|_0 \leq \epsilon \\ & \text{rank}(L) \leq r \end{aligned} \tag{5.13}$$

assuming that the rank of matrix L and the sparsity of S are both known. To tackle the computing cost of convex relaxation, many powerful and novel non-convex methods are introduced. For example, Rodriguez and Wohlberg [2013] employed the alternating projection method which was proved to be more efficiently than convex relaxation methods. However, this method is lacking of convergence results and it only provides computational evidences to show its convergence behaviour. The matrix factorization approach was introduced by Zhou and Tao [2013], provided that the approximation results of their proposed solver is not far away to optimum. Alternating minimization over low rank and sparse constraints iteratively was used by Zhou and Tao [2011] and Netrapalli et al. [2014]. Zhou and Tao [2011] proved that the alternating projection method local minimal convergence result at linear rate, given the assumption that the initial guess is close to the optimal solution, which may be quite strict in practice. All these researches on non-convex solvers inspired us to employ the pMAP scheme for this RPCA problem.

5.2.2 The Majorization Penalty Approach

In this section we demonstrate how Problem (5.13) can be tackled via the penalty majorization method framework. Firstly we introduce the penalization function $g_r(L)$ of pMAP as defined in last chapter:

$$g_r(L) = \frac{1}{2}\|L - \Pi_{M_r}(L)\|^2 = \frac{1}{2}\|L\|^2 - h_r(L), \qquad \forall L \in \mathcal{M}$$

Here $h_r(L)$ is defined the same as (4.3). Then according to the pMAP scheme, we can rewrite (5.13) into the following equivalent formulation:

$$\begin{aligned} \min \;\; & \theta_\rho(L,S) := \|M - L - S\|^2 + g_r(L) \\ \text{s.t.} \;\; & \|S\|_0 \leq \epsilon \end{aligned} \tag{5.14}$$

One may note that Problem (5.14) has binary variables, so a natural approach to deal with (5.14) is to alternatively minimise the objective function over two variables. However, minimising $\theta_\rho(L)$ over L is not a easy task and another iteratively framework may be required. Our proposed approach is to combine the alternating projection method together with the penalty majorization approach. Considering the surrogate function $g_r^m(L,Z)$ defined as

$$g_r^m(L,Z) := \frac{1}{2}\|L\|^2 - h_r(Z) - < \Pi_{M_r}(Z), L - Z >, \qquad \forall L, Z \in \mathcal{M}$$

We further define $\theta_\rho^m(L,Z,S) = \|M - L - S\|^2 + g_r^m(L,Z)$, then it is straightforward to have the following property:

Lemma 5.5. *Consider the function $g_r^m(L,Z)$ defined in 4.7. According to Prop.4.2, $g_r^m(L,Z)$ can be seen as the surrogate function of $\theta_\rho(L)$ by satisfying the following conditions:*

$$\theta_\rho^m(L,L,S) = \theta_\rho(L,S) \tag{5.15}$$

$$\theta_\rho^m(L,Z,S) \geq \theta_\rho(L,S) \tag{5.16}$$

for all $L, Z, S \in \mathbb{R}^{l\times k}$.

We propose our pMAP method for RPCA problem as following:

Algorithm 10: Algorithm: pMAP for Stable Principle Component Pursuit

Result: Approximated low rank matrix $\hat{L}$ and the sparse noise matrix $\hat{S}$.

Initialization observed incomplete matrix M, rank constraint r, sparsity ϵ, penalty parameter ρ and stop criterion $STOP$, initial guess L^0 and S^0. Set $\nu = 0$;

while *The stop condition STOP is not met* **do**

Compute $L^{\nu+1}$

$$L^{\nu+1} = \arg\min_{L} \theta_\rho^m(L, L^\nu, S^\nu) \tag{5.17}$$

Compute $S^{\nu+1}$

$$S^{\nu+1} = \arg\min_{S} \theta_\rho^m(L^{\nu+1}, L^{\nu+1}, S) \qquad \text{s.t. } \|S\|_0 \le \epsilon \tag{5.18}$$

$\nu \to \nu + 1$

At each iteration of Alg.10, the penalised problem is minimised over two variables sequentially. Then the following lemma holds.

Lemma 5.6. *Let the sequence* $\{L^\nu, S^\nu\}$ *be the* ν*-th iterate computed through Alg.10, we have*

$$\theta_\rho(L^\nu, S^\nu) \ge \theta_\rho(L^{\nu+1}, S^{\nu+1}) \qquad \textit{for } k = 0, 1, ... \tag{5.19}$$

That is to say, the function value $\theta_\rho(L^\nu, S^\nu)$ *is non-increasing to* ν.

Proof. From Prop.5.5 we have

$$\theta_\rho(L^{\nu+1}, S^\nu) \le \theta_\rho^m(L^{\nu+1}, L^\nu, S^\nu) \;\text{ and }\; \theta_\rho(L^\nu) = \theta_\rho^m(L^\nu, L^\nu, S^\nu)$$

We further note that $\theta_\rho^m(L^{\nu+1}, L^\nu, S^\nu) \le \theta_\rho^m(L^\nu, L^\nu, S^\nu)$ because $L^{\nu+1}$ is the optimal solution to (5.17). As a result we have

$$\theta_\rho(L^{\nu+1}, S^\nu) \le \theta_\rho^m(L^{\nu+1}, L^\nu, S^\nu) \le \theta_\rho^m(L^\nu, L^\nu, S^\nu) = \theta_\rho(L^\nu)$$

The proof completes. □

Now we solve two sub-problems (5.17) and (5.18). We will show that both sub-problems have closed form solution hence they can be solved easily. Firstly we have the following proposition.

Proposition 5.7. *We have the following equivalent minimization problem to Problem (5.17)*

$$\arg\min_L \ \theta_\rho^m(L, L^\nu, S^\nu) = \arg\min_L \ \frac{1}{2}\|\sqrt{\rho+1}(L - L_\rho^\nu)\|^2 \tag{5.20}$$

where L_ρ^ν is computed by:

$$L_\rho^\nu := \frac{1}{\rho+1}((M - S^\nu) + \rho\Pi_{\mathcal{M}_r}(L^\nu)) \tag{5.21}$$

Apparently (5.17) is solved by taken $L = L_\rho^\nu$.

Proof. We can easily get

$$\begin{aligned}
\theta_\rho^m(X, X^\nu, S^\nu) &= \frac{1}{2}\|L + S^\nu - M\|^2 + \rho g_r^m(L, L^\nu) \\
&= \frac{1}{2}\|L + S^\nu - M\|^2 + \frac{\rho}{2}\|L\|^2 - \rho h_r(L^\nu) - \rho < \Pi_{M_r}(L^\nu), L - L^\nu > \\
&= \frac{\rho+1}{2}\|L\|^2 - < L, M - S^\nu > - < L, \rho\Pi_{\mathcal{M}_r}(L^\nu) > \\
&\quad + \underbrace{\frac{1}{2}\|M - S^\nu\|^2 - \rho h_r(L^\nu) + \rho < L^\nu, \Pi_{\mathcal{M}_r}(L^\nu) >}_{:=\Delta_1} \\
&= \frac{1}{2}\|\sqrt{\rho+1}L\|^2 - \langle L, M - S^\nu + \rho\Pi_{\mathcal{M}_r}(L^\nu)\rangle + \Delta_1 \\
&= \frac{1}{2}\|\sqrt{\rho+1}L\|^2 - \langle \sqrt{\rho+1}L, \frac{1}{\sqrt{\rho+1}}((M - S^\nu) + \rho\Pi_{\mathcal{M}_r}(L^\nu))\rangle \\
&\quad + \Delta_1 \\
&= \frac{1}{2}\|\sqrt{\rho+1}(L - \frac{1}{\rho+1}((M - S^\nu) + \rho\Pi_{\mathcal{M}_r}(L^\nu)))\|^2 \\
&\quad \underbrace{-\frac{1}{2}\|\frac{1}{\sqrt{\rho+1}}((M - S^\nu) + \rho\Pi_{\mathcal{M}_r}(L^\nu))\|^2 + \Delta_1}_{:=\Delta_2} \\
&= \frac{1}{2}\|\sqrt{\rho+1}(L - \underbrace{\frac{1}{\rho+1}((M - S^\nu) + \rho\Pi_{\mathcal{M}_r}(L^\nu))}_{:=L_\rho^\nu})\|^2 + \Delta_2 \\
&= \frac{1}{2}\|\sqrt{\rho+1}(L - L_\rho^\nu)\|^2 + \Delta_2
\end{aligned} \tag{5.22}$$

where we define Δ_1, Δ_2 and L_ρ^ν as following

$$\begin{aligned}
\Delta_1 &= \frac{1}{2}\|M - S^\nu\|^2 - \rho h_r(L^\nu) + \rho < L^\nu, \Pi_{\mathcal{M}_r}(L^\nu) > \\
\Delta_2 &= -\frac{1}{2}\|\frac{1}{\sqrt{\rho+1}}((M - S^\nu) + \rho\Pi_{\mathcal{M}_r}(L^\nu))\|^2 + \Delta_1 \\
L_\rho^\nu &= \frac{1}{\rho+1}((M - S^\nu) + \rho\Pi_{\mathcal{M}_r}(L^\nu))
\end{aligned}$$

Then the Proposition 5.7 is proved because Δ_2 is a constant item that independent with variable L. This completes our proof. □

Now we focus on the second sub-problem (5.18). The following proposition shows it also enjoys closed form solution.

Proposition 5.8. *Given the next iterate $L^{\nu+1}$, the solution to problem (5.18) can be computed as*

$$S^{\nu+1} = HT_\zeta(M - L^{\nu+1}) \tag{5.23}$$

where $HT_\zeta(A)$ is denoted as the hard-thresholding operate on known matrix A, i.e. $(HT_\zeta(A))_{i,j} = A_{i,j}$ if $|A_{i,j}| \geq \zeta$ and 0 otherwise. Here ζ is selected as the ϵ-th largest element in $M - L^{\nu+1}$ in terms of absolute value.

Proof. It is straightforward that

$$\begin{aligned}
\arg\min_S \theta_\rho(L^{\nu+1}, L^{\nu+1}, S) &= \arg\min_S \frac{1}{2}\|M - L^{\nu+1} - S\|^2 + g_r^m(L^{\nu+1}, L^{\nu+1}) \\
&= \arg\min_S \frac{1}{2}\|M - L^{\nu+1} - S\|^2
\end{aligned} \tag{5.24}$$

then Problem (5.18) can be equivalently written as

$$S^{\nu+1} = \arg\min_S \frac{1}{2}\|M - L^{\nu+1} - S\|^2 \qquad \text{s.t. } \|S\|_0 \leq \epsilon \tag{5.25}$$

One optimal solution to (5.25) can be obtained as $M - HT_\zeta(M - L^{\nu+1})$. □

Remarks.

1. Given the current iterate L^{ν}, the next iterate $L^{\nu+1}$ is obtained via the following update:

$$L^{\nu+1} = M - HT_{\zeta}(M - \frac{1}{\rho+1}((M - S^{\nu}) + \rho\Pi_{\mathcal{M}_r}(L^{\nu})))$$

   And it is worth noting that if ρ approaches infinity, above update will be degenerated to the basic alternating projection which is exactly the same as GoDec. In this case the Problem (5.14) will also be degenerated to the basic robust principle component analysis problem (5.11). Prop.5.6 will still hold in this case, which implies that the basic alternating projection enjoys the non-increasing objective function value sequence.

2. Apart from the basic non-increasing sequence of objective function values, it is not an easy task to establish other convergence results without making additional assumptions, e.g., the quality of initial gauss. Since both original objective function and surrogate function is bounded below by zero, we can only say the solution at each iterate will converge to a certain point. However, it might be a local optimal point or just a stationary point.

5.2.3 Numerical Experiment

5.2.3.1 Start Study

We firstly conduct a synthetic experiment to analyse the behaviour of proposed pMAP in tackling robust principal component analysis problem. Following experiments in Yuan and Yang [2009], the low rank matrix L and the noise matrix S are generated randomly by the MATLAB scripts as

- L = randn(m,r)*randn(r,n); mgL = max(abs(L(:)));
- S = zeros(m,n); p = randperm(m*n); K = round(spr*m*n);
  - Impulsive sparse matrix: S(p(1:K)) = mgL .* sign(randn(L,1));
  - Gaussian sparse matrix: S(p(1:K)) = randn(K, 1)

- M = L + S.

Here r and spr represent matrix rank and sparsity ratio respectively. Alg.10 is implemented to approximate low rank matrix $\hat{L}$ and sparse noise matrix $\hat{S}$ from observed matrix M. We introduce three different errors to demonstrate the result quality. The relative error of estimated sparse matrix $\hat{S}$ to the original sparse matrix S is calculated as

$$\text{ErrSP} = \|\hat{S} - S\|_F / \|S\|_F$$

The error of estimated low rank matrix $\hat{L}$ to the original matrix L is calculated as

$$\text{ErrLR} = \|\hat{L} - L\|_F / \|L\|_F$$

Finally the quality of recovery is measured by

$$\text{RelErr} = \|(\hat{L}, \hat{S}) - (L, S)\|_F / \|(L, S)\|_F$$

The numerical results are listed in Table 5.4 and 5.5. Each result in these two tables is the average value of 100 instances. It can be seen that in these two tables, the errors (including ErrSP, ErrLR, RelErr) are close to zero. It means the approximating results obtained by pMAP are very close to the optimal result (input L and S).

$m = n$	r	spr	ErrSP	ErrLR	RelErr	Iter
100	10	5%	5.8e-5	6.4e-5	6.1e-5	10.7
		10%	1.9e-3	3.7e-3	2.4e-3	15.2
500	10	5%	5.1e-6	7.0e-6	5.8e-6	6.0
		10%	9.1e-6	1.8e-5	1.1e-5	7.0
	50	5%	5.1e-5	5.8e-5	5.4e-5	9.0
		10%	4.8e-5	7.6e-5	5.7e-5	11.8
1000	50	5%	1.7e-5	2.0e-5	1.8e-5	7.0
		10%	3.5e-5	6.1e-5	4.3e-5	8.0
	100	5%	4.2e-5	4.9e-5	4.5e-5	9.0
		10%	6.3e-5	1.0e-4	7.6e-5	11.0

TABLE 5.4: Results of low rank and sparse matrix decomposition experiment for the method of pMAP, by assuming the noise is impulsive sparse.

$m = n$	r	spr	ErrSP	ErrLR	RelErr	Iter
100	10	5%	8.2e-4	5.8e-5	8.1e-5	14.7
		10%	9.2e-3	9.3e-4	1.3e-3	19.9
500	10	5%	1.4e-3	9.7e-5	1.3e-4	5.7
		10%	2.5e-3	2.5e-4	3.6e-4	8.7
	50	5%	1.5e-3	4.8e-5	6.8e-5	7.0
		10%	2.2e-3	9.8e-5	1.4e-4	9.1
1000	50	5%	9.6e-4	3.0e-5	4.3e-5	5.0
		10%	1.1e-3	4.8e-5	6.8e-5	7.0
	100	5%	7.8e-4	1.7e-5	2.5e-5	7.0
		10%	1.8e-3	5.7e-5	8.0e-5	8.0

TABLE 5.5: Results of low rank and sparse matrix decomposition experiment for the method of pMAP, by assuming the noise is Gaussian sparse.

Similarly we also use this experiment to demonstrate the convergence behaviour of pMAP. Fig.5.5 shows the functional value $\theta_\rho(L^\nu, S^\nu)$ at each iterate under different cases. The computing results show that the functional value converges to zero and thus the approximation result converges to global optimal efficiently, although we can not guarantee this behaviour theoretically.

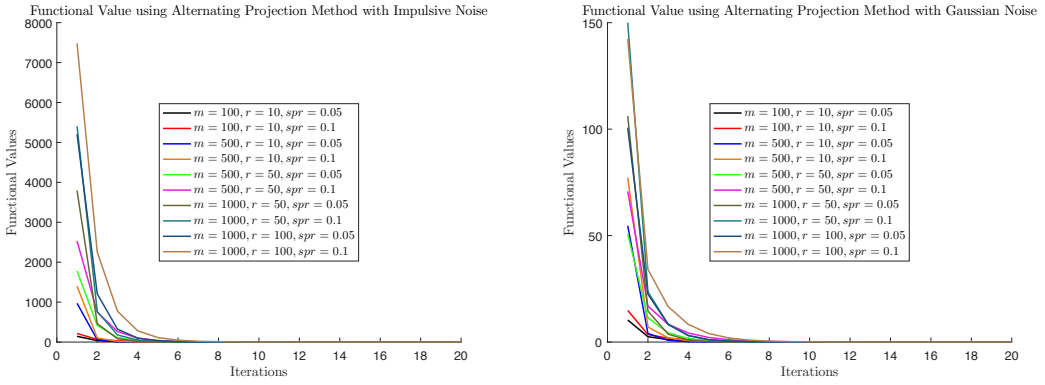

(a) Function values of $\theta_\rho(L^\nu, S^\nu)$ at each iterate in the case of Impulsive noise

(b) Function values of $\theta_\rho(L^\nu, S^\nu)$ at each iterate in the case of Gaussian noise

FIGURE 5.5: Function values of $\theta_\rho(L^\nu, S^\nu)$ in each iteration using Alternating Projection Method based on simulated data

5.2.3.2 Comparison between solvers

In this experiment the performance of our proposed method will be compared with some state-of-the-art solvers using this randomly generated synthetic dataset. Candidate solvers introduced in this experiment includes Augmented Lagrange Multiplier

Method (ALM, Lin et al. [2010]), Fast Principle Component Pursuit (FPCP, Rodriguez and Wohlberg [2013]), GreGoDec (Greedy Semi-Soft GoDec Algotithm, Zhou and Tao [2013]), Block Lanczos with Warm Start (IALM_BLWS, Lin and Wei [2010]), Fast Alternating Linearization Methods (FALM, Goldfarb et al. [2013]), Non-smooth Augmented Lagrangian Algorithm (NSA, Aybat et al. [2011]), Principal Component Pursuit (PCP, Candès et al. [2011]) and Singular Value Thresholding (SVT, Cai et al. [2010]). All these solvers share the same stopping condition such that the results are comparable.

In this experiment we will consider two different cases to test all solvers. In the first case M is constructed by L and S only and no extra noise component is added. In the second case the observations are polluted by both impulsive sparse noise and Gaussian noise as $M = L + S + N$, where N is generated by:

- N = 0.2 * randn(m,n)

The numerical results of both case for all solvers are listed in Table.5.6 and 5.7. Here we fix the objective rank to 50. We test all solvers over two *spr* instances as 0.05 and 0.1, which means the sparsity of S is 0.05 and 0.1 respectively. In Table.5.6 where only sparse noise are introduced, our first observation is that proposed pMAP always provide the most accuracy approximation results with lowest ErrLRs and ErrSPs among all solvers. At the same time, we note that pMAP is also the most efficient solver because it costs the shortest computing time in almost all instances. The only exception happens in the 1000/50/0.05 case where NSA is 0.1 seconds faster than pMAP but with much inferior results. We observed very similar behaviour in Table. 5.7 where pMAP always provides the best approximations on both low rank matrix L and sparse noise matrix S. Although only one solver (GreGoDec) spent lower computing cost than pMAP, its approximation accuracy is much worse than our proposed solver in terms of RMSE.

5.3 Conclusion

In this chapter we extend our proposed pMAP framework to solving two rank minimization problems as robust matrix completion and stable principal component pursuit.

$l/r/spr$	1000/50/0.05	1000/50/0.1	2000/50/0.05	2000/50/0.1
	ErrLR/ErrSP/Time	ErrLR/ErrSP/Time	ErrLR/ErrSP/Time	ErrLR/ErrSP/Time
ALM	1.5e-5/1.3e-5/46	1.6e-5/1.3e-5/47	1.4e-05/1.4e-05/355	1.4e-5/1.4e-5/337
FPCP	1.1e-2/9.7e-3/54	1.0e-2/6.0e-3/56	5.6e-3/4.3e-3/252	5.2e-3/3.0-e3/247
GreGoDec	8.4e-1/6.9e-1/14	4.6/2.7/14	0.86/0.66/54	5.0/2.8/55
IALM_BLWS	5.8e-1/4.7e-1/35	5.9e-1/3.5e-1/45	1.8e-1/1.4e-1/1202	2.6e-1/1.4e-1/1376
FALM	8.6e-8/7.9e-8/85	7.4e-8/6.0e-8/75	6.3-8/7.0e-8/605	5.6e-8/8.2e-8/649
NSA	3.6e-3/2.9e-3/5.4	3.2e-3/1.9e0-3/7.5	0.2e-3/1.6e-3/31	1.7e-3/9.6e-4/39
PCP	3.9e-8/6.1e-8/12	5.6e-8/5.5e-8/12.7	2.4e-8/4.2e-8/90	3.9e-8/4.2e-8/90
SVT	8.3e-4/2.7e-4/85	1.1e-3/3.1e-4/100	8.4e-4/2.2e-4/340	1.1e-3/2.6e-4/394
pMAP	**2.6e-8/2.1e-8/5.5**	**3.8e-8/2.2e-8/6.8**	**8.9e-9/6.8e-9/18**	**2.4e-8/1.3e-8/22**

TABLE 5.6: The RMSE incurred by 10 different methods for robust principal component analysis problem where only spare noise is taken into consideration

$l/r/spr$	1000/50/0.05	1000/50/0.1	2000/50/0.05	2000/50/0.1
	ErrLR/ErrSP/Time	ErrLR/ErrSP/Time	ErrLR/ErrSP/Time	ErrLR/ErrSP/Time
ALM	1.9e-2/1.7e-2/63	2.1e-2/1.3e-2/60	1.4e-05/1.4e-05/355	1.4e-5/1.4e-5/337
FPCP	1.2e-2/2.0e-2/55	1.2e-2/1.5e-2/54	5.6e-3/4.3e-3/252	5.2e-3/3.0-e3/247
GreGoDec	0.84/0.68/14	4.6/2.7/14	0.86/0.66/54	5.0/2.8/55
IALM_BLWS	0.65/0.52/30	0.73/0.42/28	1.8e-1/1.4e-1/1202	2.6e-1/1.4e-1/1376
FALM	1.9e-2/1.7e-2/33	2.1e-2/1.3e-2/32	6.3-8/7.0e-8/605	5.6e-8/8.2e-8/649
NSA	1.6e-2/2.0e-2/26	1.7e-2/1.4e-2/27	0.2e-3/1.6e-3/31	1.7e-3/9.6e-4/39
PCP	1.9e-2/1.7e-2/88	2.1e-2/1.3e-2/91	2.4e-8/4.2e-8/90	3.9e-8/4.2e-8/90
SVT	9.4e-3/7.4e-3/357	9.8e-3/6.8e-3/357	8.4e-4/2.2e-4/340	1.1e-3/2.6e-4/394
pMAP	**9.1e-3/5.4e-3/21**	**9.4e-3/5.5e-3/21**	**8.9e-9/6.8e-9/18**	**2.4e-8/1.3e-8/22**

TABLE 5.7: The RMSE incurred by 10 different methods for principal component pursuit problem where both sparse noise and Gaussian noise are taken into consideration

We demonstrate our non-convex approach to tackle these two problems, which can be considered as a special weighted alternating projection method.

Several experiments based on both synthetic and real-life datasets are conducted to measure the performance of pMAP in tackling these two problems. Both theoretical and empirical results show that pMAP outperforms most state-of-the-art solvers in terms of computing time and approximation accuracy.

Chapter 6

Conclusion

Weighted Hankel structured low rank matrix approximation problem arises from many applications of time series study and signal processing. This optimization problem aims to find a Hankel matrix X such that $\text{rank}(X) \leq r$ while weighted distance to observed Hankel matrix Y is minimised. In this thesis, we introduced the majorization minimization framework and penalty method together to tackle this problem via some non-convex methods.

In Chapter 3, we proposed a sequential majorization method to tackle this NP-hard optimization problem. The $(\mathbf{p}, \mathbf{q})$-norm is introduced such that a majorization surrogate function is proposed and then the majorization minimization framework can be employed. As a result, SMM guarantees the functional value at each iterate will be non-increasing. The subproblem of SMM at each iteration step is well defined and can be solved by the Cadzow method. We use numerical examples to demonstrate the superiority of SMM based on several dataset. But one may note by introducing majorization surrogate function, the problem SMM aim to solve is different from the original one because the weights matrix has been changed.

In Chapter 4 we further proposed another new approach to solve Problem (1.2) as penalised method of alternating projection method. Different from SMM, we apply both majorization minimization and penalization technique to tackle the rank constraint such that it enjoys two advantages as (i) the subproblem of pMAP at each iteration has

analytical solutions which are easily computed and (ii) pMAP keeps the original weight matrix so that it has better performance in some specific applications like spectrally signal recovery. We further propose some theoretical result showing that pMAP will converge to at least a ϵ-KKT point at a linear rate. Numerical experiments are conducted to test pMAP against some state-of-the-art solvers. Promising results are provided to support that pMAP is a competitive solver in both recovering accuracy and computing cost.

Chapter 5 extended the application of pMAP framework into a wider range of rank minimization problems including robust matrix completion and stable principal component pursuit. We show that once the sandwich inequalities chain can be satisfied, the class of rank minimization problem can be easily tackled by our proposed framework. Further convergence result may depend on the convexity of extra constraints and objective functions. Numerical results show that the performance of pMAP in these applications are also competitive comparing with some state-of-the-art solvers.

References

Necdet Serhat Aybat, Donald Goldfarb, and Garud Iyengar. Fast first-order methods for stable principal component pursuit. *arXiv preprint arXiv:1105.2126*, 2011.

Basuraj Bhowmik, Manu Krishnan, Budhaditya Hazra, and Vikram Pakrashi. Real-time unified single-and multi-channel structural damage detection using recursive singular spectrum analysis. *Structural Health Monitoring*, 18(2):563–589, 2019.

Nicolas Boumal and Pierre-antoine Absil. Rtrmc: A riemannian trust-region method for low-rank matrix completion. In *Advances in neural information processing systems*, pages 406–414, 2011.

Thierry Bouwmans, Andrews Sobral, Sajid Javed, Soon Ki Jung, and El-Hadi Zahzah. Decomposition into low-rank plus additive matrices for background/foreground separation: A review for a comparative evaluation with a large-scale dataset. *Computer Science Review*, 23:1–71, 2017.

George EP Box, Gwilym M Jenkins, Gregory C Reinsel, and Greta M Ljung. *Time series analysis: forecasting and control*. John Wiley & Sons, 2015.

Holly Butcher and Jonathan Gillard. Simple nuclear norm based algorithms for imputing missing data and forecasting in time series. *Statistics and Its Interface*, 10(1):19–25, 2017.

Ricardo Cabral, Fernando De la Torre, Joao Paulo Costeira, and Alexandre Bernardino. Matrix completion for weakly-supervised multi-label image classification. *IEEE transactions on pattern analysis and machine intelligence*, 37(1):121–135, 2015.

Jian-Feng Cai, Emmanuel J Candès, and Zuowei Shen. A singular value thresholding algorithm for matrix completion. *SIAM Journal on optimization*, 20(4):1956–1982, 2010.

Jian-Feng Cai, Tianming Wang, and Ke Wei. Spectral compressed sensing via projected gradient descent. *SIAM Journal on Optimization*, 28(3):2625–2653, 2018.

Jian-Feng Cai, Tianming Wang, and Ke Wei. Fast and provable algorithms for spectrally sparse signal reconstruction via low-rank hankel matrix completion. *Applied and Computational Harmonic Analysis*, 46(1):94–121, 2019.

Léopold Cambier and P-A Absil. Robust low-rank matrix completion by riemannian optimization. *SIAM Journal on Scientific Computing*, 38(5):S440–S460, 2016.

Emmanuel J Candès and Benjamin Recht. Exact matrix completion via convex optimization. *Foundations of Computational mathematics*, 9(6):717, 2009.

Emmanuel J Candès, Xiaodong Li, Yi Ma, and John Wright. Robust principal component analysis? *Journal of the ACM (JACM)*, 58(3):1–37, 2011.

Emmanuel J Candes, Yonina C Eldar, Thomas Strohmer, and Vladislav Voroninski. Phase retrieval via matrix completion. *SIAM review*, 57(2):225–251, 2015.

Venkat Chandrasekaran, Sujay Sanghavi, Pablo A Parrilo, and Alan S Willsky. Rank-sparsity incoherence for matrix decomposition. *SIAM Journal on Optimization*, 21 (2):572–596, 2011.

Yuxin Chen and Yuejie Chi. Robust spectral compressed sensing via structured matrix completion. *IEEE Transactions on Information Theory*, 10(60):6576–6601, 2014.

Yuejie Chi, Louis L Scharf, Ali Pezeshki, and A Robert Calderbank. Sensitivity to basis mismatch in compressed sensing. *IEEE Transactions on Signal Processing*, 59(5): 2182–2195, 2011.

Yuejie Chi, Yue M Lu, and Yuxin Chen. Nonconvex optimization meets low-rank matrix factorization: An overview. *arXiv preprint arXiv:1809.09573*, 2018.

Moody T Chu, Robert E Funderlic, and Robert J Plemmons. Structured low rank approximation. *Linear algebra and its applications*, 366:157–172, 2003.

Moody T Chu, Matthew M Lin, and Liqi Wang. A study of singular spectrum analysis with global optimization techniques. *Journal of Global Optimization*, 60(3):551–574, 2014.

Laurent Condat and Akira Hirabayashi. Cadzow denoising upgraded: A new projection method for the recovery of dirac pulses from noisy linear measurements. *Sampling Theory in Signal and Image Processing*, 14(1):p–17, 2015.

Jan De Leeuw. Fitting distances by least squares. *Unpublished manuscript*, 1993.

Carl Eckart and Gale Young. The approximation of one matrix by another of lower rank. *Psychometrika*, 1(3):211–218, 1936.

Sarjoui M Fazel. Matrix rank minimization with applications. 2003.

Peihua Feng, Bingo Wing-Kuen Ling, Ruisheng Lei, and Jinrong Chen. Singular spectral analysis-based denoising without computing singular values via augmented lagrange multiplier algorithm. *IET Signal Processing*, 13(2):149–156, 2018.

Florian Feppon and Pierre FJ Lermusiaux. A geometric approach to dynamical model order reduction. *SIAM Journal on Matrix Analysis and Applications*, 39(1):510–538, 2018.

Jonathan Gillard. Cadzow's basic algorithm, alternating projections and singular spectrum analysis. *Statistics and its Interface*, 3(3):335–343, 2010.

Jonathan Gillard and Vincent Knight. Using singular spectrum analysis to obtain staffing level requirements in emergency units. *Journal of the Operational Research Society*, 65(5):735–746, 2014.

Jonathan Gillard and Konstantin Usevich. Structured low-rank matrix completion for forecasting in time series analysis. *International Journal of Forecasting*, 34(4):582–597, 2018.

JW Gillard and Anatoly A Zhigljavsky. Weighted norms in subspace-based methods for time series analysis. *Numerical Linear Algebra with Applications*, 23(5):947–967, 2016.

Donald Goldfarb, Shiqian Ma, and Katya Scheinberg. Fast alternating linearization methods for minimizing the sum of two convex functions. *Mathematical Programming*, 141(1-2):349–382, 2013.

Nina Golyandina and Anton Korobeynikov. Basic singular spectrum analysis and forecasting with r. *Computational Statistics & Data Analysis*, 71:934–954, 2014.

Nina Golyandina, Vladimir Nekrutkin, and Anatoly A Zhigljavsky. *Analysis of time series structure: SSA and related techniques*. Chapman and Hall/CRC, 2001.

Michael Grant, Stephen Boyd, and Yinyu Ye. Cvx: Matlab software for disciplined convex programming, 2008.

Andreas Groth and Michael Ghil. Monte carlo singular spectrum analysis (ssa) revisited: Detecting oscillator clusters in multivariate datasets. *Journal of Climate*, 28(19):7873–7893, 2015.

Di Guo, Hengfa Lu, and Xiaobo Qu. A fast low rank hankel matrix factorization reconstruction method for non-uniformly sampled magnetic resonance spectroscopy. *IEEE Access*, 5:16033–16039, 2017.

F Maxwell Harper and Joseph A Konstan. The movielens datasets: History and context. *Acm transactions on interactive intelligent systems (tiis)*, 5(4):19, 2016.

Hossein Hassani. Singular spectrum analysis: methodology and comparison. 2007.

Hossein Hassani, Rahim Mahmoudvand, and Mohammad Zokaei. Separability and window length in singular spectrum analysis. *Comptes rendus mathematique*, 349(17-18): 987–990, 2011.

Cho-Jui Hsieh and Peder Olsen. Nuclear norm minimization via active subspace selection. In *International Conference on Machine Learning*, pages 575–583, 2014.

Yue Hu, Sajan Goud Lingala, and Mathews Jacob. A fast majorize–minimize algorithm for the recovery of sparse and low-rank matrices. *IEEE Transactions on Image Processing*, 21(2):742–753, 2012.

Guoqiang Huan, Ying Li, and Zhanjie Song. A novel robust principal component analysis method for image and video processing. *Applications of Mathematics*, 61(2):197–214, 2016.

Furong Huang, UN Niranjan, Mohammad Umar Hakeem, and Animashree Anandkumar. Online tensor methods for learning latent variable models. *The Journal of Machine Learning Research*, 16(1):2797–2835, 2015.

Weilin Huang, Runqiu Wang, Yangkang Chen, Huijian Li, and Shuwei Gan. Damped multichannel singular spectrum analysis for 3d random noise attenuation. *Geophysics*, 81(4):V261–V270, 2016.

Mariya Ishteva, Konstantin Usevich, and Ivan Markovsky. Factorization approach to structured low-rank approximation with applications. *SIAM Journal on Matrix Analysis and Applications*, 35(3):1180–1204, 2014.

Prateek Jain, Raghu Meka, and Inderjit S Dhillon. Guaranteed rank minimization via singular value projection. In *Advances in Neural Information Processing Systems*, pages 937–945, 2010.

Prateek Jain, Praneeth Netrapalli, and Sujay Sanghavi. Low-rank matrix completion using alternating minimization. In *Proceedings of the forty-fifth annual ACM symposium on Theory of computing*, pages 665–674. ACM, 2013.

Pratik Jawanpuria and Bamdev Mishra. A unified framework for structured low-rank matrix learning. In *International Conference on Machine Learning*, pages 2259–2268, 2018.

Hui Ji, Chaoqiang Liu, Zuowei Shen, and Yuhong Xu. Robust video denoising using low rank matrix completion. In *2010 IEEE Computer Society Conference on Computer Vision and Pattern Recognition*, pages 1791–1798. IEEE, 2010.

Kaifeng Jiang, Defeng Sun, and Kim-Chuan Toh. An inexact accelerated proximal gradient method for large scale linearly constrained convex sdp. *SIAM Journal on Optimization*, 22(3):1042–1064, 2012.

Xue Jiang, Zhimeng Zhong, Xingzhao Liu, and Hing Cheung So. Robust matrix completion via alternating projection. *IEEE Signal Processing Letters*, 24(5):579–583, 2017.

Kyong Hwan Jin and Jong Chul Ye. Annihilating filter-based low-rank hankel matrix approach for image inpainting. *IEEE Transactions on Image Processing*, 24(11):3498–3511, 2015.

Raghunandan H Keshavan, Andrea Montanari, and Sewoong Oh. Matrix completion from noisy entries. *Journal of Machine Learning Research*, 11(Jul):2057–2078, 2010.

Ken Kreutz-Delgado. The complex gradient operator and the cr-calculus. *arXiv preprint arXiv:0906.4835*, 2009.

Salim Lahmiri. Minute-ahead stock price forecasting based on singular spectrum analysis and support vector regression. *Applied Mathematics and Computation*, 320:444–451, 2018.

Ming Jun Lai and Abraham Varghese. On convergence of the alternating projection method for matrix completion and sparse recovery problems. *arXiv preprint arXiv:1711.02151*, 2017.

Michael Lang. Automatic near real-time outlier detection and correction in cardiac interbeat interval series for heart rate variability analysis: singular spectrum analysis-based approach. *JMIR Biomedical Engineering*, 4(1):e10740, 2019.

Hojjat Haghshenas Lari, Mostafa Naghizadeh, Mauricio D Sacchi, and Ali Gholami. Adaptive singular spectrum analysis for seismic denoising and interpolation. *Geophysics*, 84(2):V133–V142, 2019.

Dongwook Lee, Kyong Hwan Jin, Eung Yeop Kim, Sung-Hong Park, and Jong Chul Ye. Acceleration of mr parameter mapping using annihilating filter-based low rank hankel matrix (aloha). *Magnetic resonance in medicine*, 76(6):1848–1864, 2016.

Kiryung Lee and Yoram Bresler. Admira: Atomic decomposition for minimum rank approximation. *IEEE Transactions on Information Theory*, 56(9):4402–4416, 2010.

Hongze Li, Liuyang Cui, and Sen Guo. A hybrid short-term power load forecasting model based on the singular spectrum analysis and autoregressive model. *Advances in Electrical Engineering*, 2014, 2014.

Min Li, Defeng Sun, and Kim-Chuan Toh. A majorized admm with indefinite proximal terms for linearly constrained convex composite optimization. *SIAM Journal on Optimization*, 26(2):922–950, 2016.

Zhouchen Lin and Siming Wei. A block lanczos with warm start technique for accelerating nuclear norm minimization algorithms. *arXiv preprint arXiv:1012.0365*, 2010.

Zhouchen Lin, Minming Chen, and Yi Ma. The augmented lagrange multiplier method for exact recovery of corrupted low-rank matrices. *arXiv preprint arXiv:1009.5055*, 2010.

Zhouchen Lin, Chen Xu, and Hongbin Zha. Robust matrix factorization by majorization minimization. *IEEE transactions on pattern analysis and machine intelligence*, 40(1): 208–220, 2017.

Guangcan Liu, Zhouchen Lin, Shuicheng Yan, Ju Sun, Yong Yu, and Yi Ma. Robust recovery of subspace structures by low-rank representation. *IEEE transactions on pattern analysis and machine intelligence*, 35(1):171–184, 2013.

Tianxiang Liu, Zhaosong Lu, Xiaojun Chen, and Yu-Hong Dai. An exact penalty method for semidefinite-box constrained low-rank matrix optimization problems. *to appear IMA Journal of Numerical Analysis*, pages 1–22, 2018.

Zhang Liu and Lieven Vandenberghe. Interior-point method for nuclear norm approximation with application to system identification. *SIAM Journal on Matrix Analysis and Applications*, 31(3):1235–1256, 2009.

Canyi Lu, Jinhui Tang, Shuicheng Yan, and Zhouchen Lin. Nonconvex nonsmooth low rank minimization via iteratively reweighted nuclear norm. *IEEE Transactions on Image Processing*, 25(2):829–839, 2015.

Julien Mairal. Incremental majorization-minimization optimization with application to large-scale machine learning. *SIAM Journal on Optimization*, 25(2):829–855, 2015.

Ivan Markovsky and Konstantin Usevich. Structured low-rank approximation with missing data. *SIAM Journal on Matrix Analysis and Applications*, 34(2):814–830, 2013.

Mantas Mazeika. The singular value decomposition and low rank approximation, 2016.

Hossein Mobahi, Zihan Zhou, Allen Y Yang, and Yi Ma. Holistic 3d reconstruction of urban structures from low-rank textures. In *Computer Vision Workshops (ICCV Workshops), 2011 IEEE International Conference on*, pages 593–600. IEEE, 2011.

Praneeth Netrapalli, UN Niranjan, Sujay Sanghavi, Animashree Anandkumar, and Prateek Jain. Non-convex robust pca. In *Advances in Neural Information Processing Systems*, pages 1107–1115, 2014.

Thanh Ngo and Yousef Saad. Scaled gradients on grassmann manifolds for matrix completion. In *Advances in neural information processing systems*, pages 1412–1420, 2012.

Hien M Nguyen, Xi Peng, Minh N Do, and Zhi-Pei Liang. Denoising mr spectroscopic imaging data with low-rank approximations. *IEEE Transactions on Biomedical Engineering*, 60(1):78–89, 2013.

Jorge Nocedal and Stephen Wright. *Numerical optimization*. Springer Science & Business Media, 2006.

Giorgio Ottaviani, Pierre-Jean Spaenlehauer, and Bernd Sturmfels. Exact solutions in structured low-rank approximation. *SIAM Journal on Matrix Analysis and Applications*, 35(4):1521–1542, 2014.

Hou-Duo Qi and Xiaoming Yuan. Computing the nearest euclidean distance matrix with low embedding dimensions. *Mathematical programming*, 147(1-2):351–389, 2014.

Hou-Duo Qi, Jian Shen, and Naihua Xiu. A sequential majorization method for approximating weighted time series of finite rank. *Statistics and Its Interface*, 2017.

Donya Rahmani. *Bayesian singular spectrum analysis with state dependent models*. PhD thesis, Bournemouth University, 2017.

Benjamin Recht, Maryam Fazel, and Pablo A Parrilo. Guaranteed minimum-rank solutions of linear matrix equations via nuclear norm minimization. *SIAM review*, 52(3): 471–501, 2010.

R Tyrrell Rockafellar and Roger J-B Wets. *Variational analysis*, volume 317. Springer Science & Business Media, 2009.

Paul Rodriguez and Brendt Wohlberg. Fast principal component pursuit via alternating minimization. In *2013 IEEE International Conference on Image Processing*, pages 69–73. IEEE, 2013.

Richard Roy and Thomas Kailath. Esprit-estimation of signal parameters via rotational invariance techniques. *IEEE Transactions on acoustics, speech, and signal processing*, 37(7):984–995, 1989.

Nasir Saeed, Abdulkadir Celik, Tareq Y Al-Naffouri, and Mohamed-Slim Alouini. Robust 3d localization of underwater optical wireless sensor networks via low rank matrix completion. In *2018 IEEE 19th International Workshop on Signal Processing Advances in Wireless Communications (SPAWC)*, pages 1–5. IEEE, 2018.

Tara N Sainath, Brian Kingsbury, Vikas Sindhwani, Ebru Arisoy, and Bhuvana Ramabhadran. Low-rank matrix factorization for deep neural network training with high-dimensional output targets. In *2013 IEEE international conference on acoustics, speech and signal processing*, pages 6655–6659. IEEE, 2013.

Ralph Schmidt. Multiple emitter location and signal parameter estimation. *IEEE transactions on antennas and propagation*, 34(3):276–280, 1986.

Nauman Shahid, Vassilis Kalofolias, Xavier Bresson, Michael Bronstein, and Pierre Vandergheynst. Robust principal component analysis on graphs. In *Proceedings of the IEEE International Conference on Computer Vision*, pages 2812–2820, 2015.

Jian Shen. Daily crude oil price analysis and forecasting based on the sequential majorization method. In *Transforming Energy Markets, 41st IAEE International Conference, Jun 10-13, 2018*. International Association for Energy Economics, 2018.

Xin Shen and John E Mitchell. A penalty method for rank minimization problems in symmetric matrices. *Computational Optimization and Applications*, 71(2):353–380, 2018.

Yuan Shen, Zaiwen Wen, and Yin Zhang. Augmented lagrangian alternating direction method for matrix separation based on low-rank factorization. *Optimization Methods and Software*, 29(2):239–263, 2014.

Lei Shi. Sparse additive text models with low rank background. In *Advances in Neural Information Processing Systems*, pages 172–180, 2013.

Suwarna Shukla and Krishna Prasad Yadav. Forecasting indian stock market index using singular spectrum analysis: A comparison with arima and artificial neural network. 2017.

Emmanuel Sirimal Silva, Hossein Hassani, and Saeed Heravi. Modeling european industrial production with multivariate singular spectrum analysis: A cross-industry analysis. *Journal of Forecasting*, 37(3):371–384, 2018.

Dan Simon and Jeff Abell. A majorization algorithm for constrained correlation matrix approximation. *Linear Algebra and its Applications*, 432(5):1152–1164, 2010.

Nathan Srebro and Tommi Jaakkola. Weighted low-rank approximations. In *Proceedings of the 20th International Conference on Machine Learning (ICML-03)*, pages 720–727, 2003.

Chi Su, Fan Yang, Shiliang Zhang, Qi Tian, Larry S Davis, and Wen Gao. Multi-task learning with low rank attribute embedding for person re-identification. In *Proceedings of the IEEE international conference on computer vision*, pages 3739–3747, 2015.

Defeng Sun. A majorized penalty approach for calibrating rank constrained correlation matrix problems. 2010.

Ying Sun, Prabhu Babu, and Daniel P Palomar. Majorization-minimization algorithms in signal processing, communications, and machine learning. *IEEE Transactions on Signal Processing*, 65(3):794–816, 2017.

Gongguo Tang, Badri Narayan Bhaskar, Parikshit Shah, and Benjamin Recht. Compressed sensing off the grid. *IEEE transactions on information theory*, 59(11):7465–7490, 2013.

Kim-Chuan Toh and Sangwoon Yun. An accelerated proximal gradient algorithm for nuclear norm regularized linear least squares problems. *Pacific Journal of optimization*, 6(615-640):15, 2010.

Kim-Chuan Toh, Michael J Todd, and Reha H Tütüncü. Sdpt3—a matlab software package for semidefinite programming, version 1.3. *Optimization methods and software*, 11(1-4):545–581, 1999.

Poornima Unnikrishnan and V Jothiprakash. Daily rainfall forecasting for one year in a single run using singular spectrum analysis. *Journal of Hydrology*, 561:609–621, 2018.

Konstantin Usevich. On signal and extraneous roots in singular spectrum analysis. *arXiv preprint arXiv:1006.3436*, 2010.

Konstantin Usevich and Pierre Comon. Hankel low-rank matrix completion: Performance of the nuclear norm relaxation. *IEEE Journal of Selected Topics in Signal Processing*, 10(4):637–646, 2016.

Konstantin Usevich and Ivan Markovsky. Variable projection for affinely structured low-rank approximation in weighted 2-norms. *Journal of Computational and Applied Mathematics*, 272:430–448, 2014.

Bart Vandereycken. Low-rank matrix completion by riemannian optimization. *SIAM Journal on Optimization*, 23(2):1214–1236, 2013.

Ke Wei, Jian-Feng Cai, Tony F Chan, and Shingyu Leung. Guarantees of riemannian optimization for low rank matrix recovery. *SIAM Journal on Matrix Analysis and Applications*, 37(3):1198–1222, 2016.

Zaiwen Wen, Wotao Yin, and Yin Zhang. Solving a low-rank factorization model for matrix completion by a nonlinear successive over-relaxation algorithm. *Mathematical Programming Computation*, 4(4):333–361, 2012.

Wilhelm Wirtinger. Zur formalen theorie der funktionen von mehr komplexen veränderlichen. *Mathematische Annalen*, 97(1):357–375, 1927.

John Wright, Arvind Ganesh, Shankar Rao, Yigang Peng, and Yi Ma. Robust principal component analysis: Exact recovery of corrupted low-rank matrices via convex optimization. In *Advances in neural information processing systems*, pages 2080–2088, 2009.

Shanzhi Xu, Hai Hu, Linhong Ji, and Peng Wang. Embedding dimension selection for adaptive singular spectrum analysis of eeg signal. *Sensors*, 18(3):697, 2018.

Xiaoqiang Xu, Ming Zhao, and Jing Lin. Detecting weak position fluctuations from encoder signal using singular spectrum analysis. *ISA transactions*, 71:440–447, 2017.

Gao Yan. *Structured low rank matrix optimization problems: a penalty approach*. PhD thesis, 2010.

Jiaxi Ying, Hengfa Lu, Qingtao Wei, Jian-Feng Cai, Di Guo, Jihui Wu, Zhong Chen, and Xiaobo Qu. Hankel matrix nuclear norm regularized tensor completion for n-dimensional exponential signals. *IEEE Transactions on Signal Processing*, 65(14): 3702–3717, 2017.

Jiaxi Ying, Jian-Feng Cai, Di Guo, Gongguo Tang, Zhong Chen, and Xiaobo Qu. Vandermonde factorization of hankel matrix for complex exponential signal recovery—application in fast nmr spectroscopy. *IEEE Transactions on Signal Processing*, 66(21):5520–5533, 2018.

Xiaoming Yuan and Junfeng Yang. Sparse and low-rank matrix decomposition via alternating direction methods. *preprint*, 12:2, 2009.

Jaime Zabalza, Jinchang Ren, Zheng Wang, Huimin Zhao, Jun Wang, and Stephen Marshall. Fast implementation of singular spectrum analysis for effective feature

extraction in hyperspectral imaging. *IEEE Journal of Selected Topics in Applied Earth Observations and Remote Sensing*, 8(6):2845–2853, 2015a.

Jaime Zabalza, Jinchang Ren, Jiangbin Zheng, Junwei Han, Huimin Zhao, Shutao Li, and Stephen Marshall. Novel two-dimensional singular spectrum analysis for effective feature extraction and data classification in hyperspectral imaging. *IEEE transactions on geoscience and remote sensing*, 53(8):4418–4433, 2015b.

Shenglong Zhou, Naihua Xiu, and Hou-Duo Qi. A fast matrix majorization-projection method for penalized stress minimization with box constraints. 2018.

Tianyi Zhou and Dacheng Tao. Godec: Randomized low-rank & sparse matrix decomposition in noisy case. In *Proceedings of the 28th International Conference on Machine Learning, ICML 2011*, 2011.

Tianyi Zhou and Dacheng Tao. Greedy bilateral sketch, completion & smoothing. *Journal of Machine Learning Research*, 2013.

Zhihui Zhu, Qiuwei Li, Gongguo Tang, and Michael B Wakin. Global optimality in low-rank matrix optimization. *IEEE Transactions on Signal Processing*, 66(13):3614–3628, 2018.

N Zvonarev and N Golyandina. Modified gauss-newton method in low-rank signal estimation. *arXiv preprint arXiv:1803.01419*, 2018.

Nikita Zvonarev and Nina Golyandina. Iterative algorithms for weighted and unweighted finite-rank time-series approximations. *arXiv preprint arXiv:1507.02751*, 2015.